UNIVERSITÀ
DELLA CALABRIA

UNIVERSITÀ DELLA CALABRIA
FACOLTÀ DI INGEGNERIA

Dottorato in Ingegneria dell'Ambiente e del Territorio XXIV Ciclo
Dipartimento Difesa del Suolo 'V. Marone'

PhD Thesis
in
Maritime Engineering – ICAR/02

Hydrodynamic and morhodynamic study of a drained beach

PhD Student

Eng. Alessandra Saponieri

Supervisors

Prof. Eng. Leonardo Damiani

Prof. Eng. Paolo Veltri

PhD Coordinator

Prof. Eng. Francesco Macchione

2009 - 2011

Contents

Introduction

The present PhD thesis deals with the analysis of the Beach Drainage System (BDS) as a soft engineering solution for coastal defense. In particular BDS has to be considered as a system aimed to improve the beach management, in order to re-establish the initial equilibrium conditions of a sandy beach.
Emphasis is put on beach drainage effects on both nearshore hydrodynamics and moprhodynamics. BDS behavior is mainly analized by means of system field applications and physical modeling of the dominant processes.
Several field installations are available at many sites around the world and in Italy too. However even if field monitoring is useful to assess the effectiveness of the system, laboratory tests can be used in order to study the system response under different wave conditions. Moreover the physical modeling in known boundary and initial conditions allows to define the main design parameters, which are not yet well defined.
Laboratory experiments were performed in small and large scale. The former were conducted at the Laboratory of Coastal Engineering at Politecnico of Bari (Italy) in 2001. The latter were carried out at the Grosser Wellen Kanal in Hannover (Germany) in 2010. Physical models show the BDS efficiency in water table lowering with a consequent arise of the unsaturated zone inside the beach. This new hydrodynamic conditions should increase the run-u flow rate which infiltrates inside the beach. Such downward vertical filtration process causes the settlement of the suspended sediments on beach face, which otherwise would be transported off-shore during backwash phase. moreover the reduction of wave-induced set-up has been observed under all tested wave energy conditions with a slight decrease of the undertow. Suche effects on the hydrodynamics are not so evident on morphodynamic process. The most remarkable sediment volume accretion has been observed in the zone close to the drain. However it has to be highlighted that even if BDS does not totally nullify the erosion process, it is able to reduce and delay the off-shore sediment transport.
The thesis is divided in two parts. The first one deals with a general overview of hydrodynamic and morphodynamic processes in coastal regions (Chapter 1). Moreover the main coastal management strategies are discussed and coastal defense works are described (Chapter 2), focusing the attention on soft engineering

solutions and in particular on BDS (Chapter 3).
The second part deals with physical and numerical modeling on BDS. Small scale model results are sketchily presented in the beginning of Chapter 4. these results have allowed to draw some consideration on scale effects which influence results obtained from physical modeling on bed-movable models. Chapter 5 reports the main lines of the mathematical description for some groups of numerical wave models. Firstly four type of model formulations simulating free surface waves propagation on finite water depth are briefly described. Thereafter, the models for simulating groundwater flow and its interaction with the external wave motion and are reported. In particular the proposed models analyze the interaction between the water table variation inside the beach and the swash processes on the beach face. Afterwards the Chapter 5 focuses on the simulation of the influence of the BDS on the groundwater flow inside the beach by using the *HYDRUS-2D* code. A variety of analytical and numerical models are now available to predict water transfer process between the soil surface and the groundwater table. The most popular models remain the Richard's equation for variably saturated flow. Deterministic solutions of these classical equations have been used for predicting water movement, analyzing specific laboratory or field experiments involving unsaturated water flow. The *HYDRUS-2D* software package simulates two-dimensional water flow, heat movement and transport of solutes involved in sequential first-order decay reactions in unsaturated, partially saturated or fully saturated porous media. The comparison between experimental and numerical mainly allow to state that the numerical model well simulate the time variation of the water table induced by the presence of the drain. The reported simulations represents a first step for a complete numerical modeling of the phenomena interested in a drainage process.
Future applications could regard the possibility of improving the adopted numerical model by simulating the drainage efficiency under different wave attacks in order to deeply analyze the interaction between the new hydrodynamic conditions due to the drainage and the sediment transport in the swash zone. Moreover a complete modeling of the BDS which consider simultaneously field, laboratory and numerical results, would allow to define system guidelines useful in coast management by means of a drainage system.

Chapter 1

Coastal processes

1.1 Introduction

The present chapter deals with a general description of hydrodynamic and morphodynamic processes in coastal regions. They can be considered the main responsible of beaches geometry changes. Knowledge of such concepts is essential for coastal projects design, planning and design of marinas, shore protection measures and other civil coastal works.
Section 1.2 mainly pertains to the sea motion from deep to shallow waters and in particular to the description of surface waves and the forces they generate, focusing the attention on the nearshore processes. Section 1.3 covers with a theoretical discussion about the sediment transport as suspended and bed load. Moreover the effects on beach morphological evolution are depicted in both directions, parallel and perpendicular to the coastline.

1.2 Hydrodynamics of coastal zones

Wind waves born in the open sea, when the wind velocity exceeds a critical value and the energy is transferred to the sea. The wind waves, also called sea waves, are normally relatively steep (short waves) and irregular. For this reason in deep water it is difficult to distinguish defined wave fronts. Wave characteristics and propagation direction at a certain location are influenced by the wind field (speed, direction and duration), the fetch and the water depth over the wave generation area.
Under the continuous action of the wind, the waves gradually grow in height, length and period. At the same time the wave steepness decreases to a minimum value depending on the wind speed and the water depth. When the wave comes out the generating area a *swell* is formed. On the contrary of the wind waves, swell waves are regular and unidirectional. Their heights, lengths, pe-

riods, length of front and propagation direction generally follow statistic laws (i.e. wave heights normally follow the Rayleigh distribution quite well).
Propagating landward, when the water depth becomes about one half of the wave length, the waves begin to be affected by the seabed through processes such as refraction, shoaling and bottom friction. If the waves meet structures they are transformed by diffraction or reflected, if all wave power is not completely dissipated by the obstacle. When the wave reaches a height which is about equal to the water depth, the effects of seabed slope increase leading to a pronounced asymmetry and deformation of the wave profile. Waves became steepened, shorted, slowed and no longer stable. In these conditions, the breaking sets in. An overview of breaking waves in the surf zone and the transformation of waves can be found in Battjes and Peregrine ([1]; [2]). Breaking occurs when the water particles velocities exceed the wave celerity, before the wave face became vertical. Accelerations on the front face of the wave exceed gravity while an extensive region on and below the wave back-face has low accelerations. Near the breaker line the effects of shoaling and bottom friction on the wave height cause the wave height increasing up to breaking at the same time as the water depth decreases. Wave breaking occurs also in deep water where dissipation of wave energy primarily takes place in the so-called white caps.
In the surf zone different types of breaking can be found, depending mainly on bottom slope and wave length. Steep waves over flat beaches produce a gradual breaking called *spilling*. It takes place as a foam bore on the front topside of the wave. If the beach is steeper and the waves flatter (swell) the *surging* breaking occurs. In this case the lower part of the wave surges up on the beach face. The most dangerous breaking is the *plunging*, in which the wave curls over and loses a considerable amount of energy in one big collapse. This form of breaking takes place with moderately steep waves and sloping shorefaces.
Outside the surf zone it can be observed a slight depression of the mean water level, reaching a minimum value at about the breaking point (wave set-down). Inside the surf zone, as a consequence, the reduction of the wave height through the surf zone causes a mean water level raising (wave set-up). This 'super-elevation' of the mean water level generally represents a large fraction (about 30%, [3]) of the wave breaker height and about 10% of the incident wave height ([4],[5] and [6]).
These variations in the mean water level are due to changes in the so-called *radiation stress* and strictly related to the concept of the mean energy level. Under the hypothesis of wave fronts parallel to the bottom contours, the momentum equation of forces perpendicular to the shoreline, averaged on the wave period T, over the water depth h takes to following equation:

$$\frac{dF_w}{dx} = -\rho g h \frac{db}{dx} \tag{1.1}$$

in which b is the elevation of the mean water level, F_w is the radiation stress, ρ is the water density and g is the gravity acceleration. It is seen that if F_w is known, elevation b can be determined by integration. It can be also deducted from Eq. 1.1 that the tilt of the mean water level is negative when the radiation stress increases and vice versa. This demonstrates that the radiation stress increases outside the surf zone when a wave approaches the coast and the wave set-down occurs. On the contrary, after wave breaking, there is a decrease of this quantity inside the surf zone, which must be balanced by an increase of the hydrostatic force.
Upon breaking the wave energy is dissipated through the turbulence, while the momentum is never dissipated but transferred to the water column. This phenomenon causes a slope of the water surface in order to balance the onshore component of the flux momentum, resulting in a positive tilt of the mean water surface which corresponds to the wave set-up.
Wave induced set-up has been investigated theoretically and in laboratory and field conditions. Indeed it represents a relevant parameter to be considered in a number of engineering applications. For this reason it is necessary to calculate the maximum set-up value at the shoreline.
Several laboratory and field measurements of wave set-up allowed to define some factors which influence the wave set-up value ([4],[5] and [6], [7]) and some empirical formulas in order to calculate the maximum value. First laboratory investigations were performed with monochromatic waves ([8]). Later, experiments included also the examination of irregular waves. The first laboratory experience of wave set-up due to the irregular waves was conducted by Battjes ([9]). Later, Steve et al. ([10]) demonstrated the influence of wave nonlinearity. This effect can be explained considering that nonlinear wave are characterized by long troughs and peaked wave crests, resulting in a small water surface displacement ([7]). Therefore the wave energy, from which the momentum flux depends and proportional to the root-mean square of the water surface displacement, results to be less for nonlinear waves in shallow water.
In the following some formulas on wave set-up obtained by field experiments are listed:

1. $\bar{\eta} = 0.3H_s = 0.42H_{rms}$ ([3])
2. $\bar{\eta} = 0.17H_s = 0.24H_{rms}$ ([11])
3. $\bar{\eta} = 0.10H_s = 0.14H_{rms}$ ([12])
4. $\bar{\eta} = 0.052H_s \left(\frac{L_s}{H_s}\right)^{0.2}$ ([13])
5. $\bar{\eta} = 0.19H_s = 0.27H_{rms}$ ([14])
6. $\bar{\eta} = 0.04\sqrt{H_s L_0} = 0.048\sqrt{H_{rms} L_0} H_{rms}$ ([15])

When a real waves train of varying height reaches at coast, mean water level oscillations in the surf zone occur due to more or less periodic variations in the breaker height of the waves breaking on the beach. These long-period oscillations of the wave set-up, are often observed and called *surf beat*.
The mentioned wave set-up is only a part of the wave *run-up*. This represents the maximum height reached by the water surface on the beach face or on a coastal structure. It can be considered as the sum of the wave set-up and the wave swash and proportional to the wave length and the emerged beach slope. For wide surf zones, with steep waves on flat beaches, the set-up constitutes the major part of the run-up. In general for laboratory and field applications the run-up height exceeded by 2% of the run-up events is considered ($R_{2\%}$). In literature several empirical formulas have been proposed for predicting wave run-up value. Some of them are cited below:

1. $R_{2\%} = H_0 tan\alpha / \sqrt{H_0/L_0}$ ([16])
2. $R_{2\%} = 1.52 H_{mo}/(1 - exp^{-0.34\xi})$ ([17])
3. $R_{max} = 1.022 H_{mo}\xi/(1 + 0.247\xi)$ ([18])
4. $R_{2\%} = 1.5 H_{sb}\xi$ if $\xi < 2$ ([19])

   $R_{2\%} = 3 H_{sb}\xi$ if $\xi \geq 2$ ([19])

The wave and wind induced water level variations determine a high degree of water circulation in nearshore areas. Such currents can be classified in several ways. Wiegel ([20]) classified the currents as long-shore, tidal, wind drift and ocean. The *long-shore currents* are the mainly responsible of the development of the most part of sandy beaches, since they transport sediments along the coast. However a pure long-shore current does not constitute a stable system and along the coast the water returns seawards in form of strong narrow currents denoted *rip-currents*. They are local currents away from the shore, bringing back into deep waters the surplus water carried over the bars during the breaking process
.
In the surf zone the mass flux represented by the surface roller in the breakers returns as a seaward flows close to the bottom ([21]). Such kind of currents are known as *undertow*. The undertow can be conceived as a current driven by vertical differences within the water column between the radiation stress and the uniform pressure gradient force due to the wave set-up ([14]). It is generated below wave trough and it compensates the wave-induced volume flux above that level ([22]). Many authors developed theoretical models in order to describe the mechanism responsible of the undertow (see [23], [24], [25], [26], [27],[28]). The undertow was observed in laboratory by Bagnold [29]. Successively, detailed laboratory measurements were performed by Stive and Wind ([10]), Nadaoka

and Kondoh ([30]), Hansen and Svendsen ([21] and [31]) and Okayasu et al. ([32] and [33]). In particular Hansen and Svendsen underline that the undertow current is the result of the balance between three equally important forces acting on the fluid particles: the radiation stress, the pressure gradient due to the wave-induced set-up and the turbulent shear stresses created by the variation of fluid velocity along the vertical in combination with the turbulence already present due to the breaking. One of the latest works on the undertow has been conducted by Putrevu and Svendsen ([22]). Results show the different vertical structures of the undertow outside and inside the surf zone. Indeed they numerically demonstrate that in the surf zone the undertow has a large seaward component near the bottom and a small one near the wave trough. On the contrary outside the surf zone the opposite situation occurs. In this zone the undertow has a seaward component at trough level larger than near the bottom.

1.3 Sediment transport

The previous section explained the wave transformations over a coastal profile and how these processes generate wave induced set-up, longshore and undertow currents. These hydrodynamic conditions will result in the movement and transport of sediments, subject of the present section.
The interaction between hydrodynamics and sediment movement results in beach profiles changes. The sediment on the seabed is transported by the water movements under the action of large enough forces. These movements can be caused either by the wave orbital velocities or by the currents or a combination of both. The former is the main cause of the nearshore sediment transport when mean currents are weak. As a matter of fact, due to the shoaling, the wave shape becomes skewed and asymmetric. During the propagation of an asymmetric waves steep front the orbital velocity changes from the maximum offshore to the maximum onshore ([34]).
A correct description of sediment transport processes in a coastal area requires the knowledge of some relevant parameters listed in the following:

- the wave condition at the site and the possible variations over the site
- the current conditions and variation over the area
- the water level variations (i.e. tides, storms, wave induced set-up)
- the bathymetry
- the sediment characteristics (i.e. grainsize curve, fall velocity, hydraulic conductivity)

- the possible source of sediments such as rivers, eroding coasts or tidal inlets.

The following section deals with a general discussion of sediment transport as bed and suspended load, focusing on the last one. Afterwards the two transport components (perpendicular and parallel to the coast) are reviewed, discussing in depth the cross-shore transport process which is the main topic of the present work.

1.3.1 Suspended and bed load transport

A complete understanding of sediment transport is generally complicated, due to the fact that it results in simultaneously presence of both bed and suspended load transport. The magnitude of each of these component depends on beach characteristics (i.e. grainsize) and on wave motion (i.e. wave energy).
In the swash zone there is an ongoing discussion whether the bed or suspended load is most important ([35], [36]). The ratio between these two transport modes seems to vary greatly in space and time. it is observed that in general suspended load occurs near the front of up-rush, while the bed one prevails during the back-wash phase ([37]). Madsen ([38]) derived a sediment transport rate for the instantaneous bed load $q_b(t)$. The expression derived from previous shear-stress based formualae ([39], [40]) which allow to calculate the total sediment load, with properly tuned coefficients. Other formulation about bed load can be find in Hughes 1997 ([36]) or Masselink and Hughes 1998 ([41]). Outside of the surf zone sediment transport is attributed to bed load motion due to the nonlinearity of the waves and acceleration skewness. The bed load has been defined in different ways depending on the context. Bagnold ([42]) defined the bed load as that part of the total load which is supported by intergranular forces. Generally the bed-load transport rate can be expressed as

$$Q_b = \int_0^\infty c_B(z) u_s(z) dz = c_{max} L_B U_B \tag{1.2}$$

where c_{max} represents the maximum concentration which corresponds to the volumetric concentration of sediments in the immobile bed, L_B is the equivalent thickness-at-rest of the bed-load distribution and U_B is the integral of the sediment velocity distribution through the bed-load layer. It is not easy to calculate Q_B because neither $u_s(z)$ nor $C_B(z)$ are well understood ([43]). However some empirical formulas are available for predicting Q_B in steady flow conditions ([44], [45]).
When sediments are supported more by fluid drags then intergranular forces, they move as suspended load. This kind of transport is of great practical importance in coastal and fluvial engineering. The mechanics of suspended sediment transport has been the object of several researches, even if there is still much

to be learned about the concentration magnitude and about the distribution in waves, in currents ad in combined wave-current flows. The turbulence generated by breaking waves in shallow water is suspected to be directly responsible fro sediment suspension and transport inside the surf zone. The importance of wave breaking in sediment suspension process is recognized, but the exact mechanisms are not well understood. The descent and the rise of the air-water interface after the plunging and splashing of a plunging breaker is thought to cause vertical eddies. In the same time the ascent of the air pushed into the water generate the suction. The combination of these two phenomena was observed to suspend *clouds of sediments* several meters wide in the field ([46]). Stationary three-dimensional vertical eddies have been also observed after a spilling wave passes ([47]), called *obliquely descending eddies, ODS,* that may be responsible for sand suspension in the surf zone.
Predicting the suspended sediment transport at the breaking zone is not easy. Conceptual and numerical sediment concentration modeling is based on the sediment conservation equation. The sediment transport rate (per unit width) is usually given as follows ([43]):

$$Q_s(t) = \int_0^D c(z,t)u_s(z,t)dz \tag{1.3}$$

in which $c(z,t)$ is the suspended sediment concentration and $u_s(z,t)$ is the horizontal velocity of a sediment particle which can generally be assumed equal to the horizontal velocity of the immediately surrounding fluid.
Bagnold stated in 1966 (**??**) that a particle remains in suspension if the turbulent eddies have dominant vertical velocity components exceeding the particle fall velocity. Detailed studies on turbulence phenomena in boundary layer flow ([48]) suggest that the maximum value of the vertical velocity component of turbulence intensity is of the same order as the bed-shear velocity ([49], ([50]).
Sediment pickup and deposition are both distribution processes for which sediment goes from a state of rest to a state of movement and vice versa. These processes can be considered as an orderly convective process or as a disorganized, diffusive process, or, most commonly, as a combination of these two. The distinction can be schematically defined as a function of the mixing length as follows. If the mixing length is large compared to the overall scale of the sediment distribution, the process is convective. Conversely if the mixing length is small compared to the overall scale, the process may be described as diffusive. For the sake of simplicity, considering a horizontally uniform situation, the total vertical sediment flux q_z can be defined as the sum of a downward component, $-w_0c$, which represents the settling flux, and an upward flux which can be convective, q_C, or diffusive, q_D:

$$q_Z = -w_0c + q_D + q_C \tag{1.4}$$

Several models have been developed in order to estimate the suspended sediment distribution due to pure convection, to pure diffusion or to the combination of them under breaking and non breaking waves conditions (see [43]). In general sediment transport models are of two kinds. Namely, *cu*-integral (concentration times velocity integral) models and particle trajectory models. The former, as explained previously, allows to calculate the time-averaged sediment transport rate $\bar{Q}$ as a function of the sediment concentration $c(z,t)$ and of the horizontal sediment velocity $u(z,t)$. The latter is an alternative model which can lead, in some cases, to simpler and more accurate models. The time-averaged transport rate $\bar{Q}$ is expressed in terms of the time-averaged pickup rate $\bar{p}$ and the average distance l_x ([51]) traveled by the sediment grains.
In the following the two components of sediment transport, parallel and perpendicular to the shore are briefly discussed. In particular the attention is focused on the shore normal sediment transport in relation with the beach profile changes.

1.3.2 Long-shore sediment transport

The long-shore transport can be defined as the movement of non-cohesive sediment, mainly sandy, in the littoral zone along a shoreline. Generally it is described under the assumption that the shoreline is nearly straight with nearly parallel contours. This hypothesis is often valid especially if the sections of the shore are not too long.
It is well known that the sediment transport is caused by the turbulence due to the wave breaking. This processes of wave energy dissipation bring into suspension the seabed sediments. These suspended sediments plus the sediments on the seabed are then transported by the long-shore currents in the direction perpendicular to the wave motion. Usually the littoral drift is considered as the sum of both suspended and bed load.
The most important hydraulic parameter for quantifying the littoral transport is the wave condition. This because the sediments move along the coast as the sea currents increase. In particular it depends on long-shore currents. The magnitude of the littoral transport over a coastal profile depends not only on the hydrodynamics (i.e. wave height or incident angle) but also on the variation of the sediment characteristics (i.e. grain size) over profile. Coastline erosion or accretion analysis is based on the concept of *net littoral transport* which can be defined for each section of the shoreline.
The historical development of the shoreline can be extracted from historical maps and surveys, from aerial photos and from satellite images. Shoreline evolution is especially suited as calibration basis for littoral drift and shoreline development modeling.
Several methods and models have been developed in order to determine the

direction and the volume of the net long-shore transport. Mathematical models calculate the long-shore sediment transport across a selected section of the shoreline. In the following the CERC formula is briefly described (ref. CEM). It is one of the best known and simpler model to be used. It relates the long-shore sediment rate to the long-shore component of the wave energy flux P_l. Munch-Peterson ([52]) first related the littoral transport to deep water wave energy, obtaining a preliminary estimation of littoral drift direction by field applications. Afterward other field measurements ([53], [54], [55]) allowed to modify the existing formula. Finally in 1962 Savage ([56]) summarized the available data from field and laboratory studies and developed the formula which now is known as 'CERC' formula:

$$P_l = (EC_g)_b sin\alpha_b cos\alpha_b \tag{1.5}$$

where E_b is the breaking wave energy, evaluated as $\rho g H_b/8$, C_{gb} is the wave group celerity at breaker line, equal to $\sqrt{gd_b}$.
A drawback of this approach is that neither the beach profile nor the characteristics of the bed sediments are taking into account. This represents a common limit of *one-line models*. Such models resolved only spatial dimension along the shoreline. A refinement to the calculation of shoreline evolution has been added in the so-called *multi-line models* by introducing more than one line to describe the coast. The beach profile is represented by a stepped curve and the long-shore transport is calculated for each step (1.1). In addition the dis-

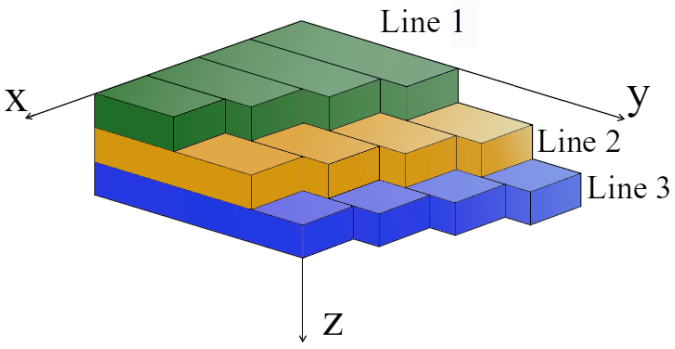

Figure 1.1: Representation of the beach profile in a multi-line model

tribution of the cross-shore sediment transport along the beach profile is also calculated and taken into account when solving the continuity equation for the transported sediment. In this way the profile evolution is modeled at the same time as changes in shoreline position are. Nevertheless the multi-line models required more data for calibration than a one-line model because of the difficulty in the specification of realistic relations for cross-shore sand transport.

1.3.3 Cross-shore sediment transport

The cross-shore sediment transport is strongly influenced by several parameters. In particular beach profile changes mainly depend on wave conditions, tide levels,bathymetry, sand grain size, the initial beach profile and sediment distribution along the profile. Varying wave conditions results in varying on-shore and offshore transport. When beach is exposed to small period and low energy waves (generally in the summer) the suspended sediment near the shoreline are transported on-shore during the up-rush phase. Under swell waves and normal water level conditions these sediments deposit on the emerged beach, resulting in a berm on shoreface. On the contrary, under storm surge conditions, off-shore sediments transport causes the erosion of the emerged beach with the formation of one or more bars. If the sediment load is transported out from the active zone, it is lost for the erosive and accretive beach cycles.
During such a sequence of profile erosion and rebuilding, certain parts of coastal profile may experience temporary erosion. This may not be recorded in profile surveys, because some rebuilding have already taken place before whether gives the possibility of carrying out surveys after storms. It is important to take such temporary profile fluctuation into account when designing structures in the coastal zone.
Shore normal sediment transport may occur in the swash zone, throughout or in parts of the surf zone and outside the surf zone if the waves are large and the sand is fine. It is generally recognized that the swash zone contributes to the major part of the total littoral drift. However, at present, little knowledge is available about the boundary layer flow and the corresponding shear stresses to even attempt a description of the basic sediment transport mechanisms in this area. Furthermore the comprehension of such processes includes the extra complication of flows perpendicular to sand surface whose details are not well understood.
In the surf zone the bed can be considered practically flat. Megaripples some times present, have no sharp crests that might cause vortex formation. While the bed topography in the surf zone may be simple, the flow structures is certainly not simple. The main difficulties lie in the modeling of the important seaward undertow currents.
Outside the surf zone the sea bed can be also considered practically flat with respect to sediment transport. Cross-shore processes can be modeled considering the sheet-flow formulas ([57]).
The study of the sediment transport and the mathematical formulation of the hydrodynamic processes are not yet completely solved because of the involved processes are not linear. For this reason simplifying assumption are used in order to predict the macros changes before reaching the equilibrium condition. As shown in the previous paragraph concerning the bed and suspended load

transport, the cross-shore transport can be expressed in terms of net sediment transport rate $Q(t)$. In literature several mathematical approaches are available in order to determine $Q(t)$ inside and outside the swash zone. Bagnold ([58], [59]) derived general relationships in order to express quantitatively the natural process of sediment transport along open channels, by reasoning from the general principles oh physics and from results of previous critical experiments. The author founded an energetics-based, depth-integrated volume transport equation which directly relates the total sediment load transport rates to instantaneous shear stresses derived from the local field $u(x)$. The form of equation is given by:

$$q_t = \frac{\rho_w c_f}{(\rho_s - \rho_w)g}\left(\left\{\frac{\epsilon_s(1-\epsilon_b)}{(\frac{w}{\langle|u|\rangle}) - tan\beta}\right\} + \left\{\frac{\epsilon_b}{tan\phi - tan\beta}\right\}\right)\langle u^3\rangle \tag{1.6}$$

where q_t represents the time-averaged, cross-shore volumetric total sediment load transport per unit width per unit time, ρ is the seawater intensity ($1.025 g/m^3$), ρ_s is the sediment density, β is the beach gradient,ϕ is the friction angle of the sediment, w is the fall velocity, g is the gravitational acceleration, c_f, ϵ_b and ϵ_s are respectively the friction, bed-load and suspended load efficiency factors as defined by the author. The foregoing theory was successively used by other authors who demonstrate the good applicability in order to determine the load transport in the cross-shore direction. The foregoing theory was successively validated by other authors to demonstrate its good applicability in the swash zone in order to determine the cross-shore direction at a given location and time with a varying beach slope ([60], [36]). Holland et al. ([61]) estimated the sediment transport rate q_t applying Bagnold's formula in order to evaluate the profile changes, using the sediment continuity equation:

$$\frac{h}{t} = \frac{1}{1-n_i}\frac{q_t}{x} \tag{1.7}$$

This relation allows to describe the profile changes due to the cross-shore sediment transport, neglecting the alongshore gradients and ignoring advection of sediment from the surf zone into the swash one.
Moreover qualitative correlation between the model and field data suggested the swash flow velocity as an important parameter affecting foreshore sediment transport.
Bagnold's formula resulted to be insufficient in some cases for predicting the magnitudes and in some cases the direction of observed transport. The work was useful to understand the importance of other factors affecting sediment transport prediction, as in example, the effects of water depth variations, infiltration, groundwater and the influx of sediment from offshore. Masselink and Hughes ([41]) modify Bagnold's model through the use of variable efficiency coefficients during up-rush and back-wash.

It is easy to understand that the knowledge of a model able to accurately reproduce the sediment transport across the swash zone is difficult, especially when the influence of other physical processes has to be simultaneously considered, as mentioned above. As a matter of fact first efforts in cross-shore sediment transport investigation revealed that coastal profile possesses an average characteristics form, which is referred to as the theoretical *equilibrium profile*. Considering the beach active zone (landward from the closure depth), an *equilibrium profile* theoretically can be reached under constant wave motion and water level conditions for a long enough period. The equilibrium profile can be rightly used only under undisturbed laboratory conditions which never occur in nature. In literature several models have been proposed in order to define the beach equilibrium condition. Bruun ([62]) firstly derived an equation in order to determine the equilibrium beach profile by using field data obtained in previous studies in Denmark and California. He proposed a simple law which relates the seaward off-shore distance (referred to the shoreline) x with the water depth h. The cross-shore profile has the following form:

$$h = Ax^m \tag{1.8}$$

where A is a sediment scale parameter and $m = 2/3$.
In 1977 Dean ([63]) examined the forms of equilibrium beach profiles that would result from different dominant forcing mechanisms and concluded that equilibrium beach profiles would take the form shown above if the dominant destructive force was the wave energy dissipation per unit volume ([64]). Considering monochromatic waves Dean confirmed the value of m equal to $2/3$ in Eq. 1.8 and that the sediment scale parameter could be expressed as

$$A = \left(\frac{24}{5} \frac{D_{eq}}{\rho g \sqrt{g\gamma^2}} \right)^{\frac{2}{3}} \tag{1.9}$$

where D_{eq} represents the dissipated energy for a unit volume, depending on grains shape and diameter. Successively Moore ([65]) related A directly to sand diameter and thus to beach slope.
The main problems related to the equilibrium beach profile are that the slope is infinite at the water line and the profile does not allow for bars. Alternative forms of the equilibrium beach profile have been developed by other authors ([66], [67]), but these have more free parameters and so are less suited to making predictions as calibrations tend to be site-specific ([64]).
Under the assumption of void sediment transport in the long-shore direction, in general a beach can assume mainly two kind of profiles with respect to the equilibrium condition, the winter storm profile and the summer swell profile (bar and berm profiles of respectively).During winter storm higher wind velocities generate high steep waves (short period) with high energy. Moreover storm

surges raise water level and expose higher parts of emerged beach to wave action. The eroded material is transported offshore in large quantities and deposited on the sea bottom in the form of one or more off-shore bars. Once the bar is fully formed the surf zone reaches its maximum width and littoral drifts and currents are at maximum ([68]). During the summer the milder swell waves remobilize the off-shore bar sand back on-shore. The long waves allow the sediment to be settled on the beach face forming an emerged berm. Littoral currents and drifts decrease ([68]) as the bar is removed and the profile reverts back to the swell-built curve.

A number of investigation has been made in attempt to predict what wave conditions would results in a shift between onshore and offshore sand transport transport. However a complete understanding of the critical wave conditions that govern the shift between summer and winter profiles is still incomplete. The first factor in determining the character of a beach profile and the direction of net sediment transport was the wave steepness. Johnson ([69]) associated the direction old the sediment transport with a critical incident wave steepness in deep water (H_0/L_0):

$$\frac{H_0}{L_0} > 0.025 \div 0.030 \Rightarrow \text{Erosion} \tag{1.10}$$

Successively several laboratory experiments demonstrated the importance of other physical parameters related to the beach (i.e. grain size distribution, cohesiveness, beach slope, fall velocity) on the profiles classifications.

Iwagaki and Noda ([70]) found that the shoreline movements depend not only on deep-water wave steepness, but also on the ratio of the wave height to the mean sediment diameter H_0/d_{50}. They found different critical values as a function of wave steepness and with different initial beach slopes. They demonstrated that the critical values in correspondence of which the shoreline recession takes place decreases when the wave steepness increases. Nayak ([71]) used the ratio of wave height to the product of specific gravity in water and the mean sand diameter (H_0/SD_{50}) as referring parameter in order to predict the beach processes. Dean ([72]) in the study of beach equilibrium profile introduced the fall velocity ω. By introducing this parameter the author underlined the importance of the sediment suspension duration in a wave cycle on beach changes. He stated the following relation:

$$\frac{H_0}{L_0} > 1.7\frac{\pi\omega}{gT} \Rightarrow \text{Erosion} \tag{1.11}$$

This means that if the sand fall velocity is short with respect the wave period a landward sediment movement would occur. On the contrary if the sand is characterized by a high fall velocity with respect to the wave period the beach is exposed to erosion processes.

Sunamura and Horikawa ([73]) classified beach profiles into three types based on

the displacement of topography from the initial beach slope. The classification is well summerrized by Mimura et al. ([74]). These three types are distinguished by a nondimensional parameter:

$$C = \left(\frac{H_0}{L_0}\right) tan\beta^{0.27} \left(\frac{d}{L_0}\right)^{-0.67} \tag{1.12}$$

Horikawa et al. ([75] determined the range of C parameter for each type of profile on the basis of experimental results of regular waves as follows:

$$\begin{cases} C > 10 \Rightarrow \text{Eroding condition} \\ 3 < C < 10 \Rightarrow \text{Intermediate condition} \\ C < 3 \Rightarrow \text{Accreting condition} \end{cases} \tag{1.13}$$

Short ([76]) used a model based on variations in breaker wave power generating in order to predict beach conditions:

$$\left(\frac{\rho g^2}{16\pi}\right) H^2 T > 30 Kw/m \Rightarrow \text{Erosional trend} \tag{1.14}$$

Hattori ([77]) suggested to add the beach slope to Dean number and to use the ratio $H_0/g^{0.5}Ttan\beta$ as critical value with $tan\beta$ equal to the initial bottom slope. Kriebel et al. ([78]) performed a number of full-scale laboratory investigation on beach profile evolution and re-evaluated Dean's criteria. They modified Dean's number by introducing a coefficient which take into account the small scale effects:

$$\frac{H_0}{L_0} = c_1 \frac{\pi\omega}{gT} \tag{1.15}$$

where c_1 falls in the range $4 < c_1 < 5$. The authors suggested to use low values in small scale experiments and high values for full scale tests. Successively Krauss and Larson ([79], [80]) examined only large-scale data and found that the separation between barred and normal profiles was distinguished better by several other curves, depending on the variables chosen for analysis:

$$\frac{H_0}{L_0} = 115 \left(\frac{\pi\omega}{gT}\right)^{3/2} \tag{1.16}$$

Seymour and Castle ([81]) reviewed six simple predictors for the direction of cross-shore transport which involve the nondimensional combination from among wave height and period, sediment size and fall speed and beach slope. Dalrymple ([82]) using the Larson and Krauss results rewrote the equation in terms of a single dimensionless variable and introducing a *profile parameter*:

$$P = \left(\frac{gH_0}{\omega^2}\right) D_0 \cong 10400 \tag{1.17}$$

If the profile parameter P exceeds 10400 then the beach has a barried profile. Conversely fro small values of P the beach profile is normal. This relation is

mainly defined in terms of deep-water parameter. In shallow-waters the critical vaue of the profile parameter P is equal to 22200 referring to the breaking wave H_b. Moreover Krauss ([83] demonstrate that the Dalrymple's parameter P valid for laboratory experiments can be also use in field exeriences if the deep-water height H_0 is substituted by the deep-water significant wave height H_{0s} and the period T with the peak period T_p. Under these assumptions the Eq. 1.17 can be rewrite as:

$$P_s = \left(\frac{gH_{0s}}{\omega^2}\right)\left(\frac{gH_{0s}}{\omega T}\right) = 26500 \tag{1.18}$$

The above formulations about the evaluation of the direction of the net cross-shore sediment transport can be considered as a qualitative approach. They can be approximately applied in the first phase of a coastal analysis. The main limit is the difficulty in the application of laboratory results to real waves and beach conditions. In general the grain size distribution is far to be uniform, it is difficult to evaluate the initial beach slope and the deep-water waves characteristics to be used in order to calculate the different parameters.

Chapter 2

Coastal management strategies

2.1 General overview of coastal management

Coastal areas are vulnerable systems due to the conflict between the development on the coast and coastal stability, concerning with requirements for coast protection. Moreover the coastal zones are particularly vulnerable to hydrografic basins and global climate variabilities and changes. Key concerns include sea level rise, land loss, changes in maritime storms and flooding, responses to sea level rise and implications for water resources. There are many reason why most coastal regions throughout the world suffer from these problems. All the causes having reference to decreasing of natural supply of sand. With less sand available formerly natural and stable sandy beaches disappear. Many causes of the present situation have a long history and geographically complex background. Most of these causes can not be removed within the scope of a typical coastal protection project. There is always a delicate balance between the requirements of primary protection against coastal erosion on one hand and protection of dynamic coastal landscape and sandy shores on the other hand. Historically, protective measures have been reactive in nature and have concentrated on preventing loss due to coastal erosion. This type of protection has resulted in loss of the shore or beach and it has a serious impact on the hydrodynamics.
This calls for a skilled, powerful and, that is very important, legally backed system of Coastal Zone Management. It will be argued that these aims must be well-defined. Without well-defined aims never adequate solutions to coastal engineering problems can be found.
The exploitation of the coastal zone requires a dept study of the best resources to exploit, decision-making as to choice and constant vigilance and monitor-

ing within environmental imposed constraints. The main objective is to plan coastal zones utilization so that negative consequences from interaction between the activities and the natural resources are avoided or minimized. In order to correctly plan the coastal areas it is necessary to identify and describe the natural resources, providing a basis for the evaluation of their sustainable utilization now and in the future.
Planning of coastal area development is strategic because it is attractive for many kinds of activities, such as tourism and recreation, fishing etc. and because it is environmentally valuable and morphologically dynamic. The dynamic nature is expressed in terms of coastal accretion and erosion, of morphological mobility of dune areas, tidal inlets and in term of risk of flooding.
The coastal management deals with existing and planned development in the coastal area and its relation to actual and potential erosion and flooding and to the planning of coastal protection and sea defense schemes. Coastal management regards both spatial and sector planning. One of the main aims to be pursued by the planning is to ensure that development activities in the coastal area follow existing spatial plans and sectors requirement with any contribution or increasing in erosion processes.
Generally, planning system and sector guidelines provide no guarantee for implementation of sustainable development. Land use plan and sector guidelines tend to indicate only restriction on future development projects which are often separated from the planning policy decisions, as implementation of desired development is often based on private initiatives. These are driven by demands, such as private or public economic interests, public recreational facilities or public/private protection against erosion and/or flooding.
This is the background for the development of the *Integrated Coastal Zone Management* (ICZM). It integrates demands for development and protection of the coasts and the environment according to given sector guidelines and according to spatial plans. The basis of an ICZM is the planning of the requirements from existing regional and local spatial plans in order to make room for possible new development in relation to legal and institutional framework. In order to identify the resources and the assets in the coastal area that minimize negative consequences, a deep study of the zone is needed. Firstly historically updated information about the coastal area are required. This pertains the following analysis:

- the description of the shore and coastline development based on available historic data;
- the description of existing coastal and harbor structures;
- the study of meteomarine conditions (wave climate, currents, wind, temperature and water levels;

- bathymetric, topographic, geological and morphological information;
- mapping of existing land use.

Other important steps included in the ICZM are to establish the littoral drift budget, classify the shoreline and categorize sections of shoreline for sensitivity. In particular the littoral drift budget is decisive for erosion or accretion of the natural coast and for understanding impacts from man-made structures, existing or planned. The shoreline classification is important for understanding of morphological features and for evaluating of suitable protection works.
It is then clear that a good beach management is accompanied by a continuous beach monitoring as well. The main aim is the identification of numerical models able to reproduce the physical hydrodynamic and morphodynamic processes involving coastal areas. In order to obtain useful data, techniques have to guarantee the data real-time acquisition and their accuracy. Moreover acquired data have to be compared in order to analyze their time and spatial variation. Another important element which has to be considered in the monitoring planning is the cheapness in data time analyses and management. In this way results about shoreline changes can be quickly obtained, in order to prevent potential erosion processes in time, avoiding irreversible damages on coasts and structures in coastal areas.
In the following two sections the causes of coastal zone erosion (2.2) with the relative coasts and shore intervention (2.3) are briefly discussed.

2.2 Coastal erosion

Coastal erosion is the loss of sediments in the active zone of a beach. It can be quantified in different ways but the most common are the sediment volume variations and the shoreline movements. The latter is the most visible manifestation of an occurring coast erosion process (Fig. 2.1). Cliff erosion in hard rocks is less obvious than for unconsolidated beaches but it however occurs taking the form of long-term loss of rocks, mainly due to the continuous wave action.

Coastal erosion, of beach and cliff alike, is the result of a complex interaction of natural processes, furthered by human's actions. This anthropic factor results from a general migration of activities towards coasts. A search for easily accessible materials, sand and gravel, has contributed to exploitation of marine aggregates, contributing to beach erosion. This involves off-shore as well on-shore sand removal. In general a beach equilibrium profile is characterized by the presence of one or more offshore submerged bars. These bars constitute a natural coastal defense system because of they force the wave breaking and, as a consequence, the dissipation of the greatest part of the wave energy, far from the shoreline. As mentioned above, the coastal erosion is due to a com-

Figure 2.1: Example of coastal erosion at Otranto (LE) - Italy

plex system of both natural and anthropic causes which are difficult to classify because of they often must be considered simultaneously. In the following an attempted classification is reported, through some criteria suggested by some authors ([84]). Natural causes of shore erosion include variation in sediment supply, storm waves and surge over-wash, deflation, long-shore sediment removal and transport, and sorting of beach sediment. Other factors responsible for erosion are winds, tides, climatic conditions and biological agents. Moreover the erosional trend of a beach can be overdrawn by wave steepness, beach slope and sand characteristics. As an example an increasing gradient in transport rate in the direction of net transport can be due to gradients in the wave conditions at certain stretches, a curved coastline or special bathymetric conditions. The usual response of the beach is sand loss, off-shore migration of sediments and berm width decrease.

One of the main natural cause of coastal erosion is the natural variation in the supply of sand from a river. This is generally due to droughts in large river basins resulting in a consequent decreasing of sand supplies to the shoreline, leading to the shore erosion.

Storm surge and extreme wave conditions are responsible of the offshore movement of sand. Steeper waves generally cause the seawards moving of the bars. The high storm surges cause an offshore movement of sand due to non-equilibrium in the profile during the high surge. On hurricane-prone coasts the impact of storm surges on erosional conditions are particularly important in coast protection project.

Shoreline setback can be also caused by sea-level rise and subsidence.They are long-term changes of sea and land level respectively, which are mainly responsible of long-term shoreline and beach profile changes. Considering equilibrium

profiles, the shoreline retreat can be approximately evaluated as the sea-level rise divided by the slope of the active coastal profile. Field monitoring has shown that littoral coasts consisting of fine sediment are exposed to higher setbacks than the coasts consisting of coarser sediments. Indeed, under the effect of a same sea-level rise, in a gravel beach the smaller shoreline withdraw with respect to a sandy beach is due to the higher slope of the nearshore zone. The effect of the subsidence in morphological changes of coastal zones is a downward shift of the Earth's surface. It is a local/regional phenomenon in contrast to the sea-level rise which is global, resulting in the lowering of the upper part of coastal profile. It can be caused by many different phenomena, natural as well as human. Natural causes can be the settling of soft sediments, tectonic activity and different kind of rebound processes, whereas human causes can be the extraction of groundwater, oil or gas in the coastal area. Subsidence acts in the same ways as sea level rise in relation to shore erosion apart from the fact that a sea-level rise will always be a gradual and slow process, whereas the subsidence may occur rapidly depending on its cause.
Some authors (i.e. [85], [86], [87]) observed that rip currents could promote erosion as well. They create rip embayments that are low areas on sandy beaches that expose nearby land to higher rates of erosion by wave activity. When rip currents pull sand offshore, they leave behind rip embayments, which become *erosional hot spots* where the beach is much thinner, making the sea cliffs or land beyond these embayments more vulnerable to erosion caused by larger waves. Rip currents form in places where the water that is driven ashore with the waves drains back out to sea forming a current perpendicular to the coastline.
Although there are many natural causes of coastal erosion, most of those affecting coasts are due to human intervention in the transport processes along the coastlines and reduction in the supply of sand to the shorelines.
Anthropic causes of erosion essentially include the building of structures interfering with the littoral transport (Figure 2.2). The presence of the structures has a series of effects. They interrupt transport of material with reducing sediment supply, by improving inlets, channels, dredging and implanting 'hard' coastal protection structures. They concentrate wave energy on the beach and increase the water level variations, modifying nature's coastal protection arrangements and mining the beach for its materials or for minerals they contain.
The most evident effect of a structure is the tapping of the sand on the upstream side of the structure taking sand out of the sediment budget and thus causing erosion along adjacent shorelines, especially on the lee side.

The arise or the erosion in the nearest zone to the structures depend on many factors, as in example the wave climate and the orientation of the shoreline, the extent of the structure relative to the width of the surf zone. Obviously the impact on the coastal processes and the variation of natural morphological

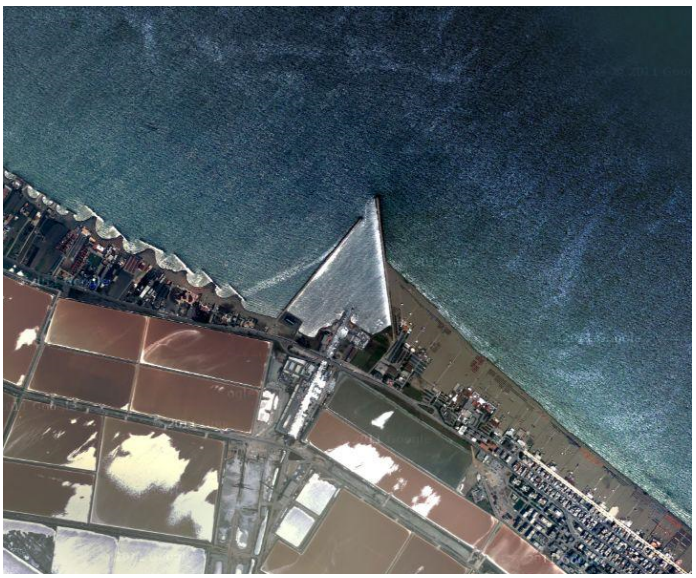

Figure 2.2: Coastal erosion at Margherita di Savoia due to structures (FG) - Italy

evolution of a coastline changes with different types of structures.
Stopping coastal erosion and halting shoreline retreat is considered almost impossible. The coastal defense works can help to hold the process, but they can not definitely stop it. Moreover the so-called hard coastal defense structures have a high environmental impact. They modify the sediment transport in the zone, causing definitive changes of the coastal dynamics. Consequently a comprehensive planning effort is required in order to secure a balanced sustainable development taking all demands and restrictions into account. In the following section the shore, coast and sea defense methods will be briefly described.

2.3 Coastal defense

Protection of the coast and the shore against the erosive forces of waves, currents and storm surge can be performed in many ways, and protection of the coast and the hinterland against flooding adds even more types to the protection defense measures. The choice of the measure in a given situation depends on the three primary conditions:

1. the problem (coast erosion, beach degradation or flooding)
2. the morphological conditions (the type of coastal profile and the type of coastline)

3. the land use (infrastructure/habitation, recreation, agriculture etc.)

Some of the measures have mainly one function, which e.g. is the case for a revetment. It protects the coast against erosion, but aggravates shore erosion. Beach nourishment, on the other hand, protects against coast erosion as well as against shore degradation. First of all it has to be stressed that with a proper system of Coastal Zone Management, some troublesome coastal protection issues can be avoided. If, for instance, it is not allowed to build too close to the brink of the mainland, a lot of (future) problems with respect to erosion due to storms and even due to structural erosion (for the time being), are avoided. With well-defined (and maintained) set-back lines, the risks of damage to, and losses of, properties are reduced. Furthermore it is not excluded that as a result of a comprehensive and honest decision making process, it is decided to renounce an intended project because of the too large adverse effects elsewhere along the coast.
In the following sub-sections the main coastal defense works are listed. Maritime literature reports different criteria for coastal defense actions classification. The works can be classified as hard/active or parallel/perpendicular with respect to the shore. In the present the coastal defense methods are divided in:

- Coast protection;
- Shore protection;
- Mixed coast/shore protection.

Coast protection

Dune stabilization
Dunes are a natural coastal feature on moderately exposed and exposed coasts. Dunes are formed by the sand, which blows inland from the beach and is deposited in the area behind the coastline.
During storm surge events, the foot of the dunes can be eroded but the dunes act as a very flexible buffer zone, which protects the hinterland from erosion and flooding. The eroded material supplies material to the littoral budget minimizing the general erosion along the entire section of shoreline. During the storm and also during more normal events, sand will be transported inland, sometimes in connection with the formation of wind alleys in the dune row. After the storm, the damaged dune will gradually be built up again, maybe slightly more inland. This means that a dune acts as a natural flexible coast protection and sea defense measures. It moves backwards parallel with the eroding coastline and at the same time it maintains its form and volume as well as a wide beach. This is a natural quasi-equilibrium situation. The erosion of dunes as a result of a severe storm surge is also referred to as dune erosion.

However, the natural balance will shift if the dune vegetation is damaged by grazing or if beach-users, etc. generate too much traffic, etc. This may cause the dunes to degrade resulting in loss of the protection provided by the natural dunes. At the same time the sand blowing inland causes various kinds of damage. Consequently, authorities normally tend to protect dunes by regulating their use.
In some cases authorities have been very eager to protect the dunes by planting marram grass and placing fascines in the wind alleys to trap the sand (Figure 2.3). (Fascines are the placing of pine or spruce branches). This has, in some cases, resulted in a complete fixing of the dune position and an unnatural growth in height. Consequently, the flexibility of the natural dune is lost resulting in a gradual disappearance of the dune due to erosion, whereby the protection, provided by the natural dune system, is lost. However, as mentioned above, the

Figure 2.3: Example of dune stabilization by planting grass

protection should not be so comprehensive that it completely fixes the dunes. Newly planted vegetation in particular can be strengthened by using fertilizer. Restrictions for their use can also protect the dunes. Grazing in dune areas is prohibited in most countries, and authorities often limit public access. Such restrictions may regulate the traffic in the dunes, e.g. by prohibiting motor traffic. Different options are paved walking passages in areas near parking lots and fencing fragile newly planted areas.
Dune stabilization is a sustainable protection measure, enhancing the natural protection ability of dune areas. It protects against wave and storm surge attack and at the same time it preserves the natural coastal landscape, if performed moderately. Dune stabilization requires a planned and co-ordinated effort. It is applicable on all coastal types where natural dunes occur. This is especially the case on moderately exposed to exposed coasts with perpendicular to very

oblique wave (wind) attacks. Artificial dunes can be also used as a sea defense structure.

Cliff stabilization
Coastal cliffs can be unstable due to the combined effect of several factors, such as:

- Erosion of the foot of the cliff caused by wave action and storm surge
- Sliding or weathering of the slope due to geo-technical overload. The erosion of the foot of the cliff normally initiates geotechnical instability, but the sliding/collapse can be of different nature depending on the geo-technical conditions of the slope.

There are basically three different situations:

1. if the material is non-cohesive material, the weathering of the cliff ill normally occur simultaneously with the erosion of the foot as a talus formation, which is the collection of fallen material forming a slope at the foot of the cliff.
2. if the material is a mixture of clay, silt, sand and boulders, such as in the case of moraine till, the slope can be very steep for a period due to the cohesive forces, but the slope will eventually collapse. Smaller or bigger fractions of the cliff will fall in connection with groundwater pressure, frost impact or general weathering, or by sliding. Sliding will especially occur in connection with groundwater pressure.
3. if the material consists of plastic clay or silty clay, the collapse of the cliff will be in the form of slides, which can go far behind the top of the cliff.

If the cliff material is sand the weathering by wind is the most pronounced phenomenon. However, also exposed cliffs consisting of other types of material can be eroded by sand blown over the cliff from the beach.
The basic cause of cliff instability is normally the marine erosion of the foot of the cliff, mitigation of this is covered under the protection method of revetment (Fig. 2.4). Installing the revetment will exclude further erosion of the foot, but at that stage the slope of the cliff may very well be so steep that weathering and sliding may still occur. This can be counteracted by the following means:

- artificial smoothing of the slope, if there is enough space at the foot as well as at top of the cliff for this. This will counteract future uncontrolled weathering and sliding.
- smoothing of the slope by filling with granular material at the foot of the cliff. This requires that there is sufficient space at the foot of the cliff for the filling.

Figure 2.4: Example of cliff stabilization by using gabion revetments

- establish a vegetation cover on the cliff. This can best be done by following the above-mentioned smoothing of the slope. Good vegetation protects against weathering and groundwater seepage, and thereby to some extent against sliding
- drainage of groundwater. This can be used if the cliff suffers from sliding due to high groundwater pressure and poor drainage conditions. Horizontal and vertical drains can be used as well as the regulation of the surface runoff.

Cliff slopes are often protected by dumping assorted rubbish, such as branches etc., over the cliff. It is a bad 'solution' because it does not stop the risk of sliding. On the contrary, it spoils the vegetation and thereby increases the risk of sliding.
Cliff stabilization presupposes that the foot of the cliff has been stabilized. Stabilization counteracts the natural behavior of cliffs to slide and weather. Such an active cliff is part of the dynamic coastal landscape and should therefore in principle be maintained as an integrated part of this landscape. Cliff stabilization can be applied at all moderately exposed to exposed coasts; however, in order to preserve the dynamic coastal landscape cliff stabilization should only be used sparingly. Preserving the active cliff at densely populated coasts is normally not feasible due to the limited space. Consequently, cliff stabilization is normally only used when there is sufficient space in the backland to allow some smoothing.

Seawall
A seawall can be defined as a structure separating land and water areas. It is designed to prevent coastal erosion and other damage due to wave action and

storm surge, such as flooding. Seawalls are normally very massive structures because they are designed to resist the full force of waves and storm surge (Fig. 2.5).
A seawall is constructed at the coastline, at the foot of possible cliffs or dunes. A seawall is typically a sloping concrete structure; it can be smooth, stepped-faced or curved-faced. A seawall can also be built as a rubble-mound structure, as a block seawall, steel or wooden structure. The common characteristic is that

Figure 2.5: Stepped seawall at Wheelers Bay Isle of Wight - England

the structure is designed to withstand severe wave action and storm surge. A rubble-mound revetment often protects the foot of such non-flexible seawalls. A rubble-mound seawall bears a great similarity to a rubble-mound revetment; however a revetment is often used as a supplement to a seawall or as a stand-alone structure at less exposed locations. An exposed dike, which has been strengthened to resist wave action, is sometimes referred to as a seawall.
The nearly vertical seawall, which was mainly used in the past, had the unfortunate function of reflecting some of the wave energy, whereby the erosion was aggravated, resulting in accelerated disappearance of the beach. However, all kinds of seawalls involve beach degradation as they are used at locations where the coast is exposed to erosion. The seawall will fix the location of the coastline, but it will not arrest the ongoing erosion in the coastal profile. On the contrary, it will to a varying degree, accelerate the erosion. It is quite normal that the beach disappears in front of a seawall, and it will most often be necessary, after some years, to strengthen the foot of the seawall with a rubble revetment. A seawall will decrease the release of sediments from the section it protects and will have a negative impact on the sediment budget along adjacent shorelines.
A seawall is a passive structure, which protects the coast against erosion and flooding. Seawalls are often used at locations off exposed city fronts, where

good protection was needed and where space was scarce. Promenades have often been constructed on top of these seawalls. They are also used along other less inhabited coasts, where combined coast protection and sea defense is urgently needed. Seawalls are primarily used at exposed coasts, but they are also used at moderately exposed coasts.

Shore protection

Nourishment

Nourishment can be regarded as a very natural way of combating coastal erosion and shore erosion as it artificially replaces a deficit in the sediment budget over a certain stretch with a corresponding volume of sand (Figs. 2.6(a) and 2.6(b)). However, as the cause of the erosion is not eliminated, erosion will continue in the nourished sand. It is thus inherent in the nourishment concept that the nourished sand is gradually sacrificed. This means that nourishment as a stand-alone method normally requires a long-term maintenance effort. In

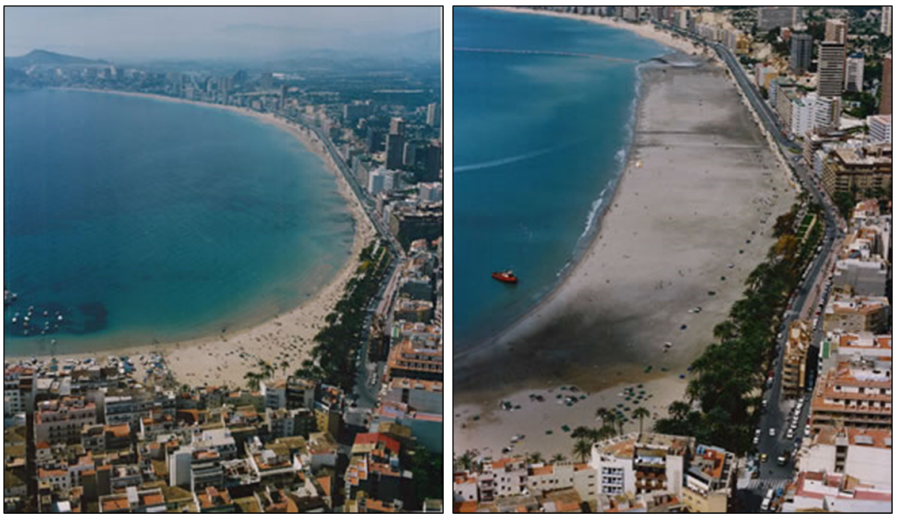

(a) Eroded beach before the intervention (b) After the nourishment

Figure 2.6: Beach nourishment - North Italy

general, nourishment is only suited for major sections of shoreline; otherwise the loss of sand to neighboring sections will be too large. Regular nourishment requires a permanent well-functioning organization, which makes nourishment as a stand-alone solution unsuitable for privately owned coastlines. The success of a nourishment scheme depends very much on the grain size of the nourished sand, the so-called borrow material, relative to the grain size of the native sand. As described in Onshore and Offshore Transport and Equilibrium Coastal Profile, the characteristics of the sand determine the overall shape of the coastal

profile expressed in the equilibrium profile concept. Furthermore, in nature the hydrodynamic processes tend to sort the sediments in the profile so that the grain size decreases with increasing water depth.
When borrow sand is placed in a coastal profile, neither the profile nor the grain size distribution will match the equilibrium conditions. Nature will attempt to re-establish a new equilibrium profile so changes will always occur in the nourished profile. There will also be changes caused by the continued long-term erosion trend and the profile response to individual events. This means that in practice it is neither possible to perform a short-term nor a long-term stable nourishment at an eroding coast. It is inherently unstable on eroding shorelines. These are the basic realities, which the public, the politicians and those who fund the projects, find it hard to accept. On the other hand, as environmental concerns and requirements for sustainability are gaining in importance, nourishment has gradually increased its share of shoreline management schemes over the last decades.
As mentioned above, the performance of a nourishment scheme very much depends on the grain size of the borrow material relative to the grain size of the native material. If the borrow sand is finer than the native sand, it will tend to form a flatter profile than the natural one. The equilibrium reshaping of the nourished sand will reach out to the closure depth. If the objective of the nourishment is to obtain a wider beach, this will require very large volumes of sand, as illustrated in the upper part of Figure 2.7. It is evident that the volume of sand needed to obtain a certain beach width increases drastically with the decreasing grain size of the nourished sand. Most coastal authorities realize this and some of them have introduced special bonuses for their nourishment contractors when they provide coarse sand. It is evident from this figure that if borrow sand with a larger grain size than that of the native sand is nourished into a coastal profile, it will tend to form a steeper profile than the natural profile. This means that a wider beach will tend to be formed, see the lower part Figure 2.7. Furthermore, coarser sand will be more stable in terms of long-shore loss. This nourishment efficiency of the nourished sand has been studied by the Danish Coastal Authority on basis of many years of nourishment along the Danish North Sea Coast[1]. The nourishment efficiency is defined as the ratio between the erosion rate for the natural sand (theoretical) and that of the nourished sand. The nourishment efficiency has been analyzed as function of the ratio between the mean grain size of the borrow sand and that of the native sand:

$$GSRNourishment = \frac{d_{50}^{B}}{d_{50}^{N}} \tag{2.1}$$

where B indicates Borrow sand and N the Native one. The analysis covers effects of cross shore as well as long-shore effects. The results are expressed as a relation between the nourishment efficiency versus the grain size ratio GSRNourishment.

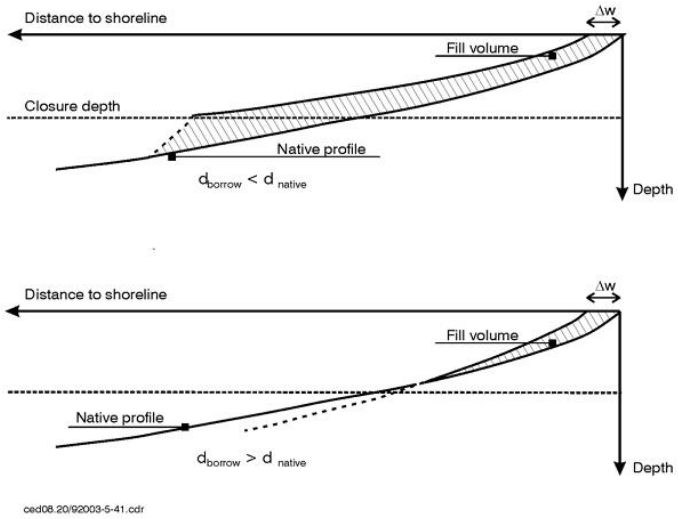

Figure 2.7: Equilibrium conditions for nourished beaches required to obtain an additional beach width Δw with borrow sand, which is finer and coarser than the native sand (upper and lower, respectively)

It is evident from the relation shown in Figure 2.8 that the nourishment efficiency increases considerably with increasing Grain Size Ratio for Nourishment.

Areas, which for a long time have been protected by hard coastal protection

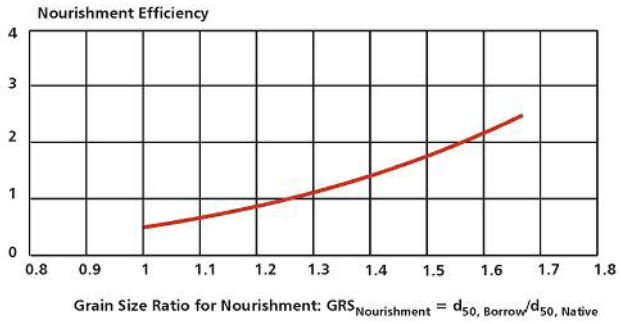

Figure 2.8: Relation between Nourishment Efficiency and the Grain Size Ratio for Nourishment

structures, have often developed steepened coastal profiles. Such areas are very far from their cross-shore equilibrium form. If nourishment is introduced in such areas it will require huge volumes of sand to restore the profile to the equilibrium profile, which is required to release the pressure on the coastal structures. In such cases, it is very important to find borrow sand, which is coarser than the native sand.

Nourishment can be divided into three types (Fig. 2.9):

1. back-shore nourishment
2. beach nourishment
3. shore-face nourishment

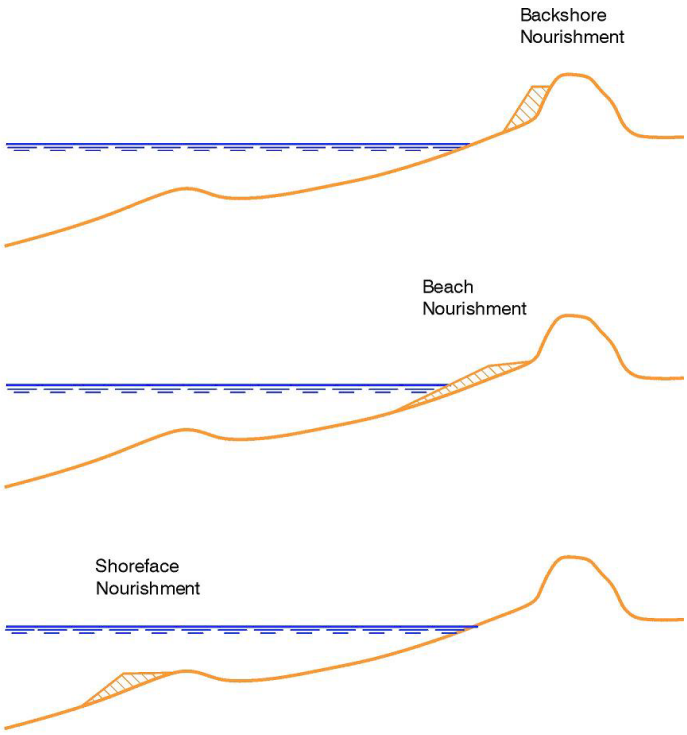

Figure 2.9: Principles in backshore nourishment, beach nourishment and shoreface nourishment

The three different nourishment methods will be discussed briefly in the following.
Back-shore nourishment is the strengthening of the upper part of the beach by placing nourishment on the back-shore or at the foot of the dunes. The main objective of back-shore nourishment is to strengthen the backshore/dune against erosion and breaching during extreme events. The material is stockpiled in front of the dunes and acts as a buffer, which is sacrificed during extreme events. This kind of nourishment works more by volume than by trying to restore the natural wide beach. The loss is normally large during extreme events, whereby steep scarps are formed. Backshore nourishment can be characterized as a kind of emergency measure against dune setback/breach; it cannot, therefore, be characterized as a sustainable way of performing nourishment and it

does not normally look very natural. Backshore nourishment can be performed by hydraulic pumping sand through pipes discharging at the foot of the dunes and later adjusted using a bulldozer. The sand source can be either an offshore supply via a cross-profile pipeline, floating or buried, or it can be supplied along the shore from, for example, a sand bypassing plant. The sand can also be supplied via land transport by dumpers.

Beach nourishment is the supply of sand to the shore to increase the recreational value and/or to secure the beach against shore erosion by feeding sand on the beach. It is not a coastal protection measure, as the beach will normally be flooded during extreme events, but it will support possible coastal protection measures. When performing beach nourishment, the borrow sand must be similar to the native sand to adjust smoothly to the natural profile. It may be an advantage to use slightly coarser sand than the natural beach sand, as this will enhance the stability of the resulting slightly steeper profile. Finer sand will very quickly be transferred to deeper water and will thus not contribute directly to a wider beach. However, the fine sand will help building up the outer part of the profile. See also experiences with beach nourishments in Portugal.

Shoreface nourishment is the supply of sand to the outer part of the coastal profile, typically on the seaside of the bar. It will strengthen the coastal profile and add sediment to the littoral budget in general. This type of nourishment is used in areas where coastal protection measures have steepened the coastal profile or in areas with a long-term sediment deficit. Shoreface nourishment is sometimes used with beach nourishment in order to strengthen the entire coastal profile. It is recommended for obtaining a nourished profile close to the equilibrium profile. Stand-alone shoreface nourishment acts only indirectly as a shore protection measure through slightly decreased wave exposure and as a shore restoration measure with considerable delay and little efficiency. Shoreface nourishment is often performed using split barges. The unloading is fast and the unit price therefore low. Shoreface nourishment can profitably be used in connection with large beach nourishment schemes, in which borrow material, which does not fulfill the requirements for beach nourishment, can be used in the outer part of the profile where it naturally belongs.

Beach Scraping

Beach scraping is recovering material from the berm at the foreshore and placing it on the back-shore at the foot of the dunes or the cliff. A beach berm consisting of coarse sand or gravel is sometimes formed during relatively mild summer wave conditions, which tend to transport seabed material towards the beach. Beach scraping is normally performed using front loaders. The purpose of beach scraping is to strengthen the upper part of the beach profile and the foot of the cliff. The material is placed in a position that reduces the erosion occurring during storm surge conditions.

This method can be used for beaches, which are mainly exposed to seasonal erosion, whereas it is probably not feasible for locations, which are exposed to long-term erosion. One disadvantage of the method is that the material used for strengthening the upper part of the beach profile is taken from the lower part of the same profile, which means that the method only contributes insignificantly to the overall stability of the beach profile. Another issue is that equipment operated during late summer may disturb recreational activities.

Mixed coast/shore protection

Mixed coastal protection and shore protection measures are schemes, which combine structures and initial nourishment, which is called beach fill. These schemes are an attempt to find a solution, which combines the ability of the structures to directly protect a section of the coast with the ability of the structures to support and maintain beach filling/nourishment. The result is protection of the beach and protection of the coast behind the beach. The advantage of this combination is that it minimizes the requirements for regular recharging of the fill, or nourishment. The relevant structures in connection with this have characteristics, which make use of the littoral processes, either the longshore littoral drift and/or the cross-shore transport. The relevant structures are listed below with links to a detailed article.

Groynes
A groyne is an active structure extending from shore into sea, most often perpendicularly or slightly obliquely to the shoreline (Figure 2.10). It works by blocking the littoral drift, whereby they trap or maintain sand on their upstream side. Groynes can have special shapes; they can be emerged, sloping or submerged, and they can be single or in groups, the so-called groyne fields.

Adequate supply of sediment and existence of satisfactorily intensive long-

Figure 2.10: Groyens at Cavallino (VE) - Italy

shore sediment transport are the sine-qua-non conditions of groynes efficiency. Catching and trapping of a part of sediment moving in a surf zone (mainly in a long-shore direction), as well as reduction of the sediment amount transported seawards, are the principle functions of the groyne. As revealed by experiments, during weak and moderate wave conditions, the groynes partly dissipate energy of water motion and lead to sand accumulation in the vicinity of a shore, thus causing its accretion. Under storm waves, mainly approaching the shore perpendicularly, the role of the groynes decreases and a beach is partly washed out. Groynes are frequently used. However, applied as a self-contained shore protection measure it is a very dubious solution. This is because of unfavorable side effects which they can cause locally. Satisfactory supply of sand and existence of longshore sediment transport are fundamental conditions for efficiency of groynes. The groins role distinctly increases if they are applied together with other (soft) shore protection measures, like artificial beach nourishment or shore nourishment.

Intensity and character of groynes influence on shore behavior depend on sea water level, parameters of waves, currents and sediment supply in the surf zone, as well as a shape and inclination of the cross-shore profile.

Protection of the shore by use of one groyne only is most often inefficient. A single groyne, long or short, on a shoreline exposed to a slightly oblique wave climate causes downstream erosion. In order to extend the length of the protected area, and to compensate for the lee side erosion, it has been normal practice to construct several groynes along the shoreline, a so-called groyne field comprising from a few to tens of individual structures. A scheme of a system of interacting groynes is given in Figure 2.11. A single groyne, besides its positive influence

Figure 2.11: Groyens at South of England

on the shore, causes numerous side effects, mainly in the form of coastal erosion on the lee side of the structure. In the case of a group of groynes, the above effect appears on the lee side of the whole system. The erosion is also observed in direct vicinity of the structures, particularly when waves approaching the shore perpendicularly predominate. Between the groynes, huge mass of water is accumulated which in turn leads to appearance of compensating flows along the structures, causing local erosion of the seabed. With respect to the surf zone width, during severe storms the groynes are 'short' structures, with frequently occurring erosion around them, while under weak wave conditions they become 'long', thus helping in sand accumulation and widening of the beach. Loss of contact between a groyne and the shore in an unfavorable effect. In such a case, long-shore flows are generated between the shoreline and the groyne root. These flows are the reason for washing out of the beach.

Appropriate choice of shapes, dimensions and location of groynes is crucial for effectiveness of shore protection. Groynes length is usually related to mean width of the surf zone and on the other hand to their longshore spacing. An active length of the groyne basically increases together with the growth of wave-to-shoreline angle. While designing groynes, one should remember that they should not trap the whole long-shore sediment flux. Numerous investigations and observations suggest that within optimal solutions the groynes spread seawards not further than to $40 \div 50\%$ of the storm surf zone width. Effectiveness of the groynes depends also on their permeability. The groynes which are either structurally permeable or submerged (permanently or during high water levels) allow more sediment to pass alongshore through them, in comparison to impermeable or high groynes.

Most often used, pile groynes are usually permeable structures which does not affect their efficiency. The groynes height influences the amount of longshore sediment transport trapped by the groynes. The same groyne can act either as emerged or submerged structure, depending on water level which is subject to changes due to astronomical tides (if they exist), as well as storm surges. Generally, the groynes are designed to stick out about h_s=0.5-1.0 m above the beach and the mean sea level (MSL). Too high groynes cause wave reflection, resulting in local scours. Considering the shape in plan view, the groynes can be straight, bent or curved, as well as L-shaped, T-shaped or Y-shaped.

In structural terms, one can distinguish between wooden groynes, sheet-pile groynes, concrete groynes and rubble-mound groynes made of concrete blocks or stones, as well as sand-filled bag groynes.

The wooden groynes are most often one- or two-row palisade structures. Effects of influence of the T-shape wooden pile groyne on the shore (local erosion on the lee side and accumulation on the other) are illustrated in Figure 3. One-row wooden groynes are most often partly permeable structures. This results

in reduced erosive lee-side effects and prevents from appearance of semi-closed nearshore water circulations. The wooden palisade groynes are cheap but on the other hand they have low durability.
Steel groynes are most often constructed of vertical sheet piling, single or double, of various profiles, located perpendicularly to the shoreline. They are impermeable structures. The experiments have shown that the groynes made of single sheet pile walls are not durable. This is due to corrosion of the material and influence (friction) of the moving sand. Besides, ice load is very harmful, causing instability and failure of the steel sheet pilings. Mixed massive structures, constituted of steel and concrete, are much more stable and durable.
Groynes built of concrete elements in the form of prefabricated boxes or other reinforced concrete items belong to the most stable and long-lasting coastal structures. Because of considerable unit weight, the elements composing a groyne of this kind require the existence of suitable soil conditions and the appropriate foundation.
Rubble-mound groynes belong to frequently applied coastal protective structures. They are built as either loose mounds of stones or mounds of various armour units, e.g. tetrapods. These groynes are often mixed structures, strengthened inside by the sheet piling. They are relatively massive, durable and impermeable. The rubble-mound groynes are advantageous with respect to the steel, concrete and wooden ones, as they better dissipate energy of waves and currents.
The sand-filled bag groynes as a protection measure should rather be considered as a short-term solution. The bags in a stacked bag groynes can either be sand- or ground-filled. Some additional protection measures are necessary, especially at the groyne head. A special filter cloth should be used under the bags to reduce settlement in soft bottom. Construction of this type of groynes requires larger bags (heavier than 50 kg), even though they are more difficult to handle and require filling on the spot.

Detached breakwaters
Detached breakwaters are straight shore-parallel structures, which partly provide shelter in their lee thus protecting the coast and decreasing the littoral transport between the structure and the shoreline (Figure 2.12). This decrease of transport results in trapping of sand in the lee zone and some distance upstream. Breakwaters can also deviate from the straight and shore-parallel layout, they can be emerged and submerged, and they can be single or in groups, the so-called segmented breakwaters. Detached breakwaters are used as shore and coast protection measures. In general terms, a detached breakwater is a coast-parallel structure located inside or close to the surf-zone.
A detached breakwater can be characterised by several parameters as shown in Figure 2.13. The most important parameters are:

Figure 2.12: Breakwater at Plymouth - England

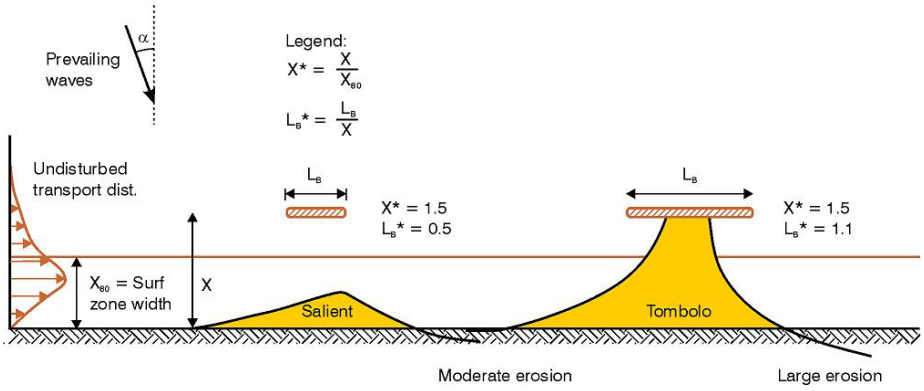

Figure 2.13: Definition of parameters characterizing detached breakwaters and accumulation forms

- LB Length of the breakwater
- x Breakwater distance to shoreline
- x80 Surf-zone width, approximately 80% of the littoral transport takes place landwards of this line
- LB* = LB/x Breakwater length relative to breakwater distance to shore-

line (dimensionless length)

- x* = x/x80 Breakwater distance relative to surf-zone width (dimensionless distance)

The breakwaters installation causes several sediments accumulation forms. When the dimensionless breakwater length $LB*$ is less than approximatively $0.6 \div 0.7$, a bell-shaped salient in the shoreline will form in the lee of the breakwater. However, parameters other than the breakwater length and distance also influence the accumulation pattern. When the dimensionless breakwater length $LB*$ is greater than approx. $0.9 \div 1.0$, the sand accumulation behind the breakwater will connect the beach to the breakwater in a tombolo formation. But again, parameters other than the breakwater length and distance influence the accumulation pattern.
If there are several breakwaters in a series, this is referred to as a segmented breakwater, where the length of the gap between the breakwaters in a segmented breakwater is denoted as LG Length of gap between breakwaters.
A detached breakwater provides shelter from the waves, whereby the littoral transport behind the breakwater is decreased and the transport pattern adjacent to the breakwater is modified. These characteristics of a breakwater are utilized in different ways for various types of breakwaters by varying relevant parameters. There are three different types of breakwaters, as can be seen in Figure 2.14.

- Offshore breakwaters
- Coastal breakwaters
- Beach breakwaters

Offshore breakwaters are located far outside the surf-zone, x* ¿ 3. The purpose of an offshore breakwater is normally to protect an offshore ship wharf against wave action, which means that an offshore breakwater is a special type of port. The offshore breakwater is used when the coastal profile is very flat. At such locations, a traditional port would have to extend far from the shoreline or extensive dredging works would have to be carried out to provide access to the port. In order to minimize the works and to avoid the associated impact, an offshore breakwater may be the answer. The offshore breakwater is normally located at a slightly greater water depth than is required for navigation, thus avoiding/minimizing capital dredging and minimizing sedimentation. Firstly it is necessary to provide shelter for a wharf; secondly, to minimize sedimentation and the impact on the coastline. The philosophy behind an offshore breakwater, in relation to its influence on transport conditions, is thus to place it as far away from the surf-zone as possible and make it as short as possible so that

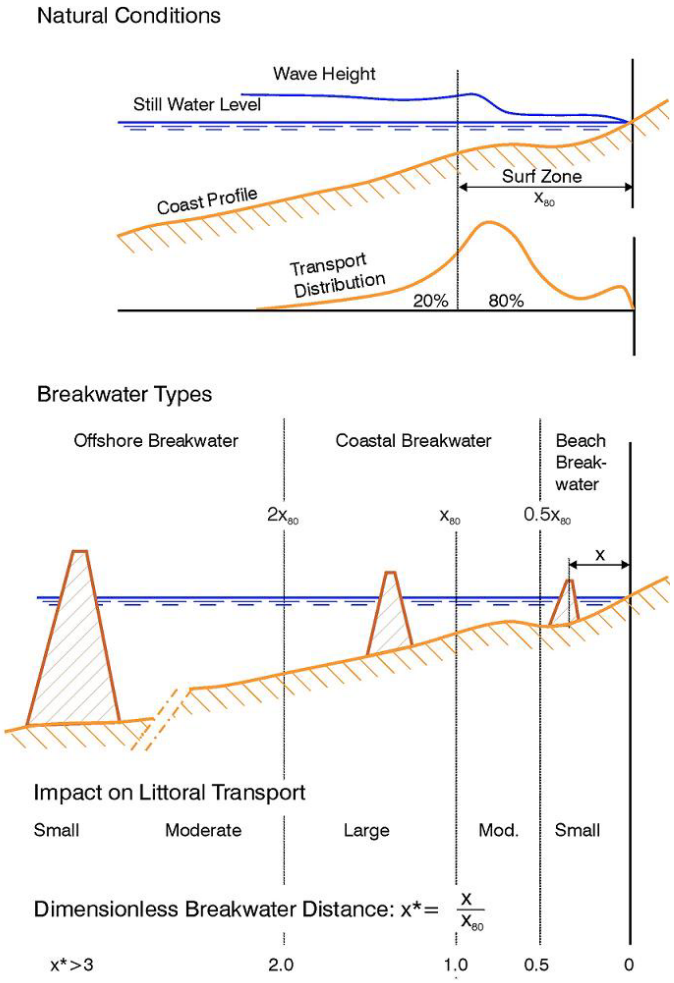

Figure 2.14: Types of detached breakwaters

its impact on the coastal morphology is negligible. However, experience shows that this is very difficult to obtain in practice; offshore-detached breakwaters often cause accumulation in their lee zone resulting in erosion effects in adjacent areas. It is thus important that the coastal impact of offshore breakwaters is taken into account when carrying out an environmental impact assessment for a port. Offshore breakwaters will not be treated further in these Guidelines as offshore breakwaters are not used as shoreline management structures.

The following two types of breakwaters are mainly used for shoreline management, where the inherent capability of a breakwater to manipulate the littoral transport is utilized.

Coastal breakwaters are located within a distance from the shoreline of half the width of the surf-zone, up to twice the width of the surf-zone, $2 > x* > 0.5$.

Such breakwaters trap sand within the part of the littoral zone they cover, thus securing that part of the coastal profile against erosion.
Beach breakwaters are located within less than half the width of the surf-zone from the shoreline, $x* > 0.5$. Beach breakwaters trap sand on the foreshore without interfering significantly with the overall transport pattern.
The philosophy behind coastal and beach breakwaters is as follows: to partly provide wave shelter for a certain part of the shore and the coast; to modify the littoral transport in predictable way, so that the combined shore-restoration and coastal protection function can be properly designed. The extent of the sand trapping, or the ability to establish the desired sand accumulation pattern, is mainly regulated by choosing the length of the breakwater, the distance of the breakwater to the shore and the number of single breakwaters in a segmented breakwater and, finally, the length of the gaps.
The advantage of a breakwater in comparison to a groyne is that it is possible to modify the littoral transport in a smoother manner than for a groyne. In this way there will be less lee side erosion on the downstream shoreline. This applies especially to breakwaters, which are so short that a permanent tombolo does not develop.
Sometimes coastal breakwaters are planned so as to provide shelter for the beach landing of small fishing boats or sheltered water for swimming. This is difficult as sufficient shelter for the boats and the swimmers requires such a long breakwater that a tombolo develops. When the tombolo has developed there is no sheltered water area left for boat landing and swimming, only a semi-protected bay downstream of the tombolo is left. This bay may be suitable for landing small boats, but it is certainly not suitable for swimming during rough wave conditions due to the eddy, which will always be present during such conditions.
Sand will be trapped behind a breakwater if initial sand fill is not performed. The trapped sand comes from the adjacent beaches, which means that both the upstream and downstream beach will suffer from erosion during the development of a salient or a tombolo. When a tombolo has been formed, the adjacent beaches are influenced in a way similar to that of a groyne with upstream accretion and lee side erosion. The influence of a salient will be smoother.
The hydrodynamic impact of a detached breakwater on the adjacent area has not to be undervalued. The breakwater shelters partly from the waves; however, as the waves diffract into the sheltered area, a complete shelter cannot be obtained. The longer the breakwater, the better the shelter. Submerged and floating breakwaters provide less shelter. Wave-overtopping of submerged or low breakwaters will cause an additional supply of water in the area behind the breakwater, and consequently some compensation currents running out the sheltered area. The wave set-up on the foreshore is less in the sheltered area

than outside, which generates local currents towards the sheltered area along the foreshore from both sides of the breakwater so that two eddies develop. These eddies also develop in the case of oblique wave approach. The long-shore current is partially blocked by the circulation currents; this causes some of the long-shore currents to be diverted outside the breakwater.
The morphological effects of a detached breakwater are various and regard different aspects.The littoral transport in lee of the breakwater decreases due to the attenuated wave and long-shore currents in the area sheltered by the breakwater. This causes the trapping of sand behind the breakwater depending on the conditions. As a rule-of- thumb, the trapping of sand will develop into a tombolo formation connecting the breakwater and the shore by sand deposits, if the length of the breakwater is equal to or longer than 0.8 times the distance between the shore and the breakwater. For shorter breakwaters, only a salient in the shoreline will develop. The diversion of the long-shore currents will cause the development of local erosion close to the heads of the breakwater. The trapping of sand, especially if a tombolo has developed, will cause lee side erosion downstream of the breakwater. This downstream erosion is very similar to what is developed for groynes. However, there are more parameters involved in breakwaters, so it is possible to manipulate the transport in a more refined manner. A breakwater traps sand under all circumstances, even if the net transport is zero. This means also that there will be a coastal impact in any case.
When several breakwaters are constructed in a row, the system is referred to as a segmented breakwater. A segmented breakwater is used to protect long sections of shoreline; the downstream coastal impact will be correspondingly larger than for a single breakwater. Generally if segmented breakwaters are constructed with too small gaps, the water exchange in the embayments between the breakwaters may be poor.
A coastal breakwaters has also an influence on the flow pattern of the long-shore current. A long breakwater causes major changes in the flow pattern. There are increasing current speeds towards the lee zone, high current speeds close to the breakwater heads and circulation in the downstream end of the lee zone. This current pattern and the corresponding sediment transport pattern cause the formation of a tombolo. There will also be local scour close to the breakwater heads. The eddy in the lee zone will remain, even after the tombolo has formed, and the current around the upstream head of the breakwater will increase with a higher offshore component. The current eddy and the scour holes will be dangerous for swimmers, and the jet directed offshore will cause a loss of sand and decreased bypass, resulting in relatively large lee side erosion. The local lee bay will tend to collect seaweed and debris. Furthermore, the tombolo provides easy access to the breakwater, which is not practical, as walking on the structure and jumping from it can be dangerous. If the breakwater is fairly short, the flow

pattern will be quite different, as seen in the above figure. There will be no high currents at the breakwater heads; there will be only a minor tendency for eddy formation and there will be only slight changes in the general pattern of the long-shore current. The morphological response to such a breakwater will be a smooth salient in the shoreline; a tombolo will not form and there will be no scour holes at the end of the breakwater heads. There will be no offshore loss of material, and the lee side erosion will be mild. These are all positive effects; the negative effect is that the protection, provided by a short breakwater, is limited. It will secure a wider beach locally, but it will not be able to stabilize a long section of shoreline by a stable sand filet. If the sand filet consists of nourished sand, frequent re-nourishment will be necessary. The optimal solution is probably somewhere between a long and a short breakwater. It must form a solid salient, but not a tombolo. This solution is balanced between the requirements for coast and shore protection, the minimization of downstream impacts and seaweed trapping, and the optimization of safety.

The above discussion was related to single breakwaters, but shoreline management schemes often utilize segmented breakwaters. A segmented breakwater scheme provides many possibilities, ranging from total coastal protection to mild shore protection. Fig. 9. below shows the characteristic shoreline development, which can be obtained with segmented breakwaters with various combinations of breakwater lengths and gap widths.

A mixture of seawalls, revetments, groynes and breakwaters has, in the past, often been used in densely populated areas as coastal protection against long-term erosion. In some places the protection was co-ordinated, but most often it was everybody's individual fight against the sea. Such areas are characterized by lost beaches, poor passage along the coastline and poor aesthetic appearance. The natural beauty of the coastal landscape is lost due to coastal protection measures and erosion continues. Such areas require an urgent upgrade to secure the values behind the coastline, as required by the landowners, and to re-establish the shore to the highest possible level, as required by the public and the authorities. This calls for a well co-ordinated shoreline management scheme. With modern techniques and sufficient funds, it will be possible to upgrade the spoiled coastline to a nearly natural condition. However, it is almost impossible to re-establish the active coastal cliff, which is also a valuable coastal resource. The only way to achieve this is to allow the natural coastal erosion to continue. However, this requires that the authorities purchase the coastal land and allow it to develop naturally. In most cases this is unrealistic, but one solution may be to leave public-owned sections without protection, provided they are of a suitable length.

In such heavily populated and mostly privately owned areas, it will normally not be practical to choose a solution using nourishment alone, as it will not provide

sufficient safety against coastal erosion, and as it is also difficult to manage. In this case a segmented breakwater scheme is a good choice, and it can be tailored to suit the requirements agreed upon by the interested parties. A pure nourishment solution requires substantial public involvement. It is evident that nearly all combinations of requirements can be met. The most difficult aspect of such projects is often the public and political process, which has to be carried through to reach consensus. The importance of this process must not be underestimated in the planning process.

Headlands
Headlands are smooth structures built from the coastline over the beach and some distance out on the shore-face. They work by blocking (part of) the littoral transport. A headland combines the effects of groynes and detached breakwaters and at the same time, minimizes some of the disadvantages of groynes and breakwaters.

All the above interventions should be considered successful as beach restoration only in connection with a good and continuous beach monitoring and planning. In order to obtain a successful shoreline restoration project, all the parties involved must have knowledge of coastal morphological processes. It is necessary to understand the causes of the present situation and to analyze the better solution. The coastal area has to be considered as a dynamic natural landscape. The preserving natural coastal resource would be the main aim of the society. When interventions are strictly required, designs would be aimed to minimize the use of coastal protection schemes and preserve the quality of coastal landscapes, also reducing pollution and enhance sustainable use of waters.

Chapter 3

The Beach Drainage System

3.1 The Beach Drainage system (BDS)

The Beach Drainage System is constituted by one or more drains placed under the beach face running parallel to the shoreline. Drains consist of PVC pipes with holes uniformly distributed on their contour in order to drain the water. Drains were connected through blind pipes with a collection point from where the water is pumped out and then transported back to the sea or to another destination. The figure 3.1 represents a sketch of the main parts of a drainage system.

The system was discovered in Hirtshals, on the north-eastern coast of Denmark (1981). The Danish North Sea Research Center required a lot of filtered sea water for filling aquarium. The Danish Geotechnical Institute installed a series of vertical wells, near the shoreline. The system would guarantee a good water quality, using the sand layers as filters. Actually, after not many weeks, the drained flow highly decreased, being insufficient for the purpose. At the beginning the Institute thought at a possible blockage of the protection layer around the wells by the sand. Finally they observed an on-shore movement of the shoreline of about $20 \div 30$ m in the zone where the wells were placed. Moreover during winter storms a reduction of shoreline withdraw occurred, resulting in a general accretive behavior of the beach. Therefore researchers of Danish Geotechnical Institute decided of using the drainage as a coastal defense intervention with some changes. The vertical wells were substituted by a sub-horizontal drain pipe. The first patent of a commercial drainage system corresponds to what is normally called Beach Management System (BMS) or Beach Drainage System (BDS). This was registered by the Danish Geotechnical Institute in 1985 ([88], [89]).
In the following section the physical process of the BDS is described and some of field and laboratory experience discussed.

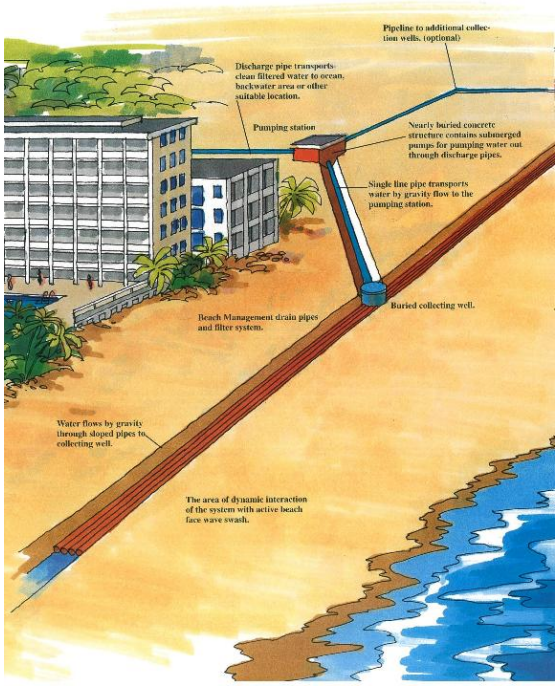

Figure 3.1: General scketch of the BDS

3.2 The physical process

As already discussed in the Chapter 2 beaches can be considered as environmental systems characterized by an unstable dynamic equilibrium. Coastal evolution is produced by combined long-shore and cross-shore sediment transport processes, due to wave action which are very different along the beach profile. In particular the cross-shore sediment transport plays a dominant role in the morphological evolution of sandy beaches profiles, above all in the near-shore zone. The direction of the net sediment transport can be considered the main cause of seasonal cycles of erosion and accretion of a beach ([36]). In particular in the swash zone it depends both on the hydrodynamic of up-rush and backwash processes ([90]; [91]) and on sand characteristics ([29]).
Although an accurate knowledge of the sediment transport in the swash zone is still developed, the analysis of the groundwater dynamics is necessary to understand the beach profile evolution ([92]).
Grant ([93] and [94]) firstly suggested a link between beach groundwater behavior and swash zone sediment transport. Indeed in the foreshore zone one of the most important causes affecting sediment moving is the infiltration inside the beach through the shore face, mainly related with the hydrodynamic conditions

during up-rush and back-wash phases, permeability and saturation degree of the beach.
In particular a critical factor of swash-groundwater interaction is the elevation of the beach groundwater table relative to the mean sea level. Field measurements and numerical modeling demonstrate that the nearshore groundwater dynamics is principally driven by tides, waves and their interactions with the beach morphology ([95]). A relative low water table is thought to enhance swash infiltration and onshore sediment transport, while a high water table suggested to promote swash ex-filtration and offshore sediment transport. The relevance of these processes for beach profile development was effectively demonstrated by Duncan ([96]), who discovered 'cut-and-fill' cycles on tidal beaches with accretion during the rising tide with a relatively low groundwater table, and erosion prevailing during the falling tide due to an elevated water table.
When the beach is interested by long-period waves the run-up flow can infiltrate into the porous medium, causing an increasing of effective stresses and thus of the sediment stability. The run-up flow infiltration inside the zone of the beach partially saturated favors the settlement of the suspended load. On the contrary when the beach is interested by winter storms (with higher wave energy and shorter period), the back-wash flux prevails on the up-rush one because of the water can not infiltrate in the sand and flushes down due to the high saturation degree of the beach. The net result of the run-up/down process is an offshore sediment transport causing, consequently, the erosion of the shore. If the sand is partially saturated the beach behavior can be compare with the summer coastal dynamics with a visible advance of the shoreline (Figure 3.2(a)). Conversely if the saturation degree of the beach is close to the unit, the beach assumes a typical winter behavior with sediment eroded from the shore zone and moved offshore (Figure 3.2(b)).
Therefore an increase in the run-up flow infiltration causes a reduction in the backwash volume and, consequently, in the suspended offshore sediment transport ([94]). Turner and Masselink ([97]) found that the in/ex filtration processes in the swash zone can increase the sediment transport rate by up to 40% of the peak transport rate during the up-rush and decrease it by 10% during backwash.
Recently the scientific research has focused the attention on the study of coastal defense structures with low environmental impact, such as the Beach Drainage System. The Beach Drainage System born as an auxiliary system for the management of the soft solution. It could for instance allows to reduce the erosive processes of a beach already interested by an artificial nourishment.
In general the system artificially increases the sand permeability, producing a lowering in the water table and, consequently, an increase in the thickness of the unsaturated zone (Figure 3.3). The local elevation of the water table and

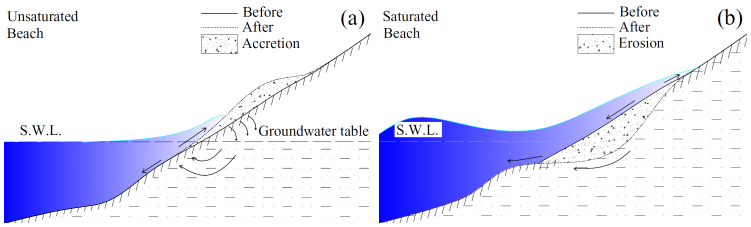

(a) Summer behavior (b) Winter behavior

Figure 3.2:

its influence on groundwater processes and on their interaction with swash zone hydrodynamics may contribute to accretionary or erosional trends at the shoreline. Beach Drainage System aims to interact with the swash hydrodynamics by favoring the deposition of sediments transported by waves during the up-rush phase and contrasting their offshore movement during the back-wash phase. The vertical infiltration of the sea water inside the sand, also allows the effective stresses carried out by soil skeleton to be increased, enhancing the beach stability.

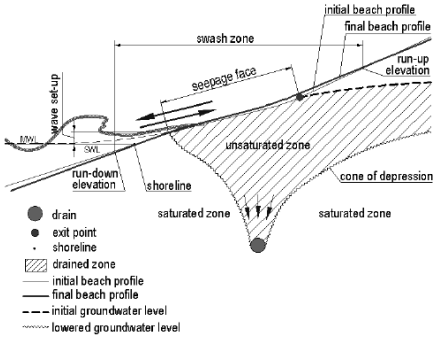

Figure 3.3: BDS interaction with the groundwater inside the beach

3.3 Field applications in Italy

Several field installations of BDS system are available at many sites around the world. The analysis of system response shows that the effective beach stabilization is not well defined. Although the different wave climates and morphological features of the sites, the BDS systems have almost the same design parameters. This confirms the lack of definitive guidelines in BDS design mainly due to the discontinuous long-term monitoring of field installations and the few laboratory

experiments available in literature. Limits and design criteria of a drainage system will be deeply discussed in Chapter 6.

The first field test was conducted in Australia by Chappell ([98]) who tested the notion that swash infiltration and therefore onshore sediment transport and beach accretion, can be promoted by artificially lowering the beach groundwater table. Tests reported qualitative evidence of sand deposition on the foreshore.
The most representative field applications were the systems realized a Hirtshals West in Denmark (1981), at Hirtshals East (1983), at Thorsminde (1985) and at Salfish Point Stuart in Florida (1988).
In Italy there are some examples at Lido di Ostia ([99]), Alassio ([100]), Lido Adriano ([101]; [102]) and Procida Island ([103]). In the following each of them will be sketchily described.

Lido di Ostia, Rome
The figure 3.4(a) is a satellite picture of the area interested by the installation of the system. Currently there is a reduction of sediment contribution from the Tevere river which leads to the erosion of the beach. Besides, the process is got worse by the presence of coastal defense structures which modify the long-shore sediment transport.
The Beach Drainage System deployed at the Lido di Ostia (Rome) is composed by three drains which covered 400 m of the shorezone. They are represented in green in the figure 3.4(b). The drains were PVC pipes with a diameter D of 160 mm covered by a geotexile layer. Drains were installed 7 m far from the shoreline, at 0.60 m below the lower tidal level. Moreover a gravel layer was put between the drain and the sand in order to avoid the blockage by the sand during the water drainage. The drains were connected to three pumping wells

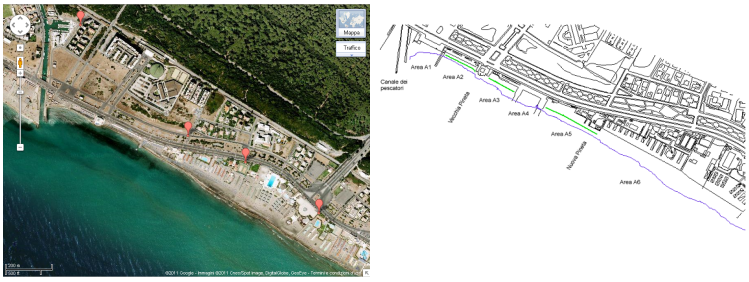

(a) Satellite picture of Lido di Ostia (Rome, Itay)

(b) Displacement of drains

Figure 3.4:

thought three blind pipes with the same diameter of drains. The water collected in the pump station was filtered and transported into the sea.
The system began to work on February 2001. It was monitored until February

2003. For all this time the system had some problems of both maintenance and management. A storm damaged one drain which was then moved onshore in order to analyze its efficacy in different position with respect to the shoreline. In general a sand volume increasing was observed on the emerged beach with the BDS activated, with a consequent seawards shoreline movement. When the system did not work, after the first sea storms, the sediment volumes previously gained were lost. The Figs.3.5(a) and 3.5(b) show the well in 2001 with the system in function and after its cut-off in 2002. The comparison between these

(a) Well in October 2001

(b) Well in October 2002

Figure 3.5:

two figures highlights the lost of sediment due to the interruption in system working. In 2001 the upper part of the well coincided to the emerged beach

surface while, after the system stopping, the well was 1.45 m higher.
Figures 3.6(a) and 3.6(b) show an example of the positive effects of drainage on the emerged beach. The drain position is represents by the red line. The figure 3.6(a) refers to the beach behavior after the reparation of the system which caused the erosion of the material gained before. After one month (Figure 3.6(b)) the BDS allowed to recover the lost material with an evident accretion of the beach.

The system at Lido di Ostia demonstrated the good efficacy of drainage in

(a) January 2003 (b) February 2003

Figure 3.6:

sand stabilization on the emerged beach. Moreover the study underlined the importance in the system management, in order to avoid any interruption which could nullify the benefits obtained by drainage. These aspect will be discussed in details in the Chapter 6.

Alassio, Savona
Alassio is located on the Italian Western Riviera in the Gulf of Genova (Figure 3.7). Over the last fifty years the site has been subjected to remarkable erosion processes which have led to the coastal dunes collapse, mainly due to the anthropic action.
A 198 m long BDS was installed in the beach at a depth of 1.5 m below the Mean Static Level, and became operative on March 2004. The diameter of its draining pipe was 160 mm. Alassio beach was monitored by using video monitoring technique. After on year of BDS working the drained beach showed a net advance of 1.1 m/year whereas the control beach regressed 1.2 m/year. Comparison of the beach sections before the draining started (February 2004) and after one year of draining (March 2005) on the drained and the control beach, demonstrate that within 5 m from the waterline the drained beach gained in all the transects 30÷40 cm in altitude (Figure 3.8(a)), while the control beach showed a small retreat (Figure 3.8(b)). Moreover a berm formation was ob-

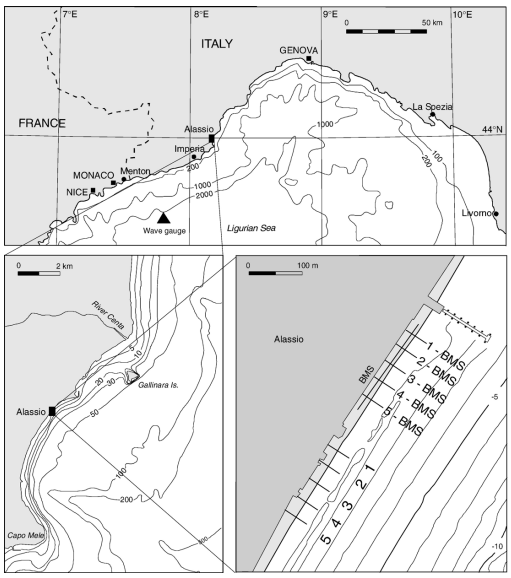

Figure 3.7: Location map of Alassio, in the Gulf of Genova with the location of the BMS

served during the drainage with a steep foreshore with a reduction of the swash zone. On the contrary the control beach exhibites a wide flat and wet foreshore.

However there was not a significant sediments accumulation on the emerged beach. In spite of this limit, the study of Alassio beach demonstrated the draining effects in shoreline migrations, characterized by a less regression in the spring and by a more propagation in the summer, although in winter compared to the control sections, no differences could be observed.

Lido Adriano, Ravenna

The study area (Figure 3.9) is located at Uniti river mouth, south of Ravenna. The BDS system consisted of two pipes100 m long and with a diameter of 160 mm. Drains were installed $1 \div 1.2$ m below the Mean Static Level. The system became operative on April 2004, but, as the above cited field installations, it initially worked intermittently. The system became fully operational on March 2005 and it is stil going on at the time of writing (ancora ora nel 2011?). The intertidal beach was surveyed monthly by GPS system. the shoreline during these years has advanced on average 20 m. This positive trend probably could be due to a natural morphological evolution of the beach profile and not directly related to the drainage. Unlike the study performed at Alassio, it is not possible to use nearby beaches as comparison with drained one. However the analysis of beach volume shows a steady increase since the beginning of monitoring period.

Procida Island, Naples

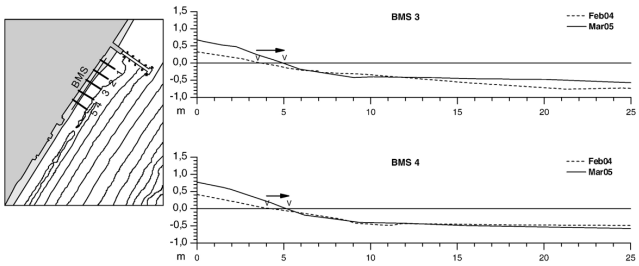

(a) Drained beach in sections 3 and 4

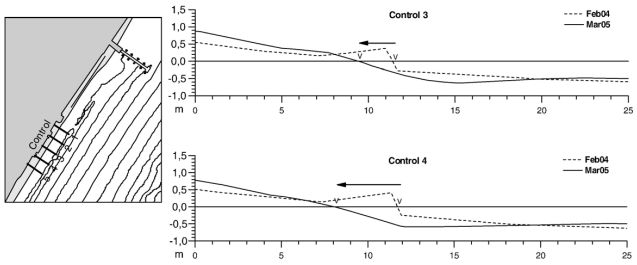

(b) Control beach in sections 3 and 4

Figure 3.8: Comparison of foreshore profiles of drained and control beach

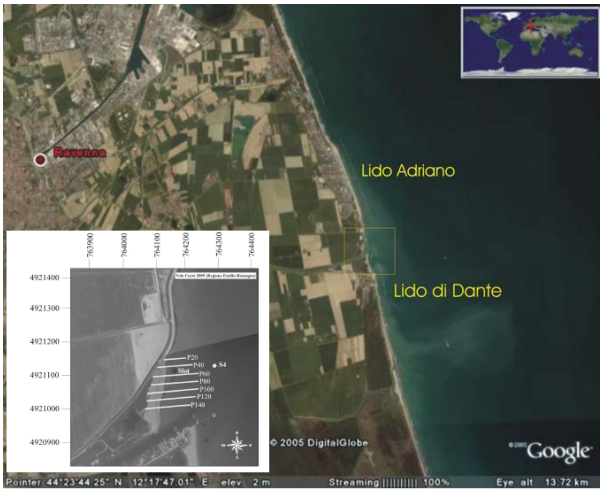

Figure 3.9: Study area at the mouth of Uniti river, Ravenna with the location of monitored sections

Procida Island is in north Gulf of Naples (Fig. 3.10). The coastal zone equipped with the BDS is about 1.5 Km long and quite straight. Over the later years the coastal erosion has caused a clearly visible shoreline retreat. This allow the cliff to be directly eroded by the sea. The drainage system was constituted by

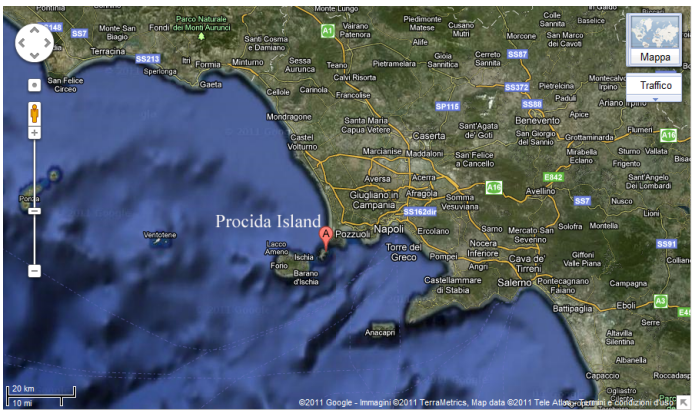

Figure 3.10: Procida Island

10 drains in PVC with a diameter D of 160 mm and covered by a geotexile layer. They were installed parallel to the shoreline at about 6 m from it and at a variable depth below the Mean Water Level, from 0.5 m to 1.3 m. Moreover a gravel layer around the drain prevented the blockage by the sand during the water drainage. The water was collected into 4 pumping well.
The system began to work on June 2002. It was subjected to several interruption. In July 2002 one drain was removed because of its bad working. A great sand volume was transported offshore by the waves motion, compromising the regular working of the drain. Another stop in system running occurred, due to the breaking of a blind pipe which connected the drains with the pumping well. This problem could be avoided by installing an air valve on the blinde pips in order to allow air to escape.
In spite of irregular functioning of the system, the performed surveys showed an increasing of the sand volume on the emerged beach with a remarkable on shore movement of the shoreline (Figures 3.11(a) and 3.11(b)).

3.4 Laboratory experiments

Even if field monitoring is very useful to assess the effectiveness of the system ([89]), laboratory tests can be used in order to clarify the system response under different wave conditions and to define the main project parameters of the system.
Laboratory studies as early as the 1970s ([104]) have observed that by artificially lowering the groundwater level it is possible to enhance the sediment stability. Kawata et al. ([105]) tested in laboratory the efficiency of a '*sub-sand system*' as system of beach erosion control, under controlled conditions. According to

(a) December 2002 (b) July 2003

Figure 3.11:

obtained results they showed the applicability of the drainage system in order to prevent or mitigate beach erosion under any wave conditions. Under swell waves the sub-sand filter allowed to accelerate the sediment accretion in the foreshore zone through the development of a berm with a consequent shoreline advance. When wave conditions change to stormy waves the decreasing of sediment loss from the foreshore was observed. Oh and Dean ([106]) performed laboratory studies at the Coastal and Oceanographical Engineering Laboratory in order to investigate the effects of groundwater table elevations on the beach profile changes over the swash zone. They investigated the changes of an initially linear profile subject to regular wave at three different water table levels. Tests confirmed the influence of beach water tables on profile dynamics. In particular the water table higher than the static water levels caused the sand erosion at the base of the beach face and the sediment transport on the upper part of it. Masselink et al. ([107]) published a work on a large-scale laboratory (Delta flume, Netherlands) investigation of the effects of the beach groundwater table on gravel beach morphology. Different ranges of wave and water level conditions were tested. Experiments demonstrated that the net onshore sediment transport was most pronounced with a steady sea level and long-period waves, while an erosion in the swash zone was observed with elevating the groundwater table.

3.5 The Beach Drainage System design

3.5.1 Design parameters

Field installations of BDS provided different responses on the efficiency of the drainage system. Firstly sites are characterized by different morphological and hydrodynamic processes. Secondly field results are difficult to be interpreted

because of many factors influence full scale system making it difficult to provide experiment control. Moreover the absence of an adequate long-term monitoring complicates the interpretation of the results and the identification of a BDS response.
Despite the detailed monitoring, it is difficult to separate many of the influencing variables, and to isolate the effect of the drainage system. As a matter of fact one of the problem in results analysis has been to isolate the natural trend of the beach from the effects of BD. Beach evolution in undrained and drained conditions is fundamental to determine the reliability of a BDS as a system of coastal protection.
Moreover the laboratory experiments on scaled models gave results quite different from that ones obtained on field, caused by the uncertainties of scale factors and the difficulty of simulating the real behavior of the aquifer under the beach face.
Design guidelines for BDS installation must be defined as a function of both dynamic and morphodynamic conditions and of the characteristics of the beach (sand grain size, fall velocity and permeability). Therefore the BDS efficiency depends on the correct design of all parameters.
Field and laboratory studies confirm the importance of a deep preliminary investigation regarding the history of the site which will be equipped with the system. One of the most important step is the analysis of the morphology of both emerged and submerged beach. If the emerged beach is not quite large or higher than the Mean Water Level, it could be completely submerged by a storm with a consequence inefficiency of the system. The water would not have the possibility of infiltrating inside the beach because of its high saturation degree.
Currently no design criteria are yet implemented. All the design parameters (number of pipes, pipe diameter, excavation depth and location, etc.) are defined only on the basis of sellers technicians experiences.
The planimetric position of drain (or drains) can be defined as a function of the design storm. At the present it is observed that the optimal position of the drain corresponds to the run-up limit. A drain positioning offshore with respect to this limit would reduce the drained flow and, consequently, the efficacy of drain. Otherwise a system place close to the shoreline causes an increasing of drained water and thus of the management costs, without any benefits in terms of beach stabilization. Besides, a drain close to the shoreline is easier to be exposed and definitively damaged.
The choice of the design wave covers an important role in the system design. It is important as well to determine the storms which mark the threshold for an effective drains. If the drain is installed in order to increase the sediment volume on the emerged beach the design wave has to be characterized by low energy. In this case the risk is that a higher energy wave would damage the sys-

tem. On the contrary if the drain has the aim of stabilizing a beach larger but subjected to more remarkable erosion process, the system design could be based on a higher return period. The drain would be deployed offshore with respect to the previous instance. A possible solution could be the installation of more than one drain at different distances from the shoreline. However the previous experiences demonstrated that simultaneously working drains do not cause increasing sand volumes and make the effects of the best placed drain for that specific wave energy negligible. The drainage system would be equipped with drains would automatically begin to work as a function of the present waves. During high energy sea storms all drains could work, reducing the damages on the closest drain to the shoreline which is more exposed to the waves action. Under low energy waves only the drain placed next to run up limit could work with lower management costs and probably system maximum efficacy.
Concerning the drain depth with respect to the Mean Water Level the performed experiments do not allow to define an optimal depth. In general drains have to be placed below the groundwater level in low tide.

3.5.2 BDS management

Every coastal protection intervention has to be taken charge during the total intervention life and not only for its design and realization. The field installations of the system described above provide results which demonstrate slight effects in reducing beach erosion. The reason was the irregular system working, generally related to administrative problems.
In these conditions the study of the effects of drainage results to be very difficult. Moreover the system is easily subjected to permanent damages. Therefore, the definition of preliminary management plans results to be necessary in order to avoid extended periods of system malfunction. Pumping system functioning and system drainage capability have to be periodically tested. Moreover a detail monitoring of both hydraulic (water table, sea-storms, wave run-up, etc.) and morphologic (shoreline movements, sediments volume changes, shorezone slope, etc.) parameters has to be conducted either with fixed instruments or with periodic measurements campaign. The monitoring aims to promptly highlight the morphodynamic beach evolution and the variation in the main hydraulic parameters in order to identify the causes of the low system efficiency. As an example a reduction of the drained discharge can be linked to the breaking of the drain pipe. In this case the pipe has to be repaired or substituted before the blockage of the pumping well by the sand. An increasing of the compaction degree of the beach or a remarkable accretion of the emerged beach can cause the reduction of beach permeability with a consequently movement of drain pipe from the shoreline. In these case the sediment movement on the emerged beach could re-establish the optimal working conditions of the system, as the

reduction of the shore slope.
In conclusion, the beach drainage can be considered an usefully work for the beach management. It has to be supported by a continuous beach monitoring and management, in order to contrast the erosion phenomena from their beginning. In coastal zones subjected by strong erosional trend, the BDS can not be considered a definitive solution to report the beach in its initial conditions without the so-called hard defense works.

3.5.3 Limits and perspectives of BDS

The available experiences on BDS performances do not allow to define fixed system applicability limits. In the previous section the importance of preliminary studies on the sand has been remarked. Sand grain size mainly influences the system response. A sand too much large or, on the contrary too much fine, would reduce the drainage efficiency. The former naturally allows water drainage. No advantages by adding an artificial drainage would be obtained. The latter has so low permeability that run-up flow can not infiltrate inside the beach and sediments are transported offshore.
When energy conditions changes from calm to erosive, material will inevitably be lost, even with working drain (although the total beach volume will remain greater with the drain in). System will begin to restore the beach profile after a length of time.
Other two important aspects limit the drainage effectiveness in beach stabilization by BDS. Firstly sand volume settled on swash zone generally comes from the shallow water. The depth of this zone represents one of the main design parameters to consider for BDS design because of it constitutes the natural reservoir of suspended sediments. Secondly the sand settlement on beach face causes the swash zone slope increasing. It is clear that the wave run-up length become large with the increasing of beach face slope. In this condition the water movement during the up-rush phase is more difficult, with a consequence decrease of sediments transport.
More data on monitored BDS sites and large scale parametric laboratory experiments are needed for a better understanding of the BDS hydraulic working principle. Too often coastal managers provide a budget that only covers installation costs and do not understand the importance of monitoring activities. These should not focus on the beach and shoreline behavior after the installation but also should be carried out before the construction of the system to have baseline datasets. Regarding future improvement of design criteria, research is needed using laboratory models with small or absent scale effects, especially for parameters like grain size and hydraulic conductivity. For this purpose the 1:1 scale experiments were undertaken at the Large Flume GWK of Hannover University. The projects involved a series of experiments using several parallel

drains under different wave conditions. The experiments and otained results will be deeply discussed in the following sections.

In the Chapter 4 small and large scale laboratory experiments on the BDS are reported. The small-scale experiments were conducted at the Laboratory of Coastal Engineering ('Laboratorio di Ingegneria delle Coste', LIC) of Politecnico di Bari (Italy) ([108]) in 2001. Experimental set-up and main results are briefly discussed and the attention is mainly focused on the scale effects. The chapter mainly deals with the description of the full-scale experiments. These were performed at the GrosserWellen Kanal (GWK) in Hannover (Germany) in 2009/2010. Experimental set-up, adopted instrumentation and measure methods are described in detail and the hydrodynamic and morphodynamic results are discussed.

Chapter 4

Physical modeling on BDS

4.1 Introduction

In the present chapter laboratory experiments on the Beach Drainage System are described. The first section 4.2 deals with a brief overview on both physical models theory and scaling analogies used for the laboratory studies. In particular the section explains the scaling criteria typically used in the study of movable bed models and their limits in the laboratory applications. The attention focuses on Darcy's criterion and Dean's scaling law. These two scaling guidances mainly pertain to the coastal transport processes and in/ex filtration ones. Next, the laboratory experiments performed in both small (section 4.3) and full (sections 4.4, 4.5 and 4.6) scale are described. The attention mainly is focused on the analysis of results obtained by large-scale experiments both on hydrodynamic and morphodynamic aspects on the study.

The small scale experiments were performed at the Laboratory of Coastal Engineering (LIC) of Politecnico di Bari in 2001. The full scale experimental activities (2009/2010) were supported by the Sixth European Community Framework Programme through a grant from the Integrated Infrastructure Initiative HYDRALAB III within the Transnational Access Activities. In particular laboratory tests on BDS were performed during the Access Project HYIII-GWK-6 'Infiltration and exfiltration on the beach face' (contract no. 022441), at the Large Wave Flume (Grosser WellenKanal, GWK) of Hannover, Germany.

The experiments were planned in order to deeply analyze the influence of the drainage system on the near-shore hydrodynamic processes. In the previous Chapter it was shown that field installations did not give good results in reducing erosion. The failure of some project is certainly due do the fact that the design criteria are not well defined. A final assessment on the efficiency of the system requires both theoretical and experimental deeper studies, in order to discuss the effects of a drainage system on a beach and its efficacy in stabilizing

the suspended sediments.
Previous experiments performed at LIC in a 1:10 scaled model of BDS indicated a general efficiency of the system under both nourishing and erosive wave conditions. Small-scale experiments gave an accurate qualitative description of the investigated phenomena, but there are doubts about the quantitative interpretation of the obtained results ([108]).

4.2 Physical models and scale effects

In technical literature, many works on influence of scale effects on beach morphology are available, even if this problem is not still completely solved. The discussion aims to delve into the correct reproduction of the hydrodynamic processes and morphological changes in the shore zone, where filtration assumes a relevant role and can not be neglected.
In movable bed models nearshore accretion and erosion processes are related to the mechanics of surface-subsurface flow interaction. If all the above phenomena have to be considered simultaneously, difficulties arise from the uncertainty in recognizing a good analogy to accurately reproduce all sediment characteristics of the prototype. If the selected scaling law requires that the grain size has to be scaled as the same as the geometric length, there is the possibility that non-cohesive sediments may be scaled with the grain diameters of cohesive sediment (grain diameter ¡ 0.08 mm). In that case the model would not be a dynamic representation of the prototype ([109]) and a different transport process would be reproduced. These issues illustrate the importance of carefully designing the tests, using different scaling laws at different zones along the profile, always considering the dominant process in each area. In particular, one of the most difficult problems facing the modeler is the fact that different types of sediment transport processes dominate inside and outside the surf zone. All the analogies useful to study the transport processes in the surf zone (i.e. Dean analogy) are suitable for simulating the suspended load transport but they are not acceptable to analyze the in/ex-filtration processes (i.e. Darcy analogy). The main limit of Dean analogy has to be found in the inconsistency in reproducing bed load transport, which, joint with suspended one, is highly influential in the beach profile evolution. In general the scale effects are due to the wrong reproduction of the sediments transport rates. This mainly depends on the hydrodynamics in the shorezone: a significant development of the turbulence increases the suspended load transport compared to the bed one and vice versa. Consequently, as the model size decreases, and thus the n scale factor increases, the ratio between the suspended and bed load is not preserved and the latter prevails ([110]).
About hydrodynamic phenomena, the usual Froude criterion is universally ac-

cepted in order to give a consistent interpretation of the results. However the most part of physical models do not take into account the mechanics of in/ex-filtration processes. Consequently the hydrodynamics in the shore-zone (i.e. wave set-up, run-up, etc.) and thus the evolution of the beach profile are distorted during laboratory tests.

The above statement confirm the importance of sediment choice in physical models, according to suitable scaling laws not only for morphological aims but also in hydrodynamic analysis.

Filtration is clearly related to sediment characteristics and porous medium conditions, like as permeability, saturation degree, compaction, etc. A wrong scaling of sediment influences the mechanical response of the beach and causes the misinterpretation of hydrodynamic processes. As an example the maximum wave run-up on a gravel beach is lower than in a sandy one, because of the higher permeability. The influence of the permeability, and thus of the saturation degree, is usually disregarded because of the filtration flows have not been considered in wave/beach interaction, unless a generic classification in gravel beach, sandy beach, etc.

Confirming the above statement, it can be considered that nourishing or erosive behavior of waves are described by means of many parameters ([72], [111]), which do not include any reference to filtration flow. With reference to sandy beach profile classification (winter or summer) all physical models results are obtained by analyzing different wave conditions and by using natural beach saturation degree. Also in coastal protection works, traditional defense structures are aimed to modify wave hydrodynamics. In recent years, some innovative systems were introduced in order to modify beach behavior by taking into account in/ex-filtration processes. It is clear that in laboratory the simulation of this kind of systems, permeability effects cannot be disregarded in defining a suitable scaling criterion.

In order to discuss the use of these two different analogies, four sands are here considered. Table 4.1 reports the fall velocities, d_{10}, d_{50} and their ratio of each sand used as prototypes for the present work.All sand characteristics were measured in laboratory. In the Udden-Wentworth scale the sands 1, 2 and 3 (Tab.

Table 4.1: Characteristics of sands

Sand	d_{50} (mm)	d_{10} (mm)	w (cm/s)	d_{10}/d_{50}
1	0.155	0.11	1.91	0.71
2	0.18	0.15	2.6	0.83
3	0.233	0.17	2.55	0.73
4	0.33	0.192	4.8	0.58

4.1 represent fine sands [$0.125mm \div 0.25mm$], while the fourth one is a medium sand [$0.25 \div 0.50$ mm]. In the following n_s will indicate the ratio between the size in the prototype (S_p) and the size in the scaled model (S_m). Taking into account the Froude analogy as hydrodynamic scaling guidance, it follows that

$$n = n_l = n_d = n_H = n_T^2 \tag{4.1}$$

where
n = the geometrical scale
l = the length
d= the depth
H= height
T = the time. Considering Dean analogy as scaling law, it imposes the parameter H/wT (in which is ω the sand fall velocity) equal in both prototype and model

$$\left(\frac{H}{\omega T}\right)_p = \left(\frac{H}{\omega T}\right)_m \tag{4.2}$$

This leads to the relation between the fall velocity, length and time scale factors

$$\frac{\omega_p}{\omega_m} = \frac{H_p}{H_m}\frac{T_m}{T_p} \Rightarrow n_\omega = n_H \frac{1}{T} = \sqrt{n_H} \tag{4.3}$$

Fixed the geometrical scale n_H, scale factors for the time and the fall velocity are directly defined. Thus, known the fall velocity of the sand in the prototype (ω_p), the fall velocity in the model (ω_m) is determined by using Dean analogy. Model sand d_{50} is calculated using Stokes' law, which expresses the mean sand diameter as a function of the fall velocity

$$d_{50} = \sqrt{\frac{\omega_p 18 \eta_{water}}{\gamma_s - \gamma_{water}}} \tag{4.4}$$

The model sand d_{50} is also calculated by using Darcy scaling guidance, which allows to reproduce the filtration processes inside the beach. Darcy's law can be expressed as follows

$$J = \frac{kv^2}{gd_{10}} \tag{4.5}$$

where J is the hydraulic grade line, k the sand permeability (expressed as a function of the Reynolds number ($\rho v d/\mu$), g the gravity acceleration and d_{10} is referred to grain size of material. Imposing $n_J = 1$, the relations between the permeability, the velocity and the sand d_{10} is defined

$$\frac{D_p}{D_m} = \frac{k_p}{k_m}\frac{v_m}{v_p} \Rightarrow n_D = n_k n_v^2 \tag{4.6}$$

Considering that the permeability is in inverse proportion to the Reynolds number, its scale factor results

$$n_k = n_v n_D \tag{4.7}$$

Substituting the expression of n_k in the Eq. 4.6, it follows that $n = n_D d^4$, where d is the sand d_{10}. The same ratio between d_{10} and d_{50} in both prototype and model is adopted in order to derive d_{50} the in the model. Figure 4.1 shows the results of applying both Dean (blue markers) and Darcy (red markers) criteria for different geometrical scale ratio from $1:10$ to $1:60$. On the x-axis and the y-axis there are respectively prototype and model sand diameters. The graphs

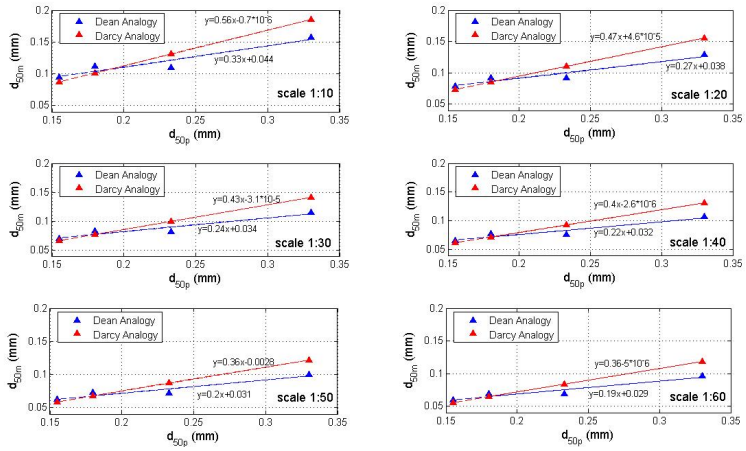

Figure 4.1: Prototype sand d_{50} values by using both Dean and Darcy analogies

first of all confirm the different results in the choice of sand diameter in the model applying respectively the analogy by Dean and Darcy. This choice would be based on the phenomena that the modeler wants to represent in the physical model. For the sands with a d_{50} in the prototype smaller than or equal to 0.2 mm the scale factor is almost the same for both analogies. In this case the model would represent simultaneously the sediment transport in the surf zone and the filtration processes in the shore zone. With a d_{50} in the prototype greater than 0.2 mm, the two analogies give different results. Moreover with the reduction of geometrical scale ratio, the slope of the fitted lines decreases. This means that small scale factors (i.e. $1:50$, $1:60$, etc) impose the use of a fine sand in the model. As a consequence possible changes in sand mechanical behavior could arise during experiments and affect reliability of the results (i.e. capillarity).

4.3 Small scale laboratory experiments

The present section deals with a general description of the small scale laboratory experiments performed at the laboratory of Coastal Engineeering (Laboratorio di Ingegneria delle Coste, LIC)of the Politecnico di Bari. The experimental set-up is briefly described and the main results on hydrodynamics and morpho-

dynamics are reported.

4.3.1 Experimental set-up

Small-scale 2D laboratory experiments on a BDS were conducted at the Research and Experimentation Laboratory for Coastal Defense (LIC) of Technical University of Bari, Italy ([112], [108]). These tests furnished suggestions to understand measurement techniques and the system performance. The LIC flume, deeply described in previous works ([113]), is 48.8 m long and 2.5 m wide; the sand has a D_{50} equal to 0.18mm, permeability between $2.7 \div 3.71^{10^-2}$ cm/s and a fall velocity equal to 2.6 cm/s. The initial beach profile slope was about 1:20 and the maximum sea water depth was 80 cm. Four PVC drain pipes (Fig. 4.2) were located under the emerged beach profile at a depth of about 10 cm under the still water level and at a distance from the shoreline variable from 20 cm to 170 cm. The drain pipes collect water in a wheel through blind pipes, each

Figure 4.2: BDS model at LIC - 1:10

one equipped with a gate: this configuration makes possible to use single drain or more than one. In order to evaluate the mean water table position, 8 'static' level probes were used, covering the swash zone and the emerged beach. Just before and after each test, the beach profile was assessed by means of automatic beach profilers. Tests were performed in static conditions and under different wave attacks. Static conditions were tested with two different water levels in the channel equal to 0.80 m and 0.82 m. The dynamic wave attacks were characterized by JONSWAP spectra, which can be representative of natural, nourishing and erosive waves in a 1:10 Froud analogy.

4.3.2 Hydrodynamics

Obtained results allow to study the water table qualitative behavior both in drained and undrained conditions ([108]). It has been observed that drains are able to lower the water table and to make available a larger unsaturated beach, where run-up flow can be absorbed. By this way, vertical in-filtration flux can stabilize sediments on the emerged beach. On the other side, the back-wash is reduced, promoting sand deposit on the foreshore zone and, as a consequence, the formation of a berm. In all investigated cases, beach drainage reduces the maximum wave induced set-up, thus affecting the near-shore circulation. During tests the drained flow was measured. Results showed that it depends on many parameters (i.e. permeability, pipe diameter, etc.) which were not deeply investigated during the experiment. In general a reliance of the drained flow on both drain pipe distance from the shoreline and water table lowering was observed. The Fig. 4.3 shows flows drained by single drains as a function of the

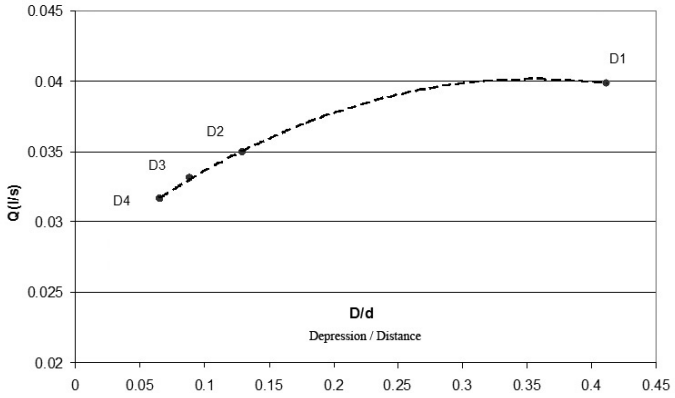

Figure 4.3: Drained flows vs the rate between the w.t. lowering and the distance from the shoreline (single drain open)

rate between the water table lowering D and the distance from the shoreline d. It can be observed that a deeper depression induced by the drain corresponds to a greater drained flow. Moreover the tests demonstrated that drains placed far from the shoreline drained less water volume with respect to the drain close to submerged beach.

Another important aspect of tests was the analysis of the hydraulic regime inside the drain. During static tests the spatial variation of water table analysis show a flow regime inside the drain as an open-channel flow. As Fig. 4.4 shows, in the most cases the water table intersect the drain diameter. During wave attacks (Fig. 4.5) the water table did not intersect the drain diameter. This allow to suppose a drain behavior under pressure. However any instruments was placed inside the drain in order to confirm these assumptions. For this reason in

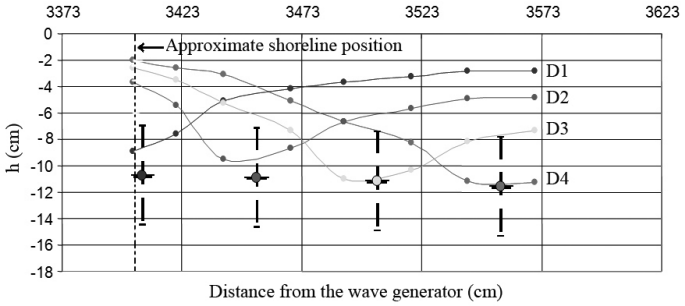

Figure 4.4: Spatial variation of water table for static test with SWL=0.8 m and with single drains open

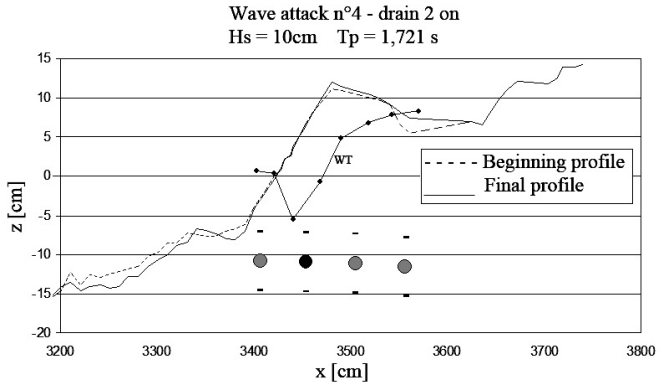

Figure 4.5: Spatial variation of water table for dynamic test with SWL=0.8 m and with drain D2 open

the experiments performed at GWK, described in the following, each drain was equipped with a pore pressure transducers inside aimed to analyze the hydraulic regime of the pipe.

4.3.3 Morphodynamics

The analysis of data collected in laboratory during the experimental activity has allowed to evaluate the drainage effects on the morphodynamics.
Tests performed in undrained conditions showed that the accretive wave attack did not produce evident morphodynamic changes. This kind of attack caused the formation of a berm on the emerged beach, but no seaward shoreline movement could be observed. On the contrary during tests the shoreline moved back landward, also in drained conditions. However the beach configuration after drained tests is comparable with the equilibrium profile typical of gravel

beaches, confirming the effect of drainage in increasing the beach permeability. The analysis of sediment volume showed an offshore erosive trend probably due to the non perfect equilibrium initial beach profile. Moreover in drained conditions a slight landward sediment transport was observed.
Under erosive wave attacks a singular behavior was observed. In both undrained and drained conditions the net sediment transport was directed landward with a consequent accretion in the submerged beach swash zone. This phenomena could be due to the presence of the berm which produced a sediment retaining on the emerged beach. However the drain effects were evident on both shoreline movement and sediment volume analysis. As a matter of fact, drains were able to slow down the shoreline landward movement with respect to undrained conditions and to produce a sand accretion on the emerged beach.
The data analysis in all tested wave energy conditions allowed to state some consideration on the planimetric drain position. Considering both hydrodynamic and morphodynamic effect induced by the activation of one drain or more drains simultaneously, the best position seemed to be close to the run-up limit.
The obtained results confirm that the model characteristics, first of all the sand permeability, assure the drain effectiveness and a quick reaching of stationary condition, even if this result could be affected by scale effects. For this reason, similar tests have been performed at GWK where a BDS prototype has been reproduced. The new tests are aimed to confirm the effectiveness of the BDS and to analyze scale effects, in order to allow a consistent interpretation of LIC results from a quantitative point of view. moreover results provide useful suggestions for understanding measurement techniques and the performance of the system.

4.4 Large scale laboratory experiments

4.4.1 Experimental set-up

The laboratory investigation on the full-scale model of Beach Drainage System (BDS) was performed at the Coastal Research Centre (FZK) of Technical University of Brounischweig in Hannover (Germany). Tests were carried out at the Large Wave Flume ('Grosser WellenKanal'- GWK), which represents an unique test facility to perform basic and applied research on coastal engineering phenomena(Fig. 4.6). Water waves up to a height of 2.00 m under quasi-prototype conditions can be simulated in the 307 m long, 7.00 m deep and 5.00 m wide flume. The facility is equipped with a piston type paddle for generating regular and irregular waves. The installed power of the piston type wave generator combined with an upper flap is about 900 kW. The gearwheel driven carrier gives a maximum stroke of 2.10 m to the wave paddle, which is 5 m wide and about 6.70 m high (Fig.4.7). The stroke can be superimposed by upper flap

Figure 4.6: General view of GWK wave flume

movements of 10 degree, in order to simulate natural water wave kinematics most accurately. A large cylinder integrated in the carrier compensates the water force in front of the paddle (rear is free of water). The wave generator

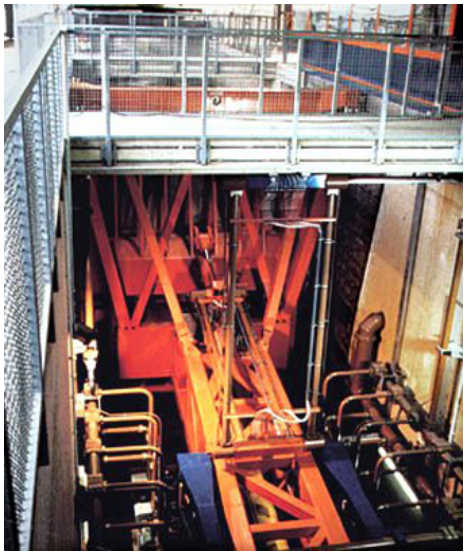

Figure 4.7: View of the wave generator

is controlled by an on-line absorption system (Fig. 4.8). This special system works with all kinds of regular and irregular wave trains. Thus, the tests are unaffected by re-reflections at the wave generator and can be carried out over nearly unlimited duration. The wave maker also allows the generation of freak

waves breaking at a predetermined point of the flume.

The wave flume is also provided with a carriage (Fig. 4.9) which travels along

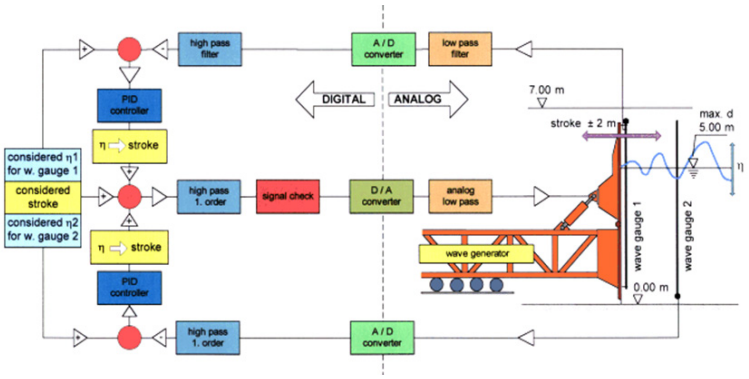

Figure 4.8: Sketch of the online absorption system

the channel. On the carriage is fixed the beach profiler which will be deeply described in the following. It is possible to install on it other instruments with the advantage of having measurements in different sections along the model.

At the end of the flume, on the opposite side of the wave generator, the beach

Figure 4.9: View of the carriage in the wave flume

was designed on basis of the previous experiments performed in Bari. The movable bed starts 99 m far from the wave generator with a planed sloped profile at 1:20 for 20 m and at 1:50 for the following 50 m (Fig. 4.10). A 50 m long flat part was shaped before reaching the beach face. The swash zone slope was about 1:10 over 30 m. The beach compaction was made on the two mentioned swash zone slopes but not for each wave test.

Beach profile in the flume consisted of a quartz sand. Grain size curve and main sand characteristics were analyzed at the laboratories of Politenico of Bari

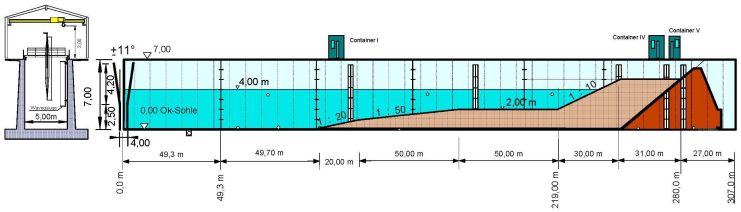

Figure 4.10: Sketch of wave flume with the beach profile

and will deeply discussed in the following subsection 4.4.2.
The adopted drainage system was constituted by 4 corrugated polyvinyl chloride (PVC) pipes installed inside the beach, under the static water level, in correspondence to the swash zone and transversally to the incident wave motion (so parallel to shoreline). Each drain had a diameter equal to 0.20 m and it was 5 m long, occupying the entire beach width (Fig. 4.11). Moreover drains

Figure 4.11: Overview of the set-up in GWK flume during the model construction

were covered by a double layer of geotexile in order to avoid the blockage due to the sand during water drainage with a probably out of action of the system. The groundwater collecting was made possible by a series of rectangular holes uniformly distributed around drains contours. The upper part of the drains D1, D2, D3 and D4 was located about 3.6 m from the bottom channel. In table 4.2 the accurate altimetric and planimetric position of the drain axis with respect to the wave paddle is shown. Variable spatial drain positions were considered to analyze their optimal distance from the shoreline in terms of morphodynamic and hydrodynamic efficiency. As can be observed the distance between the first two drains is smaller with respect to the other ones. They were placed side

Figure 4.12: Particular of the drain pipe

Table 4.2: Drains position

Drain	x (m)	y (m)	Distance from the initial shoreline (m)
D1	242.10	3.46	2.60
D2	242.40	3.47	2.90
D3	247.00	3.45	7.50
D4	252.00	3.45	12.50

by side in the same hole. This gave the possibility to simulate a drain with a double diameter in order to study the influence of drain dimensions on BDS efficiency in draining water flows. This was made possible by opening the two drains at the same time. The drains had a small longitudinal slope of about 1% to allow a connection to PVC blind pipes of same diameter and a variable length ranging from 4 m to 13 m. The blind pipes were placed along the flume walls (Fig. 4.13) and linked with the pumping well.

The end of each pipe, inside the pumping well, was provided with a gate valve to allow the drains to be switched on/off (Fig.4.14). The pumping well has a diameter equal to 2.08 m and it was made up of 7 concrete elements 0.5 m high. The total height of the well was 4.11 m and its distance from the bottom of the flume was 1.61 m. The automatic pump performance was guaranteed by two buoys placed at a relative vertical distance of 0.08 m (Fig. 4.15). During tests, the groundwater flow collected inside the concrete well was pumped and finally discharged again into the flume by means of an external iron pipe of 0.2

Figure 4.13: Rigid PVC blind pipes

m diameter.

The laboratory investigation covered a period between December 2008 to

Figure 4.14: Pumping well and valves for switching on/off of the drains

March 2009. Two sets of tests were performed. The first one (15 static tests) with two different undisturbed water levels in the channel. During the second set of tests (64 dynamic tests) drainage system was tested under different wave energy conditions (64 tests).

In table 4.3 the characteristics of the static experiments with different configu-

Figure 4.15: Pump placed in the well

rations of drains are reported. The test name, water level, status of the drains, and test duration are showed. In the name of each test 0 indicated drains off, while 1 indicated drains on. Each test, except for the test 01-S1 -1000, was defined by a first condition with drain/drains opened, followed by a successive condition without drains, having similar duration. The analysis of the water table lowering with two different water levels enables to discuss the influence of drain depth on the system efficiency.

Three kinds of irregular wave attacks characterized by a JONSWAP spectrum were performed in order to reproduce high (HE), medium (ME) and low (LE) wave energy conditions. The adopted wave conditions were chosen in order to have probable accretion or erosion on the beach. The table 4.4 shows the kind of wave attack reproduced in the laboratory according to the following different criteria:

1. $gH_0^2/\omega_s^3 T_p > 22300 \Rightarrow$ Offshore motion ([114])

   $gH_0^2/\omega_s^3 T_p < 22300 \Rightarrow$ Onshore emotion ([114])

2. $H_b/w_s T_p > 1.7 \Rightarrow$ Offshore motion ([72])

   $H_b/w_s T_p < 1.7 \Rightarrow$ Onshore emotion ([72])

3. $2\pi H_m/gt^2 > 0.0007(H_m/w_s T_p)^3 \Rightarrow$ Onshore emotion ([**?**])

   $2\pi H_m/gt^2 < 0.0007(H_m/w_s T_p)^3 \Rightarrow$ Offshore motio ([**?**])

4. $H_0/w_s T_m > 2 \Rightarrow$ Offshore motio ([78])

   $H_0/w_s T_m < 2 \Rightarrow$ Onshore emotion ([78])

Each run with or without drains has been repeated in order to identifying the temporal effect of the drains on the morphodynamic beach changes inside the

Table 4.3: Overview of the experimental program of static test

Test name	Static level (m)	Drains on	Drains off	Test duration (min)
01S1-1000	4.00	1	2-3-4	60.00
02S1-0100	4.00	2	1-3-4	68.60
02S1-0000	4.00	-	1-2-3-4	51.40
03S1-1100	4.00	1-2	3-4	45.28
03S1-0000	4.00	-	1-2-3-4	48.95
04S1-0010	4.00	1-2	3-4	48.87
04S1-0000	4.00	-	1-2-3-4	42.78
05S1-0001	4.00	4	1-2-3	49.37
05S1-0000	4.00	-	1-2-3-4	52.32
06S1-0011	4.00	3-4	1-2	49.38
06S1-0000	4.00	-	1-2-3-4	70.62
07S1-1110	4.00	1-2-3	4	48.02
07S1-0000	4.00	-	1-2-3-4	44.53
08S2-1000	4.20	1	2-3-4	47.65
08S2-0000	4.20	-	1-2-3-4	48.90
09S2-1100	4.20	1-2	3-4	48.61
09S2-0000	4.20	-	1-2-3-4	46.81
10S2-0001	4.20	4	1-2-3	48.51
10S2-0000	4.20	-	1-2-3-4	59.41
11S2-0010	4.20	3	1-2-4	58.28
11S2-0000	4.20	-	1-2-3-4	47.40
12S2-0011	4.20	3-4	1-2	47.93
12S2-0000	4.20	-	1-2-3-4	49.08
13S2-0100	4.20	2	1-3-4	48.17
13S2-0000	4.20	-	1-2-3-4	49.82
14S2-0001	4.20	4	1-2-3	48.24
14S2-0000	4.20	-	1-2-3-4	48.93
15S2-111	4.20	1-2-3	4	49.28
15S2-0000	4.20	-	1-2-3-4	49.78

Table 4.4: Overview of the experimental program of dynamic tests

			Kind of attacks	
Wave attacks	Krauss	Dean	Buccino	Kriebel
HE	Accretive	Erosive	Accretive	Erosive
ME	Accretive	Erosive	Accretive	Erosive
LE	Accretive	Erosive	Accretive	Accretive

zone influenced by the presence of the active drain.
Main characteristics of dynamic experiments with different configurations of drains are reported in Tab. 4.5,Tab. 4.6 and Tab. 4.7 showing test name, water level, status of the drains, test duration, statistic and spectral wave characteristics (significant wave height H_s, mean wave period T_m, peak period T_p, average wave steepness S_p, spectral wave energy m_0), the repetition time T_R, (which represents the interval for each generated spectrum inside the test for defining the wave packets), the mean number of wave packets and the mean number of waves for each packet and for each test. The name of each test follows the same criteria explained for static tests. These wave characteristics have been calculated through the first offshore wave gauge (WG1), placed at 50.1 m from the wave generator and at the same water depth. Detailed information about the analyses for determining the wave characteristics can be found in section 4.4.3.

Table 4.5: High Energy dynamic tests

Test name	Static level (m)	Drains ON	Drains OFF	H_s (m)	T_m (s)	T_p (s)	S_p	Total mean number of waves
16HE-0000-1	4.00 m	-	1-2-3-4	0.80	5.29	6.40	0.012	680
16HE-0000-2	4.00 m	-	1-2-3-4	0.79	5.24	6.40	0.012	687
16HE-0000-3	4.00 m	-	1-2-3-4	0.80	5.25	6.40	0.012	686
17HE-1000-1	4.00 m	1	2-3-4	0.78	5.26	6.40	0.012	685
17HE-1000-2	4.00 m	1	2-3-4	0.76	5.20	6.40	0.012	332
17HE-1000-3	4.00 m	1	2-3-4	0.81	5.44	6.40	0.013	210
18HE-0000-1	4.00 m	-	1-2-3-4	0.83	5.27	6.40	0.013	682
18HE-0000-2	4.00 m	-	1-2-3-4	0.82	5.26	6.40	0.013	684
18HE-0000-3	4.00 m	-	1-2-3-4	0.81	5.26	6.40	0.013	685
19HE-1100-1	4.00 m	1-2	3-4	0.79	5.24	6.40	0.012	687
19HE-1100-2	4.00 m	1-2	3-4	0.82	5.25	6.40	0.013	686
19HE-1100-3	4.00 m	1-2	3-4	0.83	5.24	6.40	0.013	687
19HE-1100-4	4.00 m	1-2	3-4	0.79	5.22	6.40	0.012	690
20HE-0010-1	4.00 m	3	1-2-4	0.79	5.26	6.40	0.012	684
20HE-0010-2	4.00 m	3	1-2-4	0.80	5.25	6.40	0.012	685
20HE-0010-3	4.00 m	3	1-2-4	0.80	5.24	6.40	0.012	687
21HE-1110-1	4.00 m	1-2-3	4	0.80	5.25	6.40	0.012	685
22HE-0000-1	4.00 m	-	1-2-3-4	0.80	5.22	6.40	0.013	690
22HE-0000-2	4.00 m	-	1-2-3-4	0.78	5.15	6.21	0.013	700

4.4.2 Sand analysis

A standard analysis of the grain size distribution, by using sieves (series (mm): 6.300 5.600 4.750 4.000 3.350 2.800 2.360 2.000 1.700 1.400 1.180 0.850 0.710 0.600 0.500 0.425 0.355 0.300 0.250 0.212 0.180 0.150 0.125 0.108 0.090 0.075 0.063), allowed to state that the sand was almost uniform with an average di-

Table 4.6: Low Energy dynamic tests

Test name	Static level (m)	Drains ON	Drains OFF	H_s (m)	T_m (s)	T_p (s)	S_p	Total mean number of waves
23LE-0000-1	4.00 m	-	1-2-3-4	0.39	6.46	7.88	0.004	557
23LE-0000-2	4.00 m	-	1-2-3-4	0.39	6.41	7.88	0.004	562
23LE-0000-3	4.00 m	-	1-2-3-4	0.41	6.36	7.88	0.004	566
23LE-0000-4	4.00 m	-	1-2-3-4	0.41	6.40	7.88	0.004	563
24LE-1000-1	4.00 m	1	2-3-4	0.42	6.34	7.88	0.004	568
24LE-1000-2	4.00 m	1	2-3-4	0.40	6.35	7.88	0.004	567
24LE-1000-3	4.00 m	1	2-3-4	0.41	6.31	7.88	0.004	571
24LE-1000-4	4.00 m	1	2-3-4	0.41	6.29	7.88	0.004	573
24LE-1000-5	4.00 m	1	2-3-4	0.41	6.32	7.88	0.004	570
25LE-0000-1	4.00 m	-	1-2-3-4	0.41	6.32	7.88	0.004	570
25LE-0000-2	4.00 m	-	1-2-3-4	0.41	6.28	7.88	0.004	573
25LE-0000-3	4.00 m	-	1-2-3-4	0.41	6.25	7.88	0.004	576
25LE-0000-4	4.00 m	-	1-2-3-4	0.40	6.27	7.88	0.004	574
26LE-1100-1	4.00 m	1-2	3-4	0.41	6.25	7.88	0.004	576
26LE-1100-2	4.00 m	1-2	3-4	0.41	6.24	7.59	0.005	577
26LE-1100-3	4.00 m	1-2	3-4	0.41	6.33	7.88	0.004	568
26LE-1100-4	4.00 m	1-2	3-4	0.41	6.27	7.88	0.004	574
26LE-1100-5	4.00 m	1-2	3-4	0.41	6.25	7.88	0.004	576
26LE-1100-6	4.00 m	1-2	3-4	0.42	6.29	7.88	0.004	572
27LE-0000-1	4.00 m	-	1-2-3-4	0.42	6.26	7.88	0.004	575
27LE-0000-2	4.00 m	-	1-2-3-4	0.42	6.30	7.88	0.004	571
27LE-0000-3	4.00 m	-	1-2-3-4	0.42	6.33	7.59	0.005	569

Table 4.7: Medium Energy dynamic tests

Test name	Static level (m)	Drains ON	Drains OFF	H_s (m)	T_m (s)	T_p (s)	S_p	Total mean number of waves
28ME-0000-1	4.00 m	-	1-2-3-4	0.59	6.23	7.88	0.006	578
28ME-0000-2	4.00 m	-	1-2-3-4	0.60	6.26	7.88	0.006	575
28ME-0000-3	4.00 m	-	1-2-3-4	0.59	6.27	7.88	0.006	574
28ME-0000-4	4.00 m	-	1-2-3-4	0.60	6.25	7.88	0.006	576
29ME-1000-1	4.00 m	1	2-3-4	0.57	6.22	7.88	0.006	578
29ME-1000-2	4.00 m	1	2-3-4	0.60	6.22	7.88	0.006	579
29ME-1000-3	4.00 m	1	2-3-4	0.60	6.23	7.88	0.006	578
30ME-1100-1	4.00 m	1-2	3-4	0.60	6.20	7.88	0.006	581
30ME-1100-2	4.00 m	1-2	3-4	0.60	6.20	7.88	0.006	137
30ME-1100-4	4.00 m	1-2	3-4	0.60	6.16	7.88	0.006	585
31ME-1110-1	4.00 m	1-2-3	4	0.60	6.23	7.88	0.006	578
31ME-1110-2	4.00 m	1-2-3	4	0.60	6.21	7.88	0.006	580
31ME-1110-3	4.00 m	1-2-3	4	0.60	6.18	7.88	0.006	583
32ME-0010-1	4.00 m	3	1-2-4	0.61	6.18	7.88	0.006	583
32ME-0010-2	4.00 m	3	1-2-4	0.61	6.18	7.88	0.006	583
32ME-0010-3	4.00 m	3	1-2-4	0.60	6.16	7.88	0.006	584
33ME-0000-1	4.00 m	-	1-2-3-4	0.61	6.17	7.88	0.006	583
33ME-0000-2	4.00 m	-	1-2-3-4	0.61	6.22	7.88	0.006	579
33ME-0000-3	4.00 m	-	1-2-3-4	0.61	6.22	7.88	0.006	579
33ME-0000-4	4.00 m	-	1-2-3-4	0.61	6.22	7.88	0.006	579

ameter (d_{50}) equal to 0.33 mm as Fig.4.16(a) shows. In the Udden-Wentworth scale (Fig.4.16(b)) the sand can be classified as medium. However the sand has also a small percentage of finer fraction due to water derivation from a river near the laboratory, although it was filtered before entering in the channel.

In order to analyze the filtration processes inside the beach, the average fall velocity and the coefficient of permeability were measured on samples at the laboratories of Politecnico of Bari. The following two sections deal with the measurement method of these parameters. It is necessary to highlight that it was not possible to perform measures on the undisturbed samples. So the parameters are affect by the the effects due to the sampling, which influences saturation degree, water content and compaction index of the porous medium.

Average fall velocity

The fall velocity ω was measured by a settling tube in which a high sensitive probe (a) measures the sample weight that settles in a tank inside the tube ([115]). Moreover a probe (b) measures the pressure increasing in the water column due to the sudden immersion of the sand sample. The Fig. 4.17 shows some details of the adopted experimental facility. The mean settling velocity of the sand can be obtained as the ratio between the height covered by the sample and the average settling time ($\omega = H/T_m$). The value of T_m is calculated in-

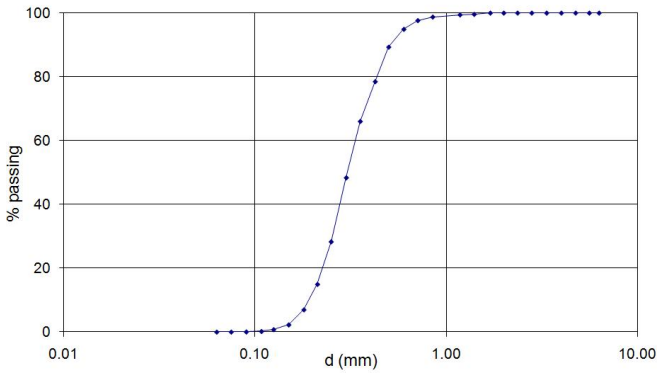

(a) Sand grainsize curve

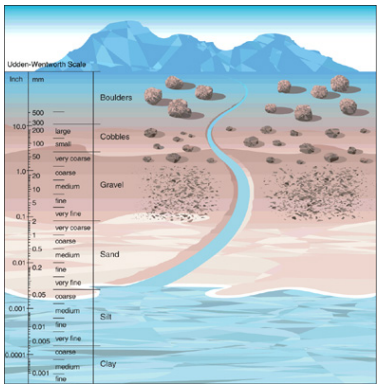

(b) Udden Wentworth scale

Figure 4.16:

tegrating the weight/time curve (Fig. 4.18) and dividing it by the difference in weight between the start and the end of the test. The sand used in laboratory had an average settling velocity equal to $4.8cm/s$.

Sand hydraulic conductivity

The sand hydraulic conductivity was measured by using a constant-head permeameter, typically adopted for coarse grained soil like as gravel and sand. In the Fig. 1.19 the sketch of the used constant-head permeameter with dimensions is shown. The sand permeability is indirectly measured from the application of Darcy's formula as the following

$$\frac{V}{t} = k\frac{h}{l}A \tag{4.8}$$

where V is the water volume which infiltrates through the soil column in the time t, k expresses the sand hydraulic conductivity, Δh represents the hydraulic head on the sample and l and A are respectively the length and the area of the soil column.

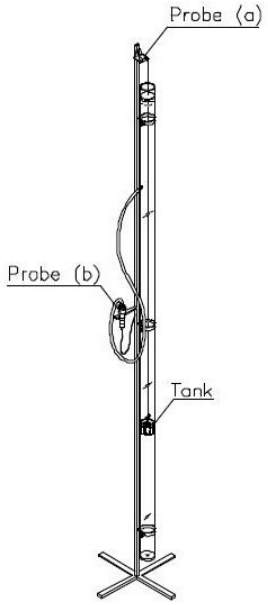

(a) Sketch of the settling tube

(b) Settling tube used in the laboratory

Figure 4.17:

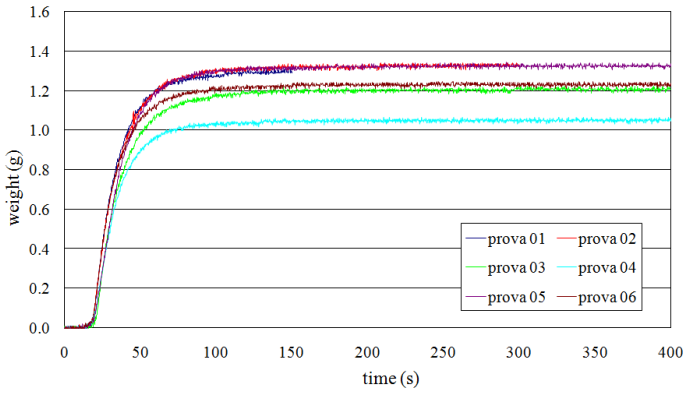

Figure 4.18: Weight/time curve

The reservoir and the cell were connected by a small pipe 1.60 m long with a diameter equal to 5 mm. The high head losses which occurred in the small pipe required two tests in order to estimate the sand permeability. The first aimed to measure the water flow discharged from the empty permeameter in a time equal to 200 s. The second one allowed to calculate the water flow filtered through the saturated soil column in the same time t of 200 s, under a constant hydraulic head. This allow to calculate the head losses in the small pipes, and then the dissipated hydraulic head in the soil column, giving a coefficient of permeability

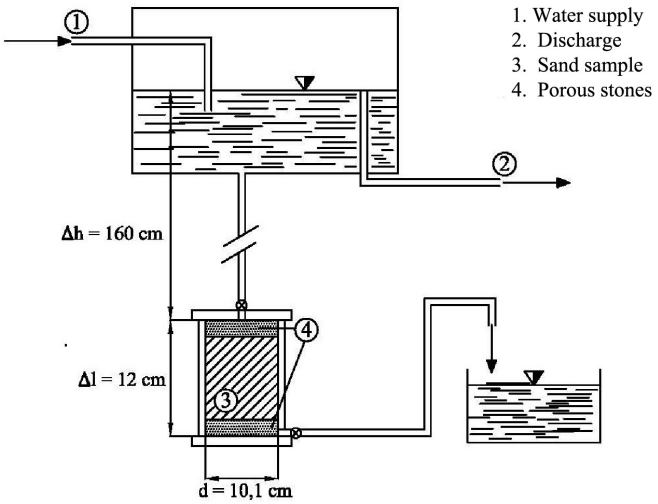

Figure 4.19: Sketch of the constant-head permeameter

equal to $3.2 * 10^{-}3$ cm/s.

4.4.3 Adopted instrumentation

During the tests the morphodynamic and hydrodynamic behavior of drained beach was analyzed by using the data sampled by a large number of instruments. Surface elevation, pressure, velocity, drainage flow and beach profile were measured in order to study nearshore processes. The installed instruments in the channel were:

- 20 wave gauges;
- 12 piezometers;
- 16 pore pressure transducers;
- 4 elettromagnetic currentmeters;
- 2 altimeters;
- 1 propeller;
- 1 flowmeter;
- 1 bottom profiler;
- 64 rods.

The time series recorded by wave gauges, pore pressure transducers, elettromagnetic currentmeters, altimeters and propeller were sampled by 64 channels

PRESTON acquisition system adopting a sampling frequency f = 20 Hz. The recording signals of adopted instruments during the tests were subjected to a processing by filtering of raw data and a successive evaluation of the principal hydrodynamic characteristics. In the following each instrument and the measurement method adopted for the present study will be deeply described.

Wave gauges

The surface elevation was evaluated by means of 20 wave gauges (WG), placed along the wave flume on the right wall with respect to the paddles (Fig. 4.20). The planimetric position is illustrated in table 4.8.

The one wire type wave gauges used in the Large Wave Channel (GWK) are

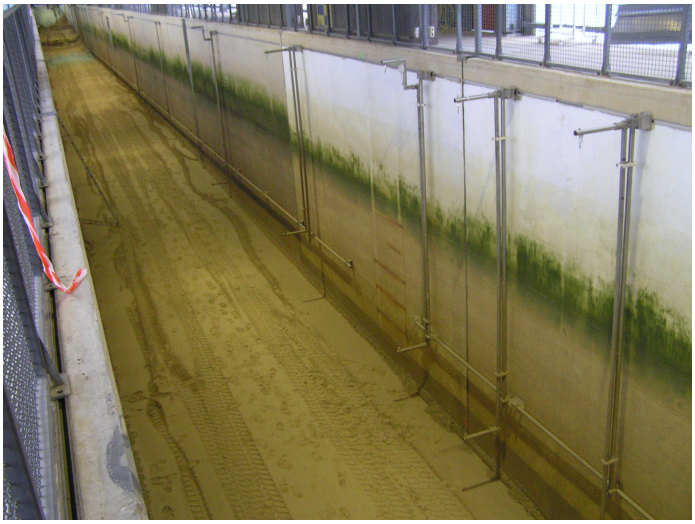

Figure 4.20: Wave gauges along the channel

based on a combined 'resistance-capacity' technique. Each of the wave gauges consists of two electrodes, a measuring wire and the ground plane. In the GWK the electrical ground is formed by the mechanical supporting frame using aluminum pipes.

The measuring principle substantially based on measuring the voltage drop which is proportional to the depth of immersion of the wire. To avoid aberrations from the length of the cable between the measuring site and the data acquisition unit for each wave gauge a water sealed pre-amplifier is used which has to be installed near the wire. The instruments measurement range goes form 2 m to 7 m. The minimum length is restricted by the required minimum electrical resistance of the measuring wire of about 5 Ohms. The maximum length is only limited by practical mechanical reasons.The measurement accurancy is around ± 1 cm while the sampling frequency is 50 Hz. Before the test starting, the wave gauges were subjected to the preliminary calibration on the

Table 4.8: Planimetric position of the 20 resistive wave gauges

Wave gauge	Distance from wave generator (m)	Wave gauge	Distance from wave generator (m)
1	50.10	11	108.00
2	52.20	12	116.00
3	55.90	13	126.22
4	61.30	14	140.00
5	79.05	15	161.90
6	81.15	16	180.00
7	84.85	17	200.00
8	90.25	18	210.00
9	97.30	19	220.00
10	102.09	20	230.00

basis of the water levels. The calibration curve is S-shaped with a nearly linear part of around 80% of the wire length.

Water table measures

A set of 12 piezometers (P) and of 10 pore pressure transducers (PT) were installed along the beach profile in order to measure the water table fluctuations during the tests (Fig.4.21).

Each pressure cell was placed at about the same depth of drains and at about

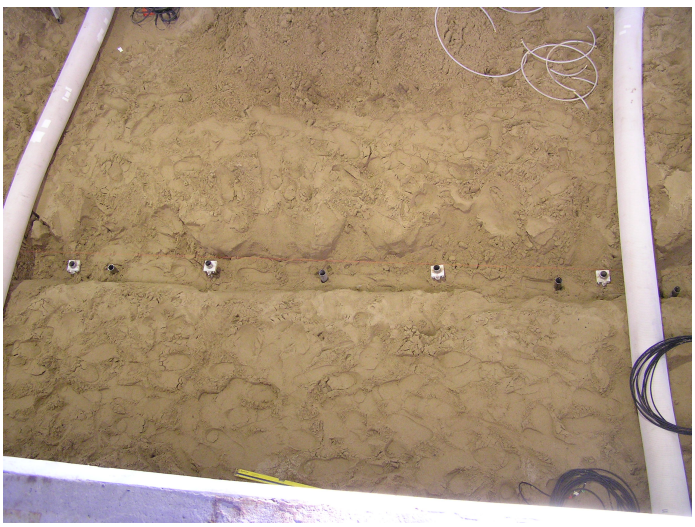

Figure 4.21: Piezometers (P) and pore pressure transducers (PT) placed inside the beach

2 m from the left wall of the flume with respect to the wave generator. Pore pressure transducers were placed at the same depth of the piezometers below the drains but at different planimetric positions. Table 4.9 reports accurately the planimetric and altimetric position of the sensors. The former with respect to the wave generator while the latter represents the distance from the bottom of the channel.

The pore pressure sensors of the piezometers (Fig.4.22(a)) were connected by a

Table 4.9: Planimetric and altimetric position of pressure cells of piezometers and pore pressure transducers

Piezometers	x (m)	y (m)	Transducers	x (m)	y (m)
P1	237.8	3.2	PT1	238.83	3.186
P2	239.79	3.2	PT2	240.80	3.182
P3	241.79	3.2	PT3	243.79	3.188
P4	242.72	3.2	PT4	246.28	3.195
P5	243.89	3.2	PT5	247.63	3.193
P6	245.55	3.2	PT6	249.56	3.191
P7	246.68	3.2	PT7	253.63	3.197
P8	247.33	3.2	PT8	242.10	3.460
P9	248.59	3.2	PT9	42.40	3.470
P10	250.50	3.2	PT10	252.00	3.450
P11	251.70	3.2			
P12	252.30	3.2			

small pipe (diameter = 0.20 mm) to 12 pvc pipes, fixed on the wall. The mean water table levels were obtained by measuring manually the water level in the pvc pipes through freatmeters (Fig. 4.22(b)). Data recording was carried out every 5 minutes during the static tests and every 10 minutes for the dynamics one. Fig. 4.22 shows an example of the time variation of relative maximum water tables,Δh_{max}, measured by a piezometer. The duration of tests was set to achieve a quasi-stationary condition of the water table evolution on the beach. The optimal setting of the duration of the tests is clear from analysis of the space-time variation of the water table lowering as figure 4.22 shows. At the beginning of each day the piezometers were calibrated with the static water level in the channel. Moreover once a day they were washed by a counter-current flow in order to avoid the blockage due to the sand particles.

The pore pressure transducers were constituted by a pressure cell protected by a filter-stone (Fig. 4.23) which seperates the soil-pressure from the pore-pressure with a range of measurement of $70 \div 100$ kPa and an accurancy of $\pm 0.06\%$. The transducers sampled continously during each run.

(a) Pressure cell of the piezometer

(b) PVC pipes of piezometers and freatmeters

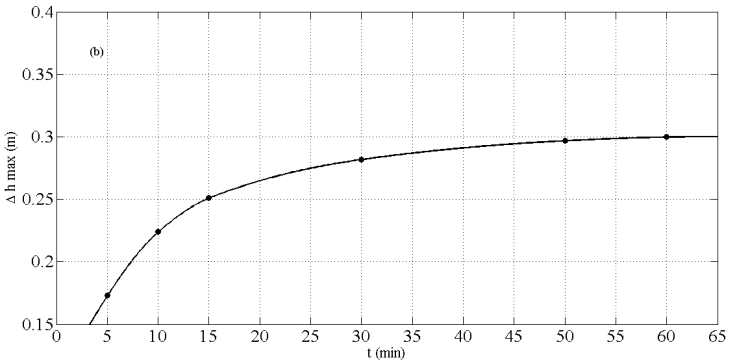

Figure 4.22: Example of the time variation of relative maximum water tables by a piezometer (S1 test - D1 on)

Other 4 pore pressure transducers with the same characteristics of the mentioned ones were located inside the lower zone of the terminal part of each drain (Fig. 4.24). These transducers were used in order to measure the hydraulic head inside drains and understand if drains work under pressure or not.

In the Table 4.10 the planimetric (with respect to the wave generator) and altimetric (referred to the bottom of the channel) position of transducers placed inside drains is reported.

Figure 4.23: Pore pressure transducer inside the sand

Figure 4.24: Pore pressure transducer inside the drain

Drained flow measures

The measurements of the drainage discharge were performed using both a flow meter and a pore pressure transducer(PT15) placed in the pumping well. The

Table 4.10: Planimetric and altimetric position of pore pressure transducers placed in the drains

PT	x (m)	y (m)
PT11	242.25	3.189
PT12	244.83	3.189
PT13	251.52	3.195
PT14	247.00	3.450

flow meter (Fig. 4.25) was located on the external pipe used for removing the drainage flow. It has an internal digital oscilloscope and his sampling frequency was set equal to 1 Hz. The pore pressure transducer was placed at 0.08 m from

Figure 4.25: Flow meter placed on the external iron pipe

bottom pump station and at 1.69 m from the bottom channel (Fig. 4.26).

With referring to the phases of the automatic switch on and switch off of the pump inside the station during the experimental tests with the drains, the water level in the pump station measured by the submerged pressure transducer

Figure 4.26: Pore pressure transducer placed in the pumping well

shows a so-called 'sawtooth profile' (Fig. 4.27). During the filling up of the pumping well, the time evolution of the water level results linear for an interval corresponding to the water time from the first to the second buoy of the pump (Fig. 4.28). Successively during the filling down of the water inside the

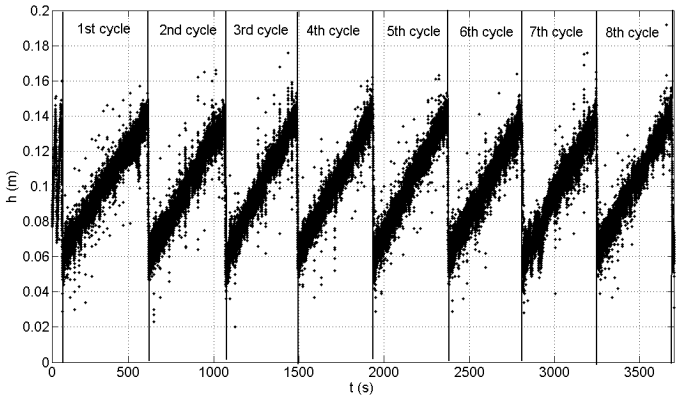

Figure 4.27: Example of time variation of water level in the pump station by the PT15

station induced by the pump, a decreasing trend has been observed. A cyclic phenomenon has been shown until the end of each experimental test having one or more drain opened. The number of cycles was variable as function of the value of the drainage discharges.

The mean drainage flows have been calculated through the measurements of pressure transducer (PT15), placed in the pump station. Starting from the evaluation of the mean time, t_m, of all pump cycles, and the mean water depth, h_m, deduced as difference between the maximum and the minimum levels of

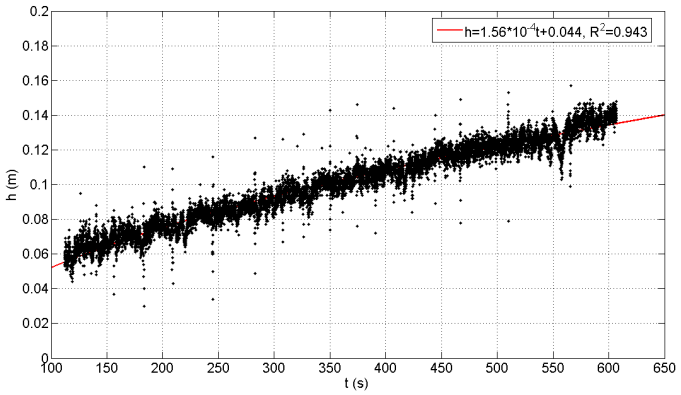

Figure 4.28: Example of the time variation of water level in the pump station for each cycle by the PT15

each cycle. The mean drained volume V_m is calculated as follows:

$$V_m = h_m A \tag{4.9}$$

where A (pump station area) = 3.4 mq. The values of the main drained discharge Q_m (l/s) were calculated as

$$Q_m = \frac{V_m}{t_m} \tag{4.10}$$

The drained flows have been calculated using a different method by the flow meter recording. Because the flow meter was placed on the external pipe of the flume, it measured the time of the water passage into the pipe, during the well emptying induced by the pump. The first step was the evaluation of the mean time, t_m, between successive signal peaks recorded by the flow meter and the mean drained volume from the water level in the pump station. The evaluated mean time corresponded to the emptying time of the pump station. The mean drained discharge has been calculated, as in the case of the pressure transducer. Fig. 4.29 shows an example of the time variation of the flow meter signal, highlighting the different filling up cycle in the pump station, and the possible passage of the water flow in the external iron pipe.

Beach profiles

After each run the submerged and emerged beach profile was measured by a profiler placed on the carriage of the flume. The profiler was made of a wheel, a metal jib and an acquisition system installed on the carriage (Fig. 4.30). A 7.60 m long sensor arm is used of which the upper end is pivoted on a test rig trolley (measuring platform) movable along the flume over a distance of about 250 m in x-direction. Its lower end is attached to a three-divided pulley that rolls over the sand bedding. The wheel was directly connected to the acquisition system

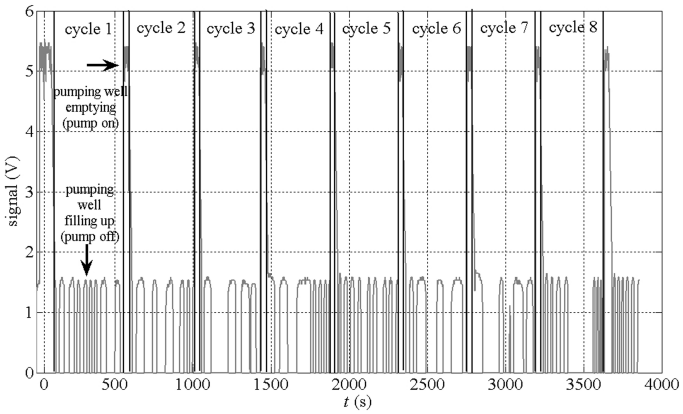

Figure 4.29: Example of the time variation of flow meter signal

and transmitted, every about 0.025 m, the exact profile position, starting from x = 206.8 m to x = 252.6 m, inside the closure depths of the beach in different wave conditions. This measured part of bottom was particularly influenced by

Figure 4.30: Beach profiler mounted on the carriage

morphodynamic effects induced by the effect of wave motion and drains. The metal jib, with its vertical movement, gave the profile vertical height, while the carriage allowed the possibility to move the profile during the acquisition of the longitudinal bottom profile.

A set of 60 metal rods with washers have been arranged along four lines spaced from the lower swash zone to the berm (Fig. 4.31). Rods had height of about 1.2 m and a relative longitudinal and transversal distance of 1 m.

These instruments have been adopted to determine the Depth of Disturbance

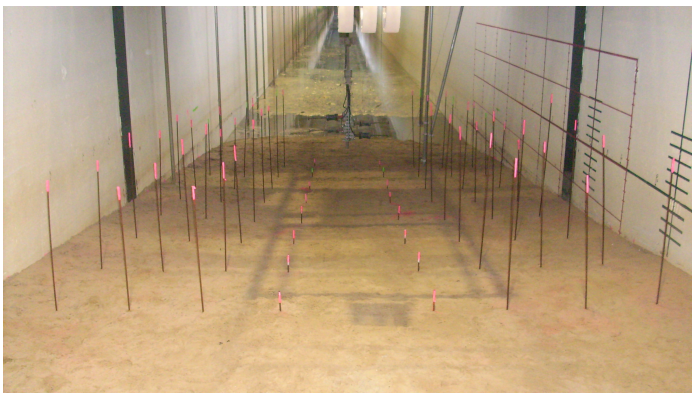

Figure 4.31: A view of the rods-grid

inside the surf zone in order to understand the near shore morphodynamic features with or without drains. Manual readings of the depth of the washer and bed elevation were undertaken at the end of each run after stopping the wave paddle using a graduated pin with millimeter precision.

4.5 Hydrodynamics of the shore-zone

4.5.1 Introduction

The presence of a singularity such as a drain in the sand leads to a substantial change in the hydraulic regime of the groundwater system inside the beach ([112], [108]). The water table trend highlights the system effectiveness in increasing the thickness of the unsaturated layer. This effect is induced by the activation of the drains for both static and dynamic conditions.
In the following sections the effects of the BDS on the nearshore hydrodynamics are discussed by showing laboratory test results. Water table (Section 4.5.2), drained flows (Section 4.5.3) and hydraulic regime inside drains (Section 4.5.4) are reported in both undrained and drained conditions for static and dynamic tests. Moreover tests under different wave energy has enabled to analyze the effects of the drainage also on the maximum set-up (Section 4.5.5) and on the undertow currents (Section 4.5.6).

4.5.2 Water table

The present section deals with the influence of the beach drainage on the groundwater behavior in static conditions and under wave attacks by means of the analysis of the water table fluctuations.
As aforementioned (section 4.4.3) water table behavior was measured by using

both piezometers and pore pressure transducers placed inside the sand. Figure 4.32 shows an example of the local hydraulic head decreasing (Δh) measured by piezometers (blu line) and transducers (red line) at the end of the static test S2 ($t = 60'$) with the working drain D2 (Tab. 4.3). The x positions refer to wave generator section. Although piezometers and transducers give static (mean) and dynamic measurements respectively, the comparison highlights the good agreement between the two kinds of measurement. For this reason in the

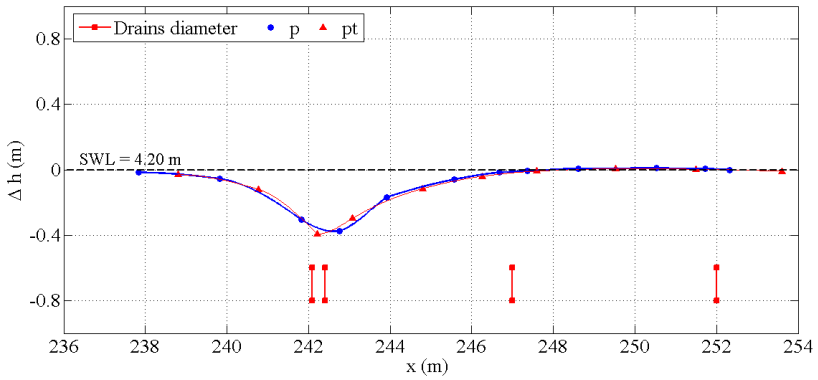

Figure 4.32: Spatial variation of relative water table by piezometers and transducers at t = 1 h for test S2 with D2 on

next graphs only data collected by the piezometers will be presented.
Figure 4.33 reports an example of the spatial variation of water tables evaluated at different time step measurements (t = 5', 10', 15', 30', 50' and 60') for S1 test with drain D1 opened. The figure 4.34 report the water table lowering (Δh) respect the initial static level for the tests S1 with single drains configurations at the end of each run ($t = 1$ h). The effect of drains on the groundwater behavior is the lowering of the saturation line, resulting in an increasing of unsaturated area inside the beach. For all tested configuration the maximum lowering occurs in correspondence of the activated drain. The drain influence decreases moving away from the section in which the drain is placed. It can be observed that the drains D1 and D2 affects the sea mean water level much more than the drains D3 and D4. This occurs because the first two drains are closer to the shoreline with respect the other two. These are placed in the inner zone of the beach. In particular the water table lowering induced by the fourth drain is localized over the drain with no influence on the saturation degree inside the run-up zone. The drains position with respect to the initial shoreline influences also the maximum water table lowering. In particular the maximum value occurs for D3 and it proves to be 0.37 m, which corresponds to about 92% of the drain upper part

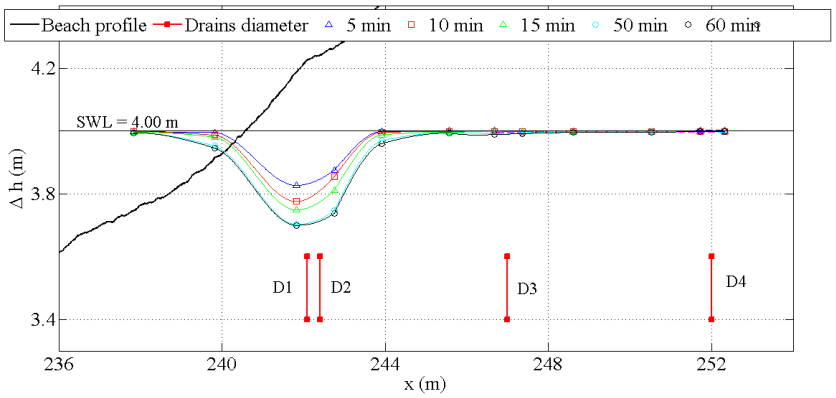

Figure 4.33: Spatial variation of the water tables evaluated by the piezometers at different time steps (Test S1 - D1 on

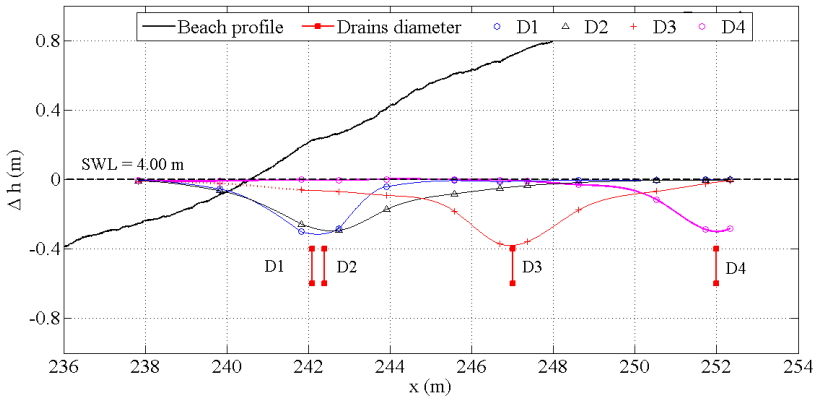

Figure 4.34: Spatial variation of the water tables at t=1h for single drains working - Test S1

of the drain depth. The opening of D1 and D4 produces a water table lowering of 75% and 72% respectevely in the depth of the upper part of the drains. The best efficiency in water table lowering given by D3 is probably due to its planimetric placement, also confirmed by dynamic tests. The drain D1 is the nearest to the shoreline and, consequently, it receives not only the vertical infiltration flux through the porous medium but also the water directly from the channel. The position of D4 proves to be influenced by the higher degree of compaction due to the upper sand weight with respect to D1 and D3.
The system was tested in different drain configurations, also opening more drains simultaneously. As an example the figure 4.35 shows the water tables with the drain D1, and the addition of D2 and D2+D3. This comparison allows to

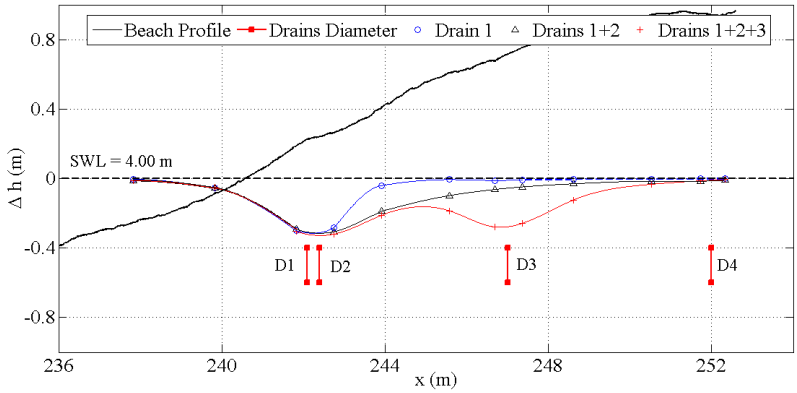

Figure 4.35: Spatial variation of water tables for test S1 with D1, D1+D2, D1+D2+D3 on

analyze the influence of the drain diameter by comparing the first two configurations. The addition of the only D2 does not produce an increasing of water table maximum lowering (see Table 4.11) but it leads to a remarkable increase of the unsaturated area emphasized by the addition of D3. The figure 4.36 reports an example of saturated and unsaturated areas considered for the D1. The saturated reference area (A_s) is defined by the grey rectangular in the figure. The basis is calculated as the difference between the x-positions of the last piezometers placed inside the sand (252.33 m) and the initial shoreline (240.55 m). The height corresponds to the drain depth with respect to the undisturbed water table (0.4 m).The unsaturated area (A_u) is bounded by the mean water table after drainage and the above initial undisturbed one (the red-colored area in the figure). The ratio between A_u and A_s has been regarded as an indicator of the system efficacy in reducing the sand saturation degree. The three drains

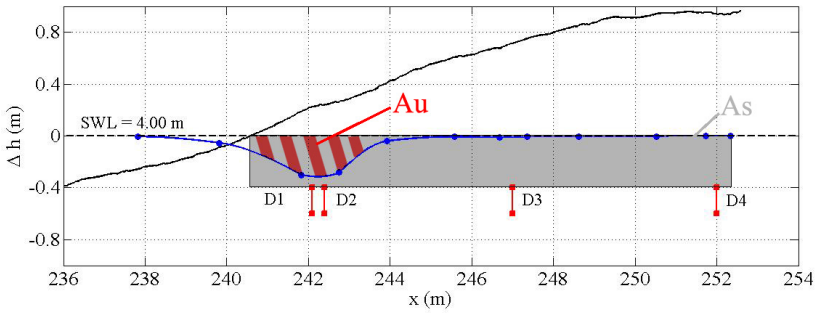

Figure 4.36: Spatial variation of water tables for test S1 with D1, D1+D2, D1+D2+D3 on

opened simultaneously were tested in order to evaluate the possible advantages in using more drains in the field application. In this case the distance between D2 and D3 leads to the suppression of their mutual influence. The water table rises between D2 and D3, reaching about the same value induced by D1 and D2. The maximum lowering occurs in correspondence to D1 and D2 because these drains simulate a single drain of double diameter.
The above system configurations were also tested with a higher static level in the channel equal to 4.20 m. Figure 4.37 reports the spatial variation of the water table for all single drain configuration tested. As observed for tests S1, the

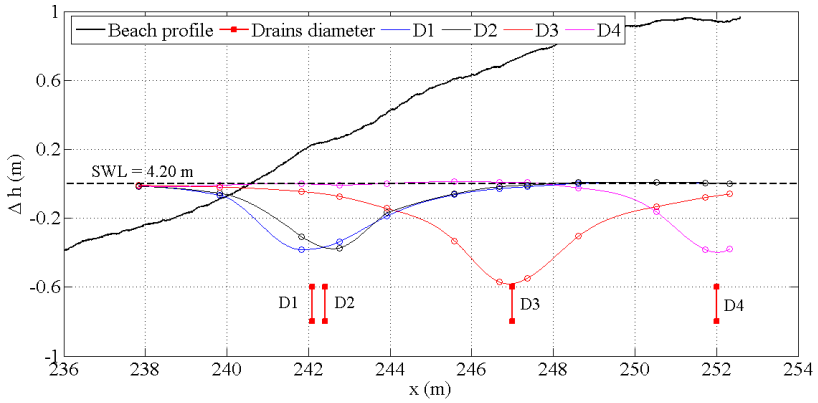

Figure 4.37: Spatial variation of the water tables at t=1h for single drains working - Test S2

maximum water table lowering occurs when the drain D3 is open and it is equal

to 0.57 m that is about 95% of the drain upper part of the drain depth. The opening of D1 and D4 produces a quite similar water table lowering of 63%. The system behaviour with more drain working simoultaneously was tested also with the higher static water level. Figure 4.38 reports the spatial variation of water tables at the end (t=60') of static test S2 with D1, D1+D2 and D1+D2+D3 opened. The addition of the drains D2+D3 causes a small increasing of water

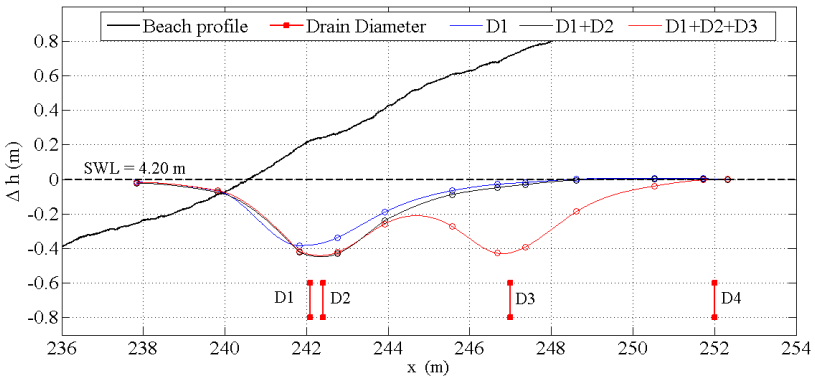

Figure 4.38: Spatial variation of water tables for test S1 with D1, D1+D2, D1+D2+D3 on

table lowering. Also with a higher water level in the channel, the most noticeable effects of using more drains together is the reduction of saturated area. As a matter of fact the ratio A_u/A_s is about 1.7 for the first drain. This values increases adding the second drain up to 3.5 for the configuration of the three drains working together (see table 4.11).

As mentioned in the section 4.4 the higher static water level in the channel allows to simulate a deeper position of drains with respect to the undisturbed water level. The comparison of water tables for all drain configurations and with both water level conditions shows that, in general, a deeper water table lowering correspond to a deeper drain placement with respect to the mean static level. As an example in figure 4.39 the water table lowering induced by the activation of D1 and D3 for both static tests are compared. It can be observed that the maximum depression of the water table is more relevant when the static water level is higher. Nevertheless the hydraulic head on drain is the same for both water levels. In all configuration sampled in laboratory the water table has never reach the drain with a consequent residual head on it. This is probably caused by the system resistances due to the characteristics of the drainage pipes or of the geotexile which covers the drains. Figure 4.40 shows the spatial variation of water table lowering for the wave energy test HE with in undrained conditions. The

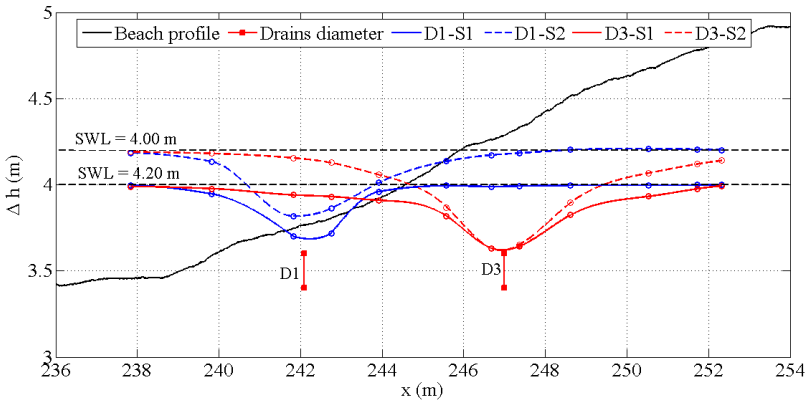

Figure 4.39: Comparison between the spatial variation of water tables for test S1 and S2 with D1 and D3 on separately

beach profile measured at the end of test (about 1h) is reported. As expected the wave motion produces a rise of the water table with respect to the static level and the maximum run-up, evaluated by video recording, is located close to the upper horizontal beach portion. This value is located offshore with respect to the maximum water table level inside the beach ([116]). Figure 4.41 shows an

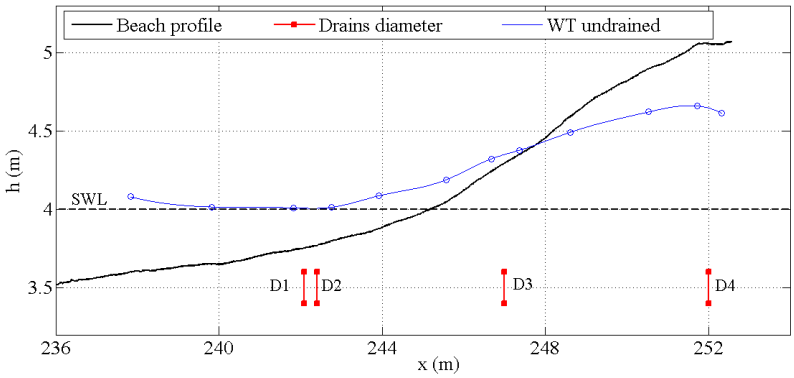

Figure 4.40: Spatial variation of water table for test HE - Undrained conditions

example of the spatial variation of water tables for test HE in both undrained and drained conditions with D1. Generally dynamic tests are characterized by a smaller lowering of the water table with respect to the static conditions due to run-up flow. An *active infiltration zone* is defined as the beach area limited by

Table 4.11:

Test	Drain	Δh_{max} (m)	$\Delta h_{max}/D_d$ (%)	A_s (m^2)	A_u (m^2)	A_u/A_s (%)
S1	D1	0.3	75	7.07	0.86	12.22
	D2	0.29	73.25	7.07	1.24	17.6
	D3	0.37	92.25	7.07	1.63	23.12
	D4	0.28	72	7.07	0.58	8.27
	D1+D2	0.31	76.5	7.07	1.41	19.7
	D1+D2+D3	0.32	80	7.07	2.11	29.8
S2	D1	0.38	63.7	8.3	1.42	17
	D2	0.37	62.16	8.3	1.23	14.8
	D3	0.57	95	8.3	2.6	31.3
	D4	0.38	63.7	8.3	0.72	8.65
	D1+D2	0.43	fare	8.3	1.7	20
	D1+D2+D3	0.43	fare	8.3	2.9	34.8

shoreline position and maximum run-up ([116]). This zone is important because it involves infiltration and ex-filtration processes during up-rush and backwash phases influencing sediment movement. An increase in the vertical flux motion produces a sediment drift which otherwise would be transported offshore during wave run-down. With reference to the active infiltration zone, the onshore zone is not influenced by the wave motion and therefore no sediment transport occurs. The present study thus focuses on the area shown in 4.41, where the mean shoreline section is evaluated at the end of the undrained test. The opening of D1 induces a water table depression along the beach which leads to a decrease in the saturated area inside the active infiltration zone of about 44% (shaded area of 4.41). This phenomenon was noted for all dynamic tests and drain configurations. In addition, the drain is able to move the maximum water table value offshore with respect to the undrained condition.

As shown for the static tests, also when waves run in the channel the maximum water table lowering occurs with the D3 on (Figure 4.42). Results for test LE are note represented because of the D3 was not tested with low energy attack. As a consequence a major unsaturated area (inserire percentuale) induced by the activation of D3 can be observed. The best efficiency of the system when D3 works is probably due to the position of the drain close to the run up zone and thus directly interested by the run-up flow which infiltrates inside the beach.

The figure 4.43 shows the maximum water table lowering for all tested drains configurations as a function of the offshore zero-order moment of wave power spectrum, m_0. It can be observed that.....

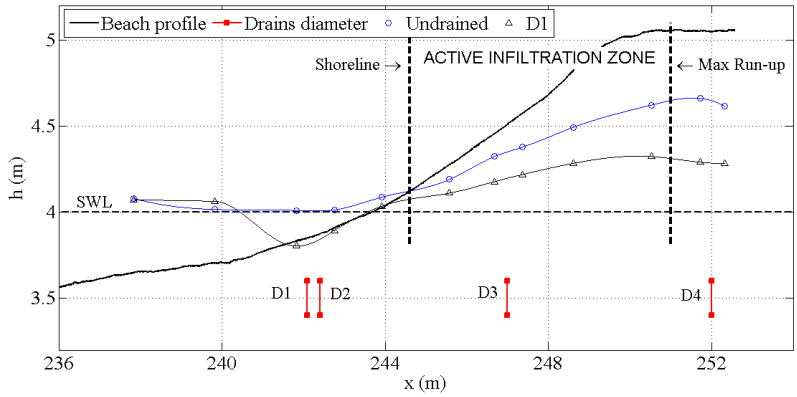

Figure 4.41: Spatial variation of water tables for undrained and drained conditions for Test HE - D1 on

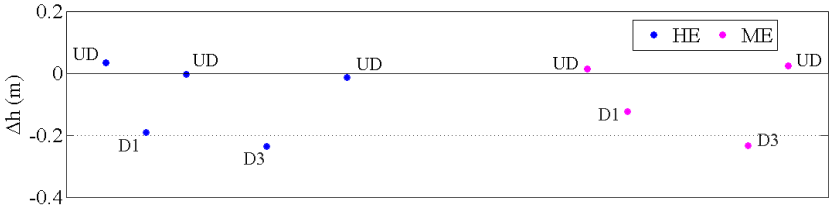

Figure 4.42: Maximum water table lowering - tests HE and ME with single drains on

4.5.3 Drained flow

In the following drained flows Q measured during tests will be reported and discussed. Moreover the obtained results will be compared with water table lowering.

Collected data on drained flow were evaluated using both flow meter installed on the external iron pipe and the pore pressure transducers placed in the pumping well (see 4.4.3). In figure 4.44 measured flows with all tested drain configuration are represented for both static tests S1 and S2 by both flowmeter and pore pressure transducer. These measurements generally well agree even if the flow meter measurements appear slightly underestimated (red circles and pink àtriangles in Fig. 4.44). This behavior can be observed for all static and dynamic tests.

The drainage discharges prove to be higher for static tests S2. This result confirm the higher values of water table lowering discussed previously.

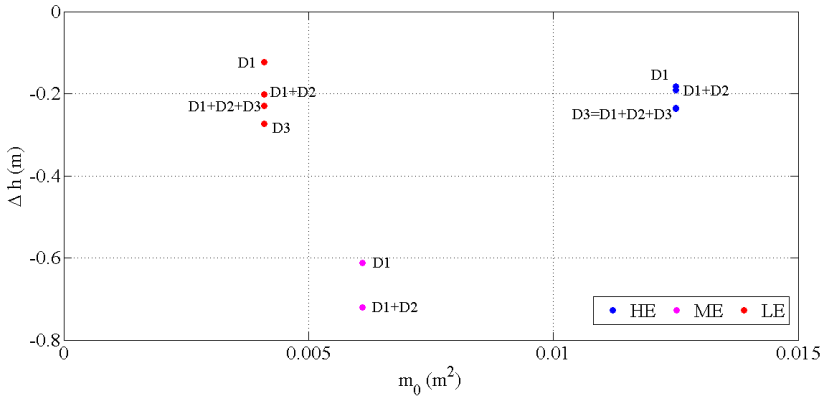

Figure 4.43: Maximum water table lowering - tests HE, ME and LE - all drains configurations

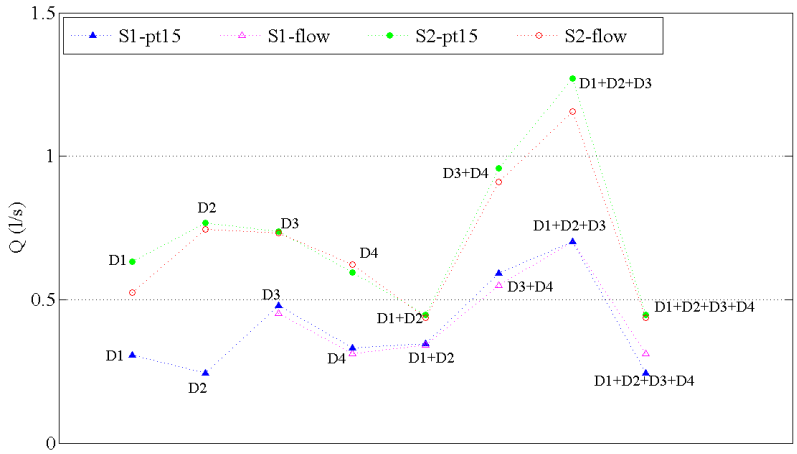

Figure 4.44: Drained discharged by flowmeter and pt15 for tests S1 and S2 - all drains configurations

The same flows are represented in figure 4.45 as a function of the distance of drains from the shoreline. The blue triangles are referred to the static test S1, while the red circles represents the Q evaluated during the static tests S2. Unlike the previous experiments performed at LIC, obtained results show that it is not possible to define a relationship between the drained flows and the

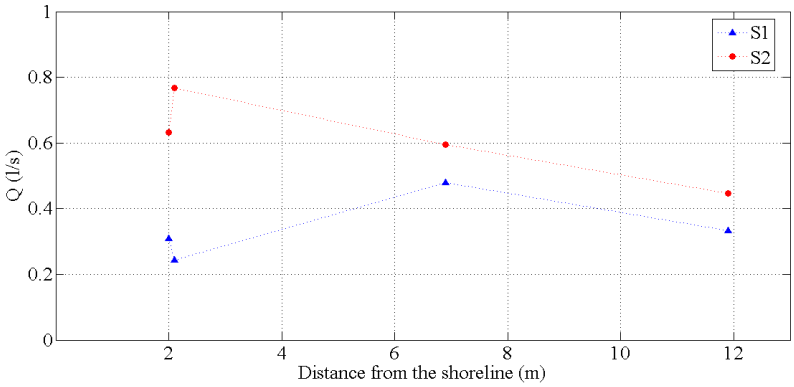

Figure 4.45: Variation of the drained discharged vs distance from the shoreline for tests S1 and S2 with D1, D2, D3 and D4 on

drain distance from the initial shoreline. For tests with static water level in the channel equal to 4.00 m, the maximum water discharge occurs when D3 works. This is equal to 0.479 l/s. During S2 tests the drained water decreases moving away form the shoreline position. As a matter of fact the Q_{max} is registered when the drain D2 works an it is equal to 0.75 l/s. Figure 4.46 reports the drained flows with the addition of D2 and D2+D3 to the first drain D1 for both tests S1 and S2. If the drains work simultaneously, the total drained flow should

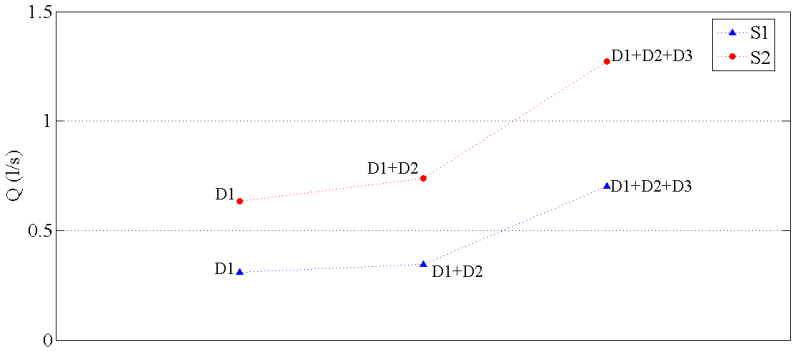

Figure 4.46: Drained flows with coupled drains working for tests S1 and S2

be equal to the sum of discharged flow of each drain pipe. This should be if there was no influence between drains. As a matter of fact the theoretical flow

has been evaluated with the previous assumption for all test configuration. The results are reported in figures 4.47(a) (test S1) and 4.47(b) (test S2). In both

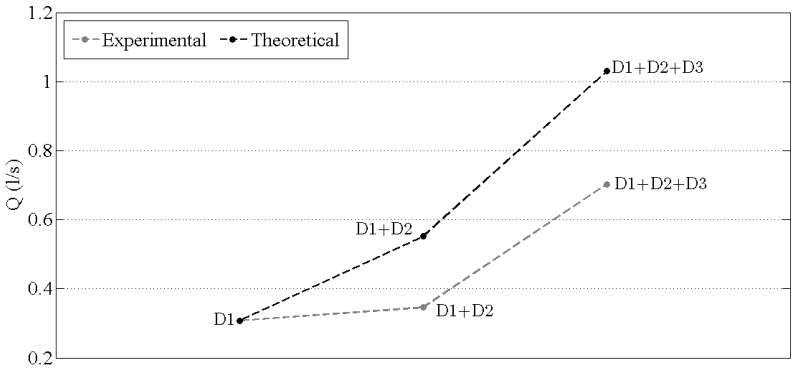

(a) Measured and theoretical drained flows - test S1

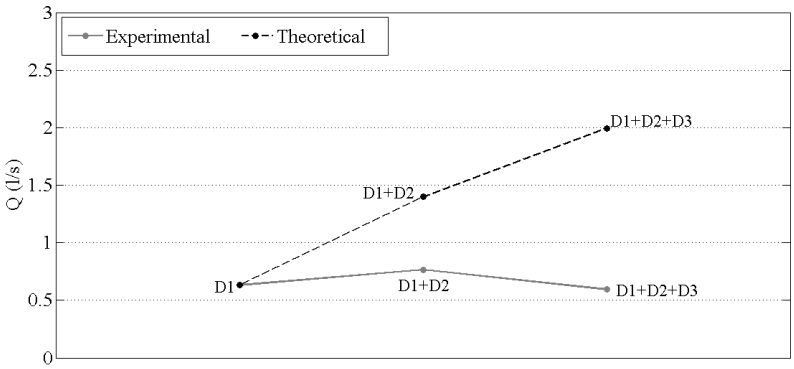

(b) Measured and theoretical drained flows - test S2

Figure 4.47:

figures the dashed lines represent the theoretical drained flows while the dotted lines represent the measured flows in the same test configurations. It can be observed that the measured flow is smaller than theoretical one for all drains configurations, showing a non linear interaction among drains.
For all tests evaluated drained flows result to be smaller than measured ones in field applications. This could be due to the hydraulic behavior of the drains which will be deeply discussed in the following section (**??**). For the static

tests, the drained discharges were higher for S2 with respect to S1, showing a poorly-defined trend during the activation of each drain and higher values when more drains were opened. With the already described procedures, the drained flows have been calculated in different drain configurations under different wave energy attacks. For all dynamic tests the drainage discharges were higher and better defined with respect to the static cases, ranging from 0.5 l/s to 1.9 l/s. However also during dynamic tests the drained flows resulted very low, probably because of the energy losses along drains during water infiltration.
As an example figure 4.48 reports the mean drained flows Q_m evaluated for all drain configurations under the high wave energy attack by the pressure transducer placed inside the pumping well. The values of Q_m deduced by the trans-

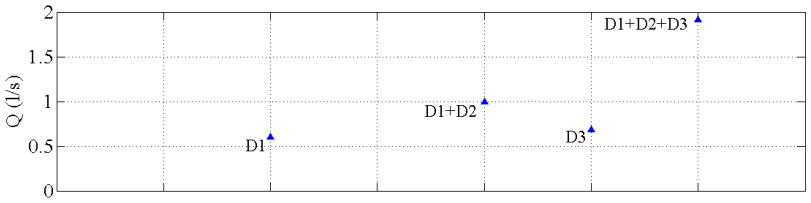

Figure 4.48: Mean drained flow for test HE - all drains configurations

ducer placed in the pumping well as a function of offshore wave parameters such as the zero-order moment of wave power spectrum m_0, mean wave celerity c_0, and mean wave energy flux P_0 are shown in Fig. 4.5.3for dynamic HE, ME and LE tests. Moreover data obtained for static test S1 are reported in the figure compared with dynamic conditions. The increasing trend of Q_m is directly associated with m_0 and P_0, showing higher values when more drains work. Note that the highest values of c_0 are not associated with the maximum drainage discharges which therefore appear to be related to the maximum incident wave energy and wave steepness. With reference to the drained flows by the system, their increase is directly associated to the values of m0, showing higher values when more drains function. This tendency corresponds to a decrease in maximum set up (Figures 4.50 and 4.51)

4.5.4 Hydraulic regime inside drains

The drain efficiency in collecting the drained discharge by the groundwater system depends on their hydraulic regime and the sand characteristics. The efficiency is also strongly influenced by the pipe characteristics and the hydraulic regime. The head losses on the external surface of drains and their capability in collecting the drained discharge influence both the water table lowering and

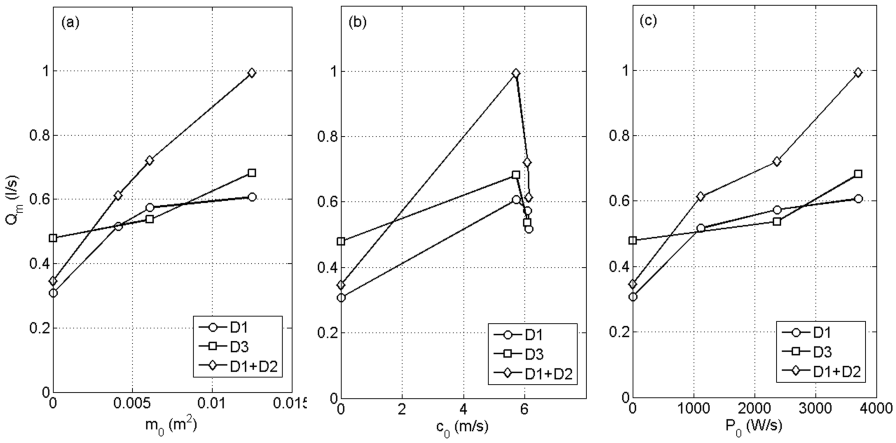

Figure 4.49: Mean drainage discharge versus offshore zero-order moment of wave power spectrum (a),mean wave celerity (b) and mean wave energy flux (c) for Tests S1, HE, ME and LE

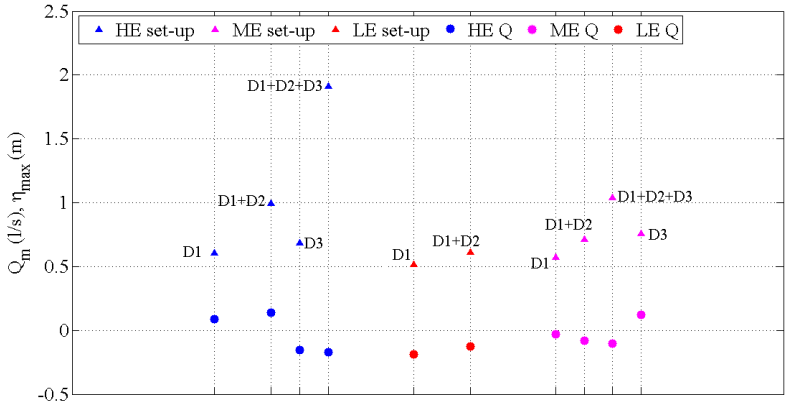

Figure 4.50: Mean drained flow Q_m for tests HE, ME and LE with all drains configurations

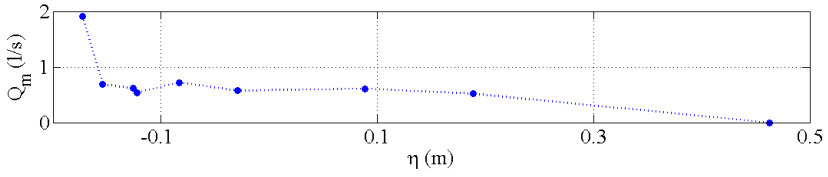

Figure 4.51: Mean drained flow Q_m vs maximum set-up η_{max}

the infiltration processes. Up to now the flow regime inside the drains has not yet been analyzed. Previous experimental ([108]) and numerical ([117], [118], [119])) BDS modeling aimed to analyze only the dynamic fluctuations on the beach but did not clarify the real drain flow regime, assuming identical hydraulic heads outside and inside the drains. The pressure transducers placed inside the drains during full scale experiments at GWK allow to measure the hydraulic head inside the pipes. Obtained results indicate that the hydraulic regime inside the drains proves to be probably different from that developed in the sand. This behavior might be related to the energy losses induced by the water infiltration phenomena. The energy losses mainly depend both on pipes and covering system of the drains. With reference to the spatial variation in the water tables and the water depths inside the drains for Test S2 with all drains opened separately (Figures 4.52(a) and 4.52(b)), low filling degrees follow from transducer measurements. A general decrease of the drain water depths as a function of the shoreline distance is noted. When more drains are opened simultaneously, the lowest filling degrees occur for combinations of 3 drains. Conversely to above, the water depth has an increasing trend. The hydraulic disconnection of the system is shown in figure 4.53(a), from where it is observed that the internal drain flow is an open-channel flow. In the figure 4.53(a) the time variation of relative water depth Δh measured by the pressure transducer placed inside drain D2 and the transducer located in the sand close to the drain for S1 is showed, including the opening phase of the drain and its successive closure phase. The value of Δh referred to the pressure transducer external to drain has a decreasing trend during the entire phase of drain opening tending to the maximum water table lowering. Its time evolution is characterized by an initial depression and a successive stabilization, followed by an increase to the initial static conditions after drain closure. The initial depression is induced by air supply due to the fast opening of the gate valve (Figure 4.53(b)). The interval between the maximum depression and the constant value Δh then corresponds to the air propagation time from the end of the pipe system to the transducer. The duration of this transitory phase is less than 1 minute for all tests and related to the length of each blind pipe. The opening phase is therefore characterized by the quick return of a different trend inside and outside the drain. Then the two mentioned flow regimes of the system attained an unique groundwater condition. With reference to the initial rising velocity of the water table given by the slope of the curve of Δh, the value of the transducer inside drain D2 proves to be about 4 times higher with respect to those deduced by the transducer outside D2. This feature is due to the different resistances offered by the air inside the drain and by the porous medium. After 300 s all velocities attain the same value, corresponding to complete air ejection from the drain. This behavior was observed in all tests.

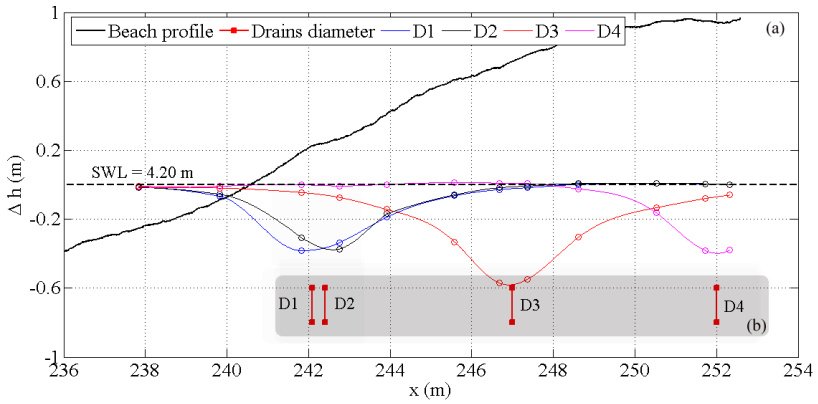

(a) Spatial variation of water table for test S2 - single drains on

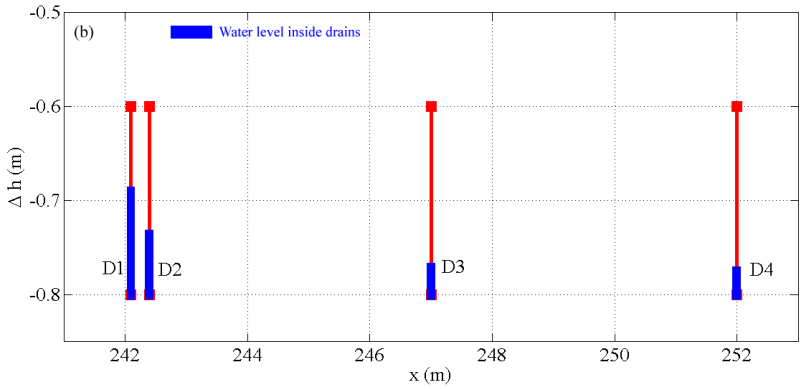

(b) Water depths inside drains for test S2 - single drains on

Figure 4.52:

4.5.5 Wave set-up

Both piezometers and pore pressure transducers located in the submerged beach measured the Sea Water Level (SWL) during the static tests and the Mean Water Level (MWL) when the waves ran along the channel. The MWL measured during dynamic tests allow to evaluate the maximum wave induced set-up in both undrained and drained conditions, from the intersection between the beach profile and the water table at the end of each test.

Figure 4.54 shows an example of the evaluated maximum wave set-up (η_{max}) for test ME in both undrained and drained conditions with the D1 on. Results demonstrate that the drainage also influences the mean water level on the sub-

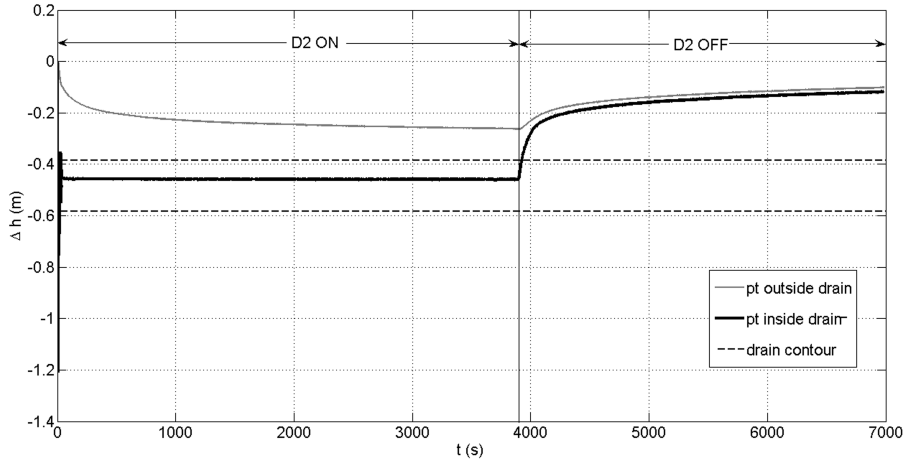

(a) Time variation of relative water depth inside drain D2 - test S1

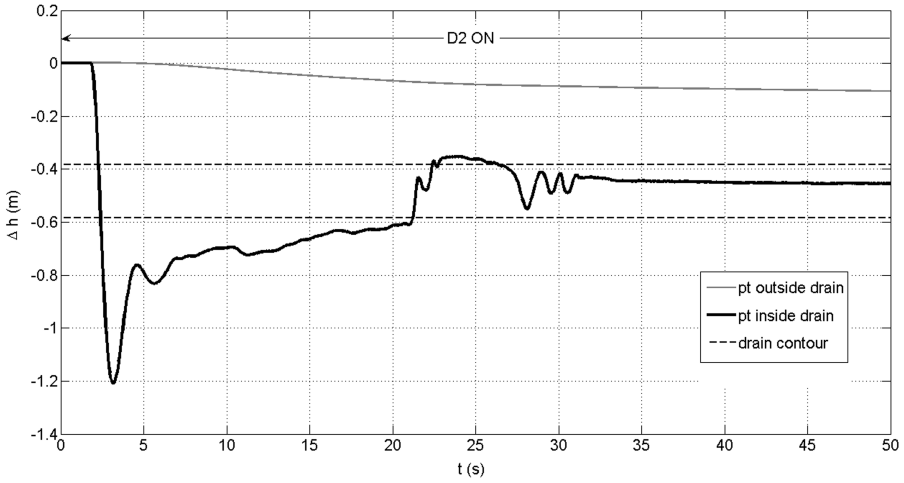

(b) Initial instants of relative water depths inside and outside the drain for Test S1 - D2 on

Figure 4.53:

merged beach. In fact the water table lowering leads to a reduction in the wave set up on the beach. As is well known the set up constitutes a hydraulic head driving undertow currents. The lower pressure gradient due to the reduction of the set-up can contribute to a reduction in the undertow currents and thus the seaward sediment transport ([120]). This aspect will be deeply discussed in the following section **??**.

Figure 4.55 shows the maximum wave set up η_{max} on the beach as a function of the offshore zero-order moment of wave power spectrum, m_0, in undrained conditions and in all single and coupled drained configurations. The values of m_0 were calculated by the first offshore wave gauge placed 50.1 m from the wave

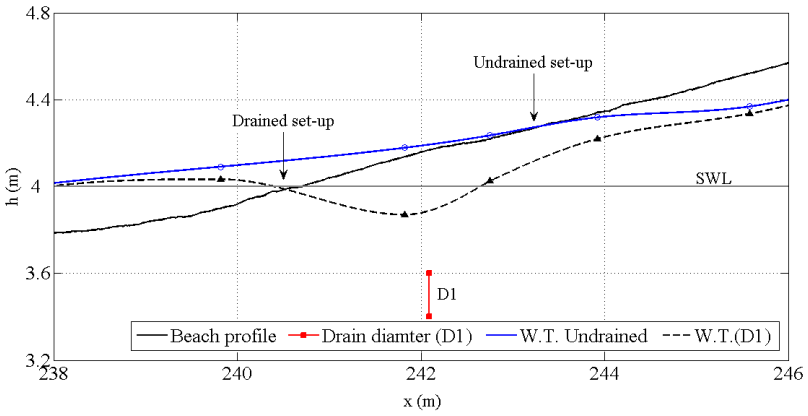

Figure 4.54: Spatial variation of water table in undrained and drained conditions (drain D1 open) for ME tests

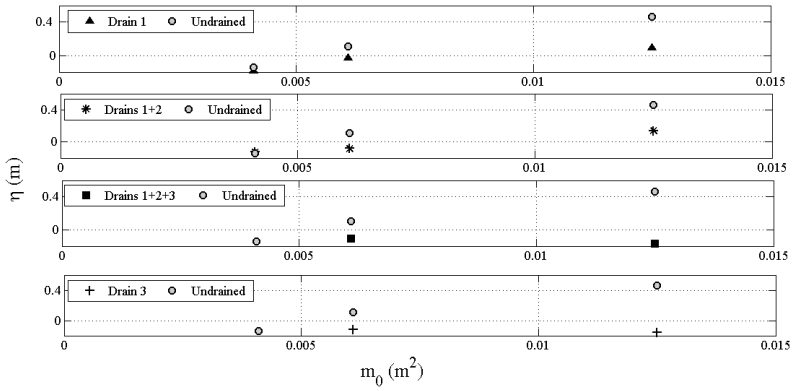

Figure 4.55: Maximum wave set-up vs. offshore zero-order moment of wave power spectrum in undrained conditions and all drain configurations

generator at the same water depth. Note that the increasing trend of set-up is associated with m_0 for both undrained and drained conditions. A higher reduction in η for high values of m_0 is noticed when D1 is opened. In general a reduction in the wave set-up due to the drainage was observed for all dynamic cases. In some HE tests η was not well related to the wave conditions because of the relevant changes in the nearshore beach profile.

4.5.6 Undertow currents

The undertow represents a mass conservation response to the associated landward drift of water under the crests of the breaking incident waves ([14]). These currents are a cause of cross-shore transport of sediments moved and suspended by turbulence due to breaking. In this section the nearshore flow field has evaluated by 4 electromagnetic currentmeters as a function of the bed evolution. The position of the instruments was suitable for measuring the seaward currents (undertow currents), flowing in the lower portion of the water column under breaking waves. The evaluation of these velocity current profiles in the presence/absence of a BDS has been performed for all wave attacks. In the following the analyses focus on comparing the undertow current for the sections where tests were performed in undrained and drained conditions. Figures 4.56(a) and 4.56(b) show the undertow current U for both undrained and drained conditions, respectively, for LE and ME wave attacks. The ordinate of such figures has a dimensionless coordinate, that pointing from the mean water level downward, is defined by the ratio $y*/y*_t$, where $y*$ and $y*_t$ are, respectively, the instrument and the beach depths for the specific test.
A larger modification of the beach depth has been observed especially comparing two tests not immediately consecutive. Therefore it is reasonable to expect that the velocity field comparison between tests in which y*t changes significantly are less reliable. Undertow currents are reported in figure 4.56(a) for the LE tests with reference to the cross-shore locations x = 227 m and 230 m. The drained conditions lead to a general reduction of the undertow current. When drains D1 and D2 are simultaneously opened a larger attenuation in the undertow current is not observed with respect to the case of activation of only D1 (figure 4.56(a)). From the analysis of LE data a general attenuation in undertow currents for almost all tests has been observed. For ME wave attacks a smaller decrease in the seaward current in drained conditions with respect to LE tests can be observed, as reported in Figure 4.56(b) under the activation of D1, also coupled with D2 in two different sections (x = 227 m and 228 m). This behavior has only been observed in some tests,. The smaller reduction in the undertow current observed in drained conditions for ME tests with respect to LE cases might depend not only on the larger wave energy attack but also on the more offshore position of the analyzed sections with respect to the position of the drains. For HE conditions the undertow current profiles do not show any sensible variation for undrained and drained conditions confirming that in storm cases the system is not working in stabilizing the beach ([121]) and it does not influence therefore the surf zone kinematics.
The low and somewhat significant influence of the BDS on the undertow currents in the swash zone suggests additional analyses on the effect of this singularity on the velocity field in both swash and surf zone.

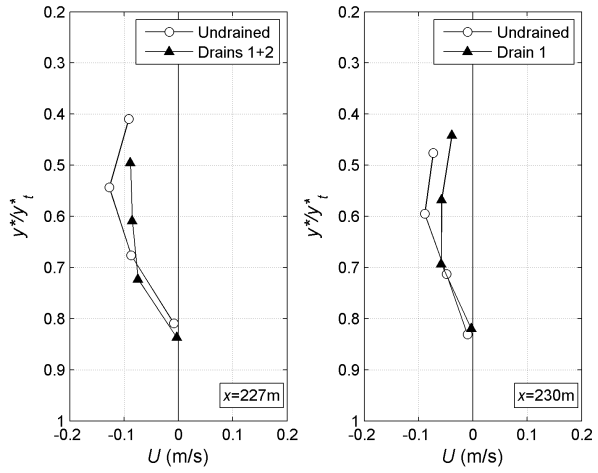

(a) Comparison of the undertow current measured by current-meters in undrained and drained conditions for LE tests

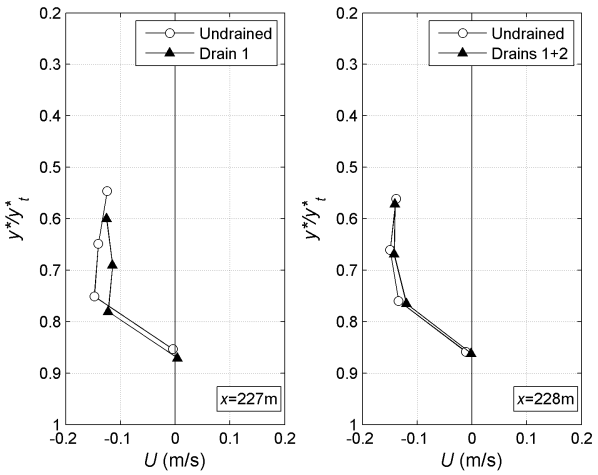

(b) Comparison of the undertow current measured by current-meters in undrained and drained conditions for ME tests

Figure 4.56:

A knowledge of possible changes in nearshore flow field due to the incident wave motion is fundamental for understanding the mechanisms of cross-shore sediment transport and, in particular, the direction of net transport ([122]). Energetic-based models consider sediment transport as a function of high-order velocity moments (skewness and kurtosis) and are able to predict nearshore bar/trough formation and evolution quite well ([123]). Therefore velocity skewness and kurtosis associated to the cross-shore flow field are calculated as predictors of sediment transport models providing a successive comparison with experimental morphodynamic data in order to define in detail BDS performances

in terms of beach stabilization. The analysis was performed on the basis of ultrasonic sensor measurements. The two sensors, called US1 and US2, were placed closer to the drains than the currentmeters and their position was variable as a function of the beach face evolution under different wave attacks. On the basis of the limits of surf and swash zones evaluated by the calculation of maximum run-up and run-down under HE, ME and LE tests, US1 was located in the surf zone for all energy wave conditions, while US2 was located in the swash zone only for the first HE test, for the first three ME tests and for all LE tests. The water heights recorded during each wave test are used here to evaluate the high-order velocity moments. According to energetic-based transport models, the flow velocity skewness, u_{sk}, is calculated as follows:

$$u_{sk} = \left\langle u^3 \right\rangle / \left\langle u^2 \right\rangle^{1.5} \tag{4.11}$$

and the flow velocity kurtosis, u_{ku}, as:

$$u_{ku} = \left\langle \left| u^3 \right| u \right\rangle / \left\langle u^2 \right\rangle^2 \tag{4.12}$$

where u is the cross-shore surface velocity, defined as normal to the shoreline and positive in the onshore direction. With reference to LE and ME tests, Figure 4.57 shows the time variation in velocity skewness for undrained and drained conditions. Higher values are observed for the most onshore ultrasonic sensor (US2). For LE wave conditions the positive values of usk confirm the

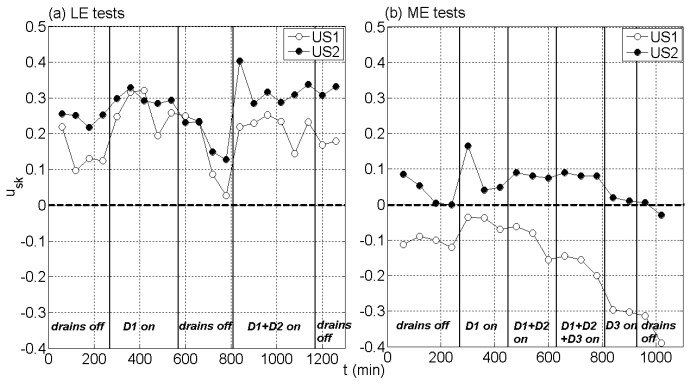

Figure 4.57: Time variation in velocity skewness measured by ultrasonic sensors US1 and US2 in undrained and drained conditions

natural accretionary tendency of the nearshore beach. Drain opening leads to higher positive values with respect to undrained conditions, in particular during the simultaneous activation of drains D1 and D2. The effect is particularly noticeable during the first drained tests. This result is linked to the beachface measurements in which the drains lead to an additional nourishing effect on the emerged beach ([121]). ME tests highlight a general beneficial effect on the

values of velocity skewness for all drained configurations and particularly for D1. The natural negative trend of u_{sk} related to offshore sediment transport beach erosion due to ME wave conditions is partially stabilized or reversed by the drain activation. This behavior is clear from US2 measurements due to its proximity to the drain location. Figure 8 highlights the time variation in velocity kurtosis in undrained and drained conditions for LE and ME tests. The positive and negative values of u_{ku} refer, respectively, to LE and ME wave conditions following the accretionary and erosional tendencies of the beach. Although the

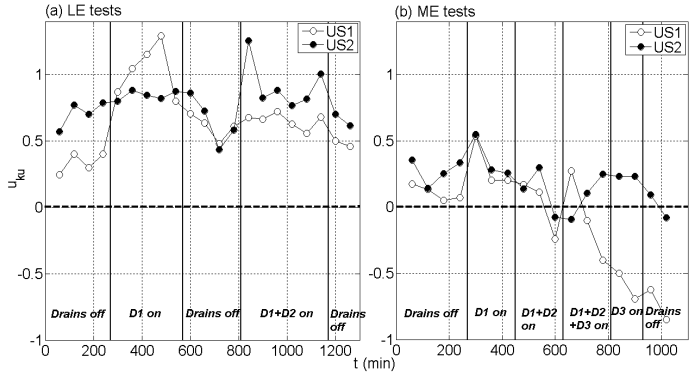

Figure 4.58: Time variation in velocity kurtosis measured by ultrasonic sensors US1 and US2 in undrained and drained conditions

values of velocity kurtosis show a larger range with respect to the skewness ones, the general trend of these two parameters is similar under the influence of the drains. Higher positive and less negative values of velocity kurtosis induced by the drains, in particular for D1, are linked to a potential reduction in offshore-directed sediment transport. Under the adopted wave conditions, the highest values of of u_{sk} and u_{ku} correspond to the transition between swash and surf zone, and prove to be in agreement with field experimental observations ([123]). As described above in the analysis of undertow currents, HE tests show the negligible contribution of the drains to a positive effect on the high-order velocity moments. The increasing negative trend of u_{sk} and u_{ku} confirm the inefficiency of the system under high wave conditions.

4.5.7 First results on scale effect analysis

First analysis concern the use of Dean analogy in order to compare the LIC model to the GWK one. This scaling guidance, consistent with the Froude hydrodynamic similitude, gives the possibility to define the geometrical and the time scales between the two models, through the knowledge of the ratio between fall velocities $\omega_{GWK}/\omega_{LIC}$ (fall velocities scale ratio n_ω, table 4.12). By using this analogy the LIC model represents a 3.41 scaled model of GWK. In figure

Table 4.12: Scale factors according to Dean analogy

n_ω	n_l=n_d=n_H	n_t	n_ω
1.85	3.41	1.85	1.91

4.59 is reported the wave set-up normalized by significant wave height as a function of $H/\omega T$ following the Dean scaling guidance. Figure 4.59(a) and 4.59(b) show results for both models, respectively in undrained and drained condition. As an example the test with the third drain from the shoreline open has been considered. Dean parameter can be seen as the ratio between $H/\omega s$ (the time

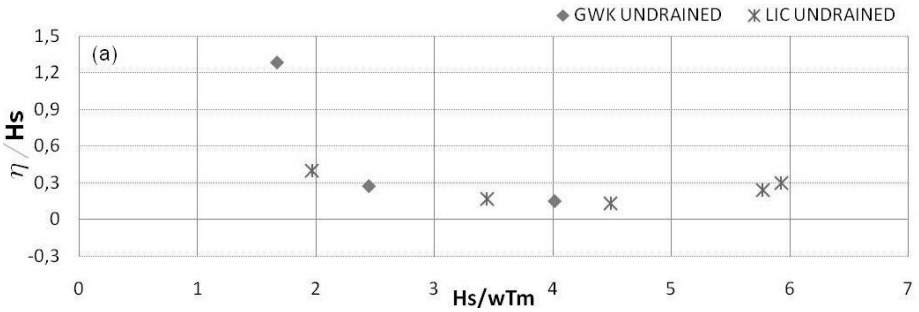

(a) Set up/Significant wave height vs. Dean Parameter (Undrained conditions)

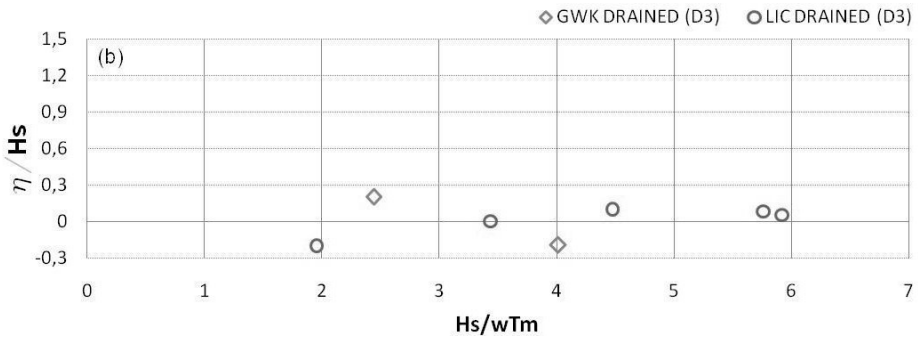

(b) Set up/Significant wave height vs. Dean Parameter (Drained conditions)

Figure 4.59:

taken for a sand particle to fall a distance equal to wave height) and the wave period T. Figures show that models above all well reproduce that the sediment transport is prevalently transported as suspended load respect to the bed one, because of Dean parameter is greater than unit in both large and small scale models. In undrained conditions (Fig. 4.59(a)) it can be observed that small scale model according to Dean scaling guidance well represents the set-up trend as a function of the Dean parameter. It is noticeable that the results obtained in both models are not immediately comparable due to the different boundary

conditions (i.e. beach face slope) which produce different wave shoaling and breaking conditions. Nevertheless the above result confirm the rightly use of this scaling guidance in the shore zone in order to reproduce the interaction between the external wave motion and the beach, when infiltration processes do not influence the beach response to the waves. In drained conditions (Fig. 4.59(b)) the beach permeability changes. Consequently the influence of the filtration processes induced by the activation of drain could create some doubts in small scale results interpretation.

4.6 Morphodynamics of the shore-zone

4.6.1 Introduction

The aim of the present analysis is to quantify the morphodynamic response of a beach equipped with a drainage system under the action of wave motion characterized by different energies. In order to study the morphological evolution of the beach, profile measurements were made at the end of each test step (1 h) by using the profiler mounted on the carriage (see section 4.4.3). Morphodynamic analysis is based on the assumption dynamic equilibrium was reached at the end of each test.
Previous experiments showed that the on-shore sediment transport due to the activation of drains cause an increasing of the shorezone slope. Consequently the run-up flow remains less time on shoreface for infiltrating inside the beach. Nevertheless large scale tests performed at GWK have show a decreasing trend of the shoreface slope. For instance in figure 4.60 ([121]) the average slope, computed between the shoreline and the bar crest, and the slope variation between subsequent beach profiles are reported for all HE tests.

The most remarkable variation of the shore slope occurr during the three steps of the first undrained tests. Next run in both drained and undrained conditions cause a minor decreasing of the shore zone slope. In almost all tests the slope variation results smaller than 5%. This is probably due to the non equilibrium condition of the beach at the beginning of run. After the first undrained three wave attacks, the beach reached a quasi-equilibrium condition with a higher degree of sand compaction. For ME cases the slope variation is always smaller than 5%, while for LE cases it is very limited amd less than 0.06%.
The effects of drainage on beach morphodynamics is analyzed by evaluating the net sediment volume variation ΔV, above the lower limit of influence of drain D1. It is computed integrating the vertical area delimited by two profiles. The greatest sediment volume for each wave condition W_{max} corresponds to the initial profile for HE and ME tests. Conversely, the initial volume for LE condition correspond to W_{min}. For the analysis the dimensionless relative volume

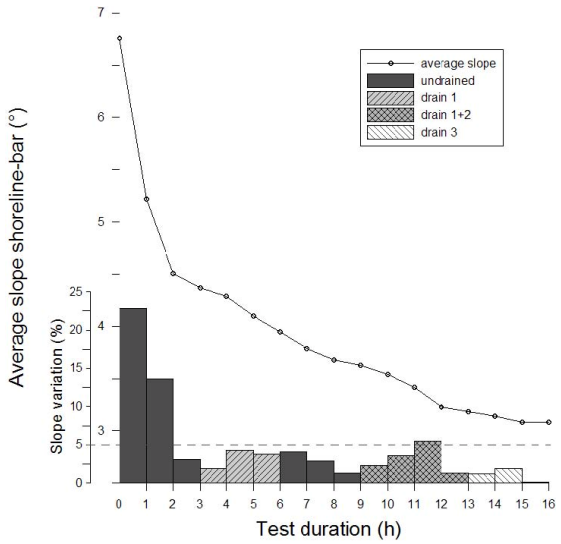

Figure 4.60: Average slope between the shoreline and the bar crest, and slope variation between successive beach profiles for the HE wave conditions

variation (Eq. 4.13) are considered:

$$\Gamma = \frac{W^j - W^{min}}{|W^{max} - W^{min}|} \tag{4.13}$$

where W^j is the sediment volume above the x position of the drain D1 per meter of cross-shore section in step j.
Positive values represents accretion, while negative one indicates erosion. In general while a positive effect are observed under low energy conditions, for medium and high energy conditions the benefit of having the drains operative is not always clear. In any case, it is evident that any positive effect of the drains on the beachface is confined by position of the cone of depression in the aquifer's surface.
In the following subsections morphodynamics response of drained beach for each tested wave energy is reported.

4.6.2 High energy conditions

Figure 4.61 ([121]) highlights the overall erosive trend of the beach. The formation of a bar far about 10 m from the initial shoreline can be observed, due to the sand movement from the swash zone to the submerged beach. The beach profiles seems to move towards a proper equilibrium configuration with an exponential shape with negligible overall effects induced by the drains.

The trend is also noticeable in the analysis of the dimensionless relative volume variation Γ. At the end of the first step without drains the erosive trend that

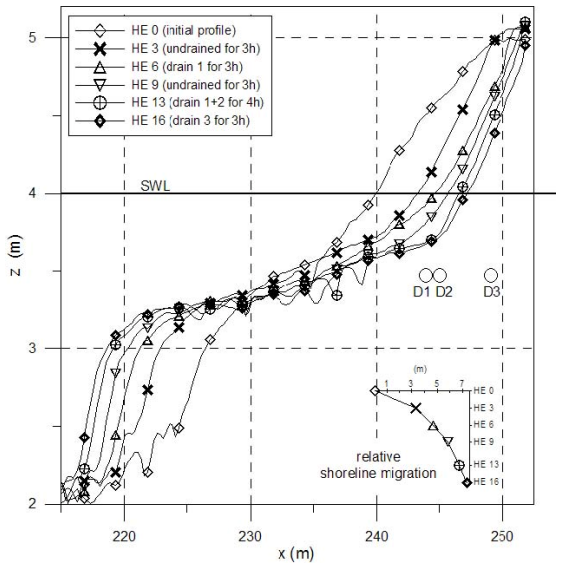

Figure 4.61: Most significant beach profiles under HE wave conditions

was observed resulted to be maximum of the test. The second and third step show a reduction in eroded sand volume. At the end of three steps, the shoreline has retreated of about 3 m (Fig. 4.61).
Switching D1 on, a sand volume loss occurs as well even if it is less than in the previous steps without drainage. Although the overall erosive tendency of the beach does not change, the drain produce some positive localized effects in the area above the cone of depression of the groundwater table, especially in correspondence of the maximum water table lowering. This stabilization effect was confirmed by a negligible bed variation during the three successive undrained steps. The switching on of D1 and D2 simultaneously confirmed again the local effect induced by the drains. The last three steps were carried out activating the drain D3. In this case the drain was acting under the emerged beach and its only effect is to slightly slow down the erosive process.

4.6.3 Medium energy conditions

Despite a reduction in wave energy in comparison with the HE tests, the ME case can still be considered erosive, with a dominance of net offshore transport. The greatest erosion occurred at about a relative depth (h/H_s) of 0.5 and it is probably related to the dominant position of the wave breaking. As in the previous HE conditions, the bar grew, but a slower rate. The activation of the drain D1 for three hours (ME 6 in Figure 4.62, [121]) does not alter this behavior. The simultaneous operation of D1 and D2 in the three hours of steps however generates a strong stabilization of the beach. It can be noticed

the coincidence of profiles ME 6 and ME 9, highlighting that 2 drains (D1+D2) operate with efficacy under ME conditions. The successive simultaneous opening of D1, D2 and D3 surprisingly triggered again the original trend of beach erosion, which persisted even using D3 alone. The last test without drains still showed beach erosion, confirming that the configuration of the beach has yet to reach equilibrium for the tested wave conditions.

An heuristic explanation of the efficacy of 2 drains and the inefficacy of 3 drains

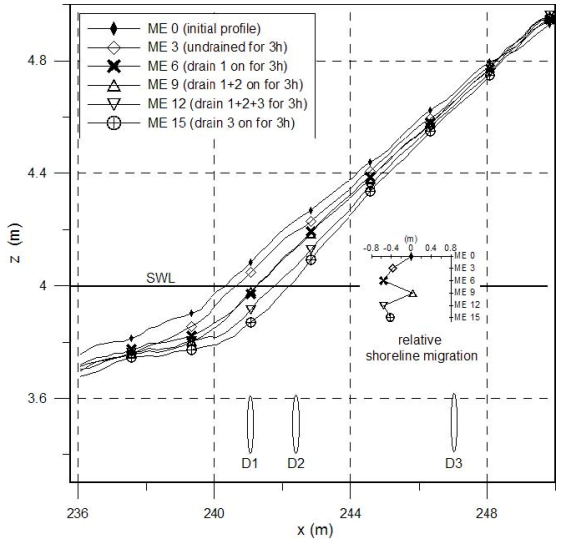

Figure 4.62: Beach profile changes under ME conditions without drain (ME 3), with D1, D2 and D3 working (ME 6, ME 9, ME 12), and with drain D3 operative (ME 15)

could be the combination of increasing/decreasing the normal and shear stress due to infiltration/exfiltration effect. In fact, the infiltration effect induces an increasing of the effective weight of the sediment by a pressure gradient in the vertical lift force ([124]) and leads to a thinning of the boundary layer and a greater shear stress ([125]) and vice versa for ex-filtration. As shown by Turner and Masselink ([126]), the boundary layer and shear stress changes appear to be dominant over the lift forces. Furthermore, when the drains D1 and D2 were operative, an increasing of the swash length due to the lowering of down rush limit, it is likely to have occurred. Thus, the increasing of the infiltration and related decreasing of exfiltration in the upper part of the beach due to drain D3 associated to D1 and D2 operating close to the shoreline, may have promoted an increase in shear stress during the backwash rather than during the uprush phase. Overall, this effect may be responsible for an overall net offshore sediment transport.

4.6.4 Low energy conditions

The tests carried out under LE wave conditions, with and without active drainage, present a slightly different picture, with a change in the morphodynamic behaviour of the beach. The tests show a slight accumulation in the emerged part of the beach as shown in Figure 4.63. Under these conditions, run-up is much more limited than in the previous test and, consequently, it was decided to use only D1 and D2. The overall accretive trend shown in the first step without drains possibly is the prolongation of a tendency already started by the previous condition with D1 operative (0.08 mc/m of accreted volume). Indeed, at the

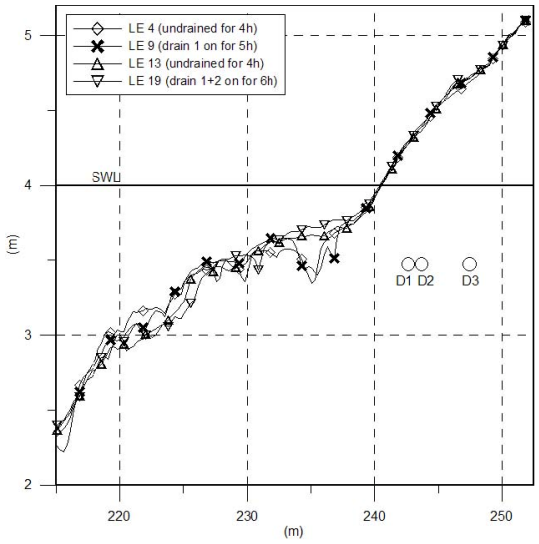

Figure 4.63: Beach profile changes under ME conditions without drain (ME 3), with D1, D2 and D3 working (ME 6, ME 9, ME 12), and with drain D3 operative (ME 15)

end of the five steps the accreted volume is substantially higher. However the general accretion trend is asymptotic. Switching off D1, a slight erosion process appears. This effect may be due to the morphodynamic beach state reached during the previous drained test. Results show that when D1 is operative, the relative bathymetry on D1 decreased while on D2 increased. In other words, the D1 promotes a steepening of the beach positioning the surrounding of the drain itself, while the undrained condition tends to re-establish the natural nourishing slope. The positive hourly average volume variation under undrained condition is comparable to the negative one obtained with D1 operative. Finally, switching on D1 and D2 triggered an initial stabilization, at first, and a successive accretive effect is observed. The trend of bed level at the location of D3 confirms the overall accretive trend under LE conditions.

Chapter 5

Numerical analysis

5.1 Introduction

Field and laboratory installations of the Beach Drainage System discussed in the previous chapters clarify that the BDS efficacy is strictly related to the interaction between the external wave motion and the groundwater inside the beach. Indeed, in coastal engineering problems one of the main pursued aim is to correctly reproduce and predict the water table variations inside the beach as a function of the wave run-up/down.
The study of filtration processes inside a partially saturated porous medium represents the first step in oder to develop such models to be used in Beach Dewatering System design. At the present time the BDS design is based on the acquired experiences on field installations and empirical formula. For this reason laboratory experiments have to be combined with numerical modeling in order to extrapolate information from a limited number of field and laboratory experiments to different drain configurations, wave climate and beach characteristics.
In the present chapter the main lines of the mathematical description for some groups of numerical wave models are discussed. Firstly four type of model formulations simulating free surface waves propagation on finite water depth are briefly described. Thereafter, the models for simulating groundwater flow and its interaction with the external wave motion are described. In particular the proposed models analyze the interaction between the water table variation inside the beach and the swash processes on the beach face. The second part focuses on the simulation of the influence of the BDS on the groundwater flow inside the beach by using the *HYDRUS-2D* code.

5.2 External wave motion modeling

A complete overview of external wave motion models available in literature was performed by van Gent ([127]). The author considered three different zones represented by three different theoretical models.
The first model regards waves propagation in deep-water. The motion of an incompressible Newtonian fluid can be accurately described by the Navier-Stokes equations. However, because solving such equations is complex, it is necessary to use approximations in order to obtain equation which are easier to solve. In deep water, before wave breaking, the flow can be assumed inviscid and irrotational. Under these the flow field can be accurately be described by models based on potential flow theory, the so called *Potential flow models* ([128], [129]).
In intermediate and shallow waters the non linear effects of wave propagation can not be always neglected. Van Gent considers two types of equations: the *finite-amplitude shallow water equations* ([130], [**?**]) and the *Boussinesq* ones. The former can be used in order to simulate wave propagation over short distances (a few wave lengths) on gentle slope, until breaking zone. After breaking up to the shoreline, these kind of equations can be used to approximate the bores originating from the breaking process. As discussed by van Gent[127], the solution of the mathematical model shows the propagation of wave crest occurs faster than the propagation of the wave troughs. This amplitude dispersion results in a continually steepening of the wave front, which would be counteracted by a frequency dispersion. This can be improved by applying high-non linear Boussinesq type equations (BTE). In general wave attack on permeable coastal structures can not be modeled accurately without modeling porous media flow. The energy dissipation, the infiltration and seepage in the swash zone and the interaction between the external and the internal wave motion often cause the effects of flow field to be quite different from the flow on impermeable structures. The above equations useful to describe the external wave motion have been extended in order to simulate also the flow motion inside a generic permeable structures ([127]). The method of study to be followed is the same if wave attack reaches a beach. Also in this case the interaction between internal and external flow is important. Indeed every changes on the swash zone hydrodynamics caused by the variations in water level inside the beach, modify the morphodynamics of the near-shore. The difference between the wave motion inside a permeable structures and inside a beach is that the flow in the first case is often turbulent, while the groundwater one is a laminar flow.
In literature several models have been proposed in order to predict the interaction between the external wave motion and the groundwater inside the beach. The study of such processes is essential for developing models aimed to BDS design. Actually any guidelines are available and the design in mainly based on previous field applications and laboratory experiments (see Chapter 6). In

the following sections some mathematical models are briefly described in order to explain the different ways in approaching the problem. The section mainly focuses the attention on the influence of water table variations on wave induced run-up on impermeable bottom.

5.3 Combined external-internal wave motion modeling

In literature several models have been proposed in order to predict the wave-induced run-up and to study the water table variations inside a beach. Unfortunately these models need complex adjustments if the analyzed beach is equipped with a drainage system. Few models have been developed in order to simulate hydrodynamic and morphodynamic processes in presence of a drain. Moreover the research is also limited by few available data obtained by field applications and laboratory experiments which would allow to validate proposed mathematical models.
Packwood ([131]) improved a model which analyzed the influence of the sand porosity on up-rush flow due to a single tide wave on a gently sloped beach initially unsaturated. The model focuses on the fact that the sediment transport on beach face is strictly related to the infiltration processes in the swash-zone. As a consequence, the sand permeability constitutes one of the main characteristics which influence the infiltrated flow rate. Indeed, experimental results showed that a fine sandy beach could be compared to an impermeable one, with respect to the infiltration process. The back-wash flux is highly reduced if beach is composed of medium coarse sand because of a greater flux can infiltrate inside beach during run-up phase. The filtration process is described by using Dicker's equation under the assumption of hydrostatic pressure distribution along the submerged beach and filtration prevailing in vertical direction. The up-rush on beach face is described by the author by using the shallow water equations. Results showed that for a medium-fine sand the effects of the porosity on the up-rush flux resulted to be less relevant than on the back.wash phase. Moreover later laboratory experiments (i.e. [132] demonstrated that the maximum run-up height on beach is not influenced by infiltration flow rate, while the back-wash is highly reduced when the sand has a high permeability.
Successively, Kobayashi ([133]) proposed a numerical model able to simulate the up-rush flow on rough beaches and the infiltration process under a perpendicular waves train. An energy equation was added to the well-know mass and continuity equations in order to evaluate the dissipated energy rate due to the breaking.
Nielsen ([134]) focused his studies on the water table variations inside the beach. He found that the water table position with reference to the mean water level

of the sea influenced many aspects of engineering projects, as i.e. the structures stability or the use of agricultural soils because of the salt water intrusion. The aim of the study was the evaluation of the water table variation as a function of tidal sea fluctuations. The process was described by using the deep aquifer solution over an impermeable bottom. Mass and continuity equations are combined in Boussinesq's equation (5.1) under the main hypothesis of a horizontal flux.

$$\frac{\partial h}{\partial t} = -\frac{1}{n}\frac{\partial}{\partial x}(hu) \tag{5.1}$$

The equation 5.1 is solved by imposing the following boundary conditions:

- water table oscillations tends to zero far from the shoreline;
- tidal level lowering slow.

In 1996 Kang and Nielsen([135]) extended the previous word conducted by Nielsen analyzing the influence on water table variations of the wave-induced up-rush flow. The authors re-wrote Boussinesq's equation including run-up effect:

$$n\frac{\partial h}{\partial t} = KD\frac{\partial^2 h}{\partial x^2} + U(x,t) \tag{5.2}$$

where $U(x,t)$ indicates the mean filtration velocity for a unit area. The study demonstrated that the filtration velocity reaches the maximum value between the shoreline and the zone were the water table tends to be horizontal. This conclusion was also confirmed by laboratory and field experiments. Li et al. ([136], [137]) defined a two-dimensional numerical model aimed to simulate the behavior of a coastal aquifer with the influence of a drainage system. The involved processes were described by using Darcy's law, the continuity equation and Laplace's law imposing the appropriate boundary conditions. Results obtained by numerical simulations showed a good agreement compared with field data. Numerical simulations gave the possibility to study the influence of drain efficiency of other parameters different to be changed in field experiments, as drain positions or diameter.

Successively also Vesterby focused his studies on the numerical simulation of a Beach Drainage System ([138]) in order to simulate hydrodynamic processes inside the beach and evaluate the water table variations. The numerical model was improved by using the hydrological model MIKE SHE for the filtration process and the model MIKE11 for the hydrodynamic of the external wave motion in the swash zone.

Successively Li et al. ([139]) derived the numerical model called *Beachwin*. It represented an evolution of the previous work performed by the authors ([136], [137]). The model allows to simulate separately the involved phenomena: the wave propagation on the beach, the filtration processes in the unsaturated zone, the sediment transport in the shore-zone and the shoreline evolution. All processes are improved in the code by the use of particular equations. Each model

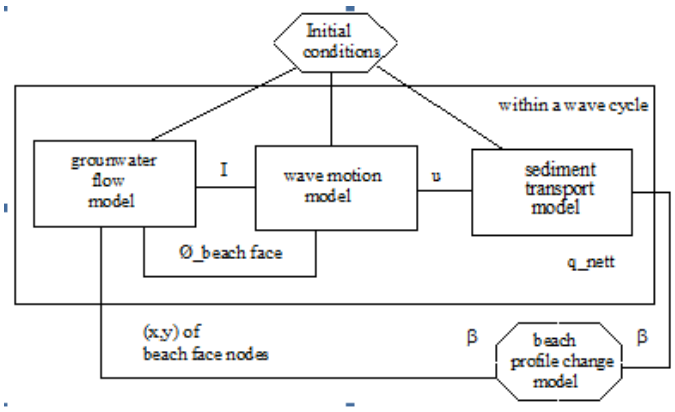

Figure 5.1: Sub-models interaction in Beachwin numerical code

interacts with each other through the boundary conditions of each process (Fig. 5.1). The wave propagation on the beach is simulated by the non-linear shallow water equations. The aquifer hydrodynamic allow to evaluate the water table variation due to both tidal variations and wave attacks. This model solve the Laplace's equations for a saturated porous medium. For the sediment transport modeling the code uses Bagnold's method (see Chapter 1), valid in the swash zone.

Recently Karambas ([140]) has developed another conceptual model for simulating the variation of the saturation line inside the beach with the presence of a drainage system. The author describes the external wave motion by using the Boussinesq equations referring to van Gent work mentioned above. The long wave equations are used to describe the porous flow model, while the sediment transport is estimated from a slightly modified meyer-peter and Muller formula ([141], [142]). Model has been validated with field data and results are quite satisfactory.

In the present work the numerical simulation has regarded the water table lowering due to the presence of a drain. Filtration processes are evaluated by using Richard's equation numerically solved by the code HYDRUS-2D. In the following the mathematical model and the numerical code used are briefly described. First results are then showed in order to understand the code accuracy in simulating the water table lowering variations in space and in time. The good results could allow to help to define the main BDS design parameters which are difficult to identify in field or in laboratory experiments.

5.4 The *HYDRUS-2D* numerical code

5.4.1 General introduction and overview of *HYDRUS-2D*

Last decades have been characterized by a considerable progress in the conceptual understanding and mathematical description of the water flow and solute transport processes in the unsaturated zone. A variety of numerical models are now available to predict water transfer process between the soil surface and the groundwater table. The most popular models remain the Richard's equation for variably saturated flow. Deterministic solutions of these classical equations have been used for predicting water movement, analyzing specific laboratory or field experiments involving unsaturated groundwater flow.
The *HYDRUS-2D* software package simulates two-dimensional water flow, heat movement and transport of solutes involved in sequential first-order decay reactions in unsaturated, partially saturated or fully saturated porous media. The program is an extension of the variably saturated flow codes *SWMS-2D* ([143]) and *CHAIN-2D* ([144]), which in turn were based in part on the early numerical work of Vogel ([145]) and Neumann ([146], [147], [148], [149]). To simplify the management of relatively complex input data file and to graphically display the final simulation results, an interactive graphics-based user-friendly interface has been developed. *HYDRUS-2D* can handle flow domains delineated by irregular boundaries and the flow region may be composed of non-uniform soils having an arbitrary degree of local anisotropy.
Saturated-unsaturated water flow and convection-dispersion type equations for heat and solute transport are described by using Richard's equation. The code numerically solves the Richard's equation using Galerkin-type linear finite element schemes. The code also includes a Marquardt-Levenberg parameter optimization algorithm for inverse estimation of soil hydraulic and solute transport and reaction parameters from measured transient or steady-state flow.
In the following only the part of code used in the present work will be described, regarding the water flow in variably saturated porous medium.

5.4.2 Governing flow equation

Consider two-dimensional isothermal Darcian water flow in a partially saturated rigid porous medium. Assuming that the air phase can be neglected in the liquid flow process, the governing equation is given by the following modified form of Richard's equation:

$$\frac{\partial \vartheta}{\partial t} = \frac{\partial}{\partial x_i}\left[K\left(K_{ij}^A \frac{\partial h}{\partial x_j} + K_{iz}^A\right)\right] - S \tag{5.3}$$

where ϑ is the volumetric water content $[L^3L^{-3}]$; t is the time [T]; h is the pressure head [L]; K_{ij}^A are components of a dimensionless anisotropy tensor K^A in which the diagonal of entries is equal one and the off-diagonal entries zero for an isotropic medium; $x_i (i = 1, 2)$ are the spatial coordinates [L]; S is a sink term $[T^{-1}]$ and it represent the volume of water removed per unit time from a unit volume of soil due to plant water uptake ([150], [151]); K is the unsaturated hydraulic conductivity function $[LT^{-1}]$ given by

$$K(h, x, z) = K_s(x, z)K_r(h, x, z) \tag{5.4}$$

where K_s is the saturated hydraulic conductivity and K_r is the relative hydraulic conductivity.
The unsaturated soil hydraulic properties $\vartheta(h)$ and $K(h)$ in Eq. 5.3 are in general highly nonlinear function of the pressure head. *HYDRUS-2D* allows to use three different models:

1) *Brooks and Corey, 1964* ([152])

$$S_e = \begin{cases} |\alpha h|^{-n} & \text{if } h < -1/\alpha \\ 1 & \text{if } h \geq -1/\alpha \end{cases} \tag{5.5}$$

where α is the inverse of the air-entry value (or bubbling pressure

$$K = K_e K_s S_e^{2/n+l+2} \tag{5.6}$$

where n is the pore distribution index and l is a pore-connectivity parameter assumed to be 20 in the original study ([152] S_e is the effective water content equal to

$$S_e = \frac{\vartheta - \vartheta_r}{\vartheta_s - \vartheta_r} \tag{5.7}$$

in which θ_r and θ_s denote the residual and saturated water content respectively. In the code the parameters α, n and l are considered empirical coefficients which affect the shape of hydraulic functions.
2) *van Genunchten, 1980* ([153])

$$\vartheta(h) = \begin{cases} \vartheta_r + \frac{\vartheta_s - \vartheta_r}{[1+|\alpha h|^n]^m} & \text{if } h < 0 \\ \vartheta_s & \text{if } h \geq 0 \end{cases} \tag{5.8}$$

$$K(h) = K_s S_e^l [1 - (1 - S_e^{l/m})^m]^2 \tag{5.9}$$

in which

$$\begin{cases} m = 1 - 1/n \quad \text{with n¿1} \end{cases} \tag{5.10}$$

The above equations contain five independent parameters ϑ_r,ϑ_s, α, n and K_s. The pore connectivity parameter l in the hydraulic conductivity function was

estimated to be about 0.5 as an average for many soils ([154]).
3) *Vogel and Cislerova* ([155])
The authors modified previous van Genuchten's equation ([153]) in order to refine the description of soil hydraulic properties near saturation. The soil water retention and hydraulic conductivity are given by

$$\vartheta(h) = \begin{cases} \vartheta_a + \frac{\vartheta_m - \vartheta_a}{[1+|\alpha h|^n]^m} & \text{if } h < h_s \\ \vartheta_s & \text{if } h \geq h_s \end{cases} \tag{5.11}$$

$$K(h) = \begin{cases} K_s K_r(h) & \text{if } h \leq h_k \\ K_k + \frac{(h-h_k)(K_s - K_k)}{h_s - h_k} & \text{if } h_k < h < h_s \\ K_s & \text{if } h \geq h_s \end{cases} \tag{5.12}$$

where

$$K_r = \frac{K_k}{K_s} \left(\frac{S_e}{S_{ek}} \right)^l \left[\frac{F(\vartheta_r) - F(\vartheta)}{F(\vartheta_r) - F(\vartheta_k)} \right]^2 \tag{5.13}$$

$$F(\vartheta) = \left[1 - \left(\frac{\vartheta - \vartheta_a}{\vartheta_m - \vartheta_a} \right)^{1/m} \right]^m \tag{5.14}$$

$$S_{ek} = \frac{\vartheta_k - \vartheta_r}{\vartheta_s - \vartheta_r} \tag{5.15}$$

In the above equation if the minimum capillary height, h_s, is non-zero the parameter ϑ_s in van Genuchten's retention function can be replaced with an extrapolated parameter ϑ_m. This value is slightly larger than ϑ (Fig. 5.4.2) and while it has little effects on the retention curve, the effect on the shape and value of the hydraulic conductivity function can be considerable, especially for fine-textured soils. To increase the flexibility of the analytical expressions, the parameter ϑ_r in the retention function was replaced by $\vartheta_a < \vartheta_r$. Eq.5.13 assumes that the predicted hydraulic conductivity function is matched to a measured value of the hydraulic conductivity at a specific water content, $K_k \leq K(\vartheta_k)$, less that or equal to the saturated water content ϑ_s. $\vartheta_k \leq \vartheta_s$ results in $K_k m \leq K_s$ ([155]). When $\vartheta_a = \vartheta_r$, $\vartheta_m = \vartheta_k = \vartheta_s$ and $K_k = K_s$, the soil hydraulic functions of Vogel and Cislerova are reduced to the original expression of van Genuchten ([153]).

5.4.3 Initial and Boundary Conditions

The solution of Eq. 5.3 requires knowledge of the initial distribution of the pressure head within the flow domain, Ω:

$$h(x, z, t) = h_0(x, z) \qquad \text{for } t = 0 \tag{5.16}$$

where h_0 is a prescribed function of x and z.
HYDRUS-2D implements three types of conditions to describe system-independent

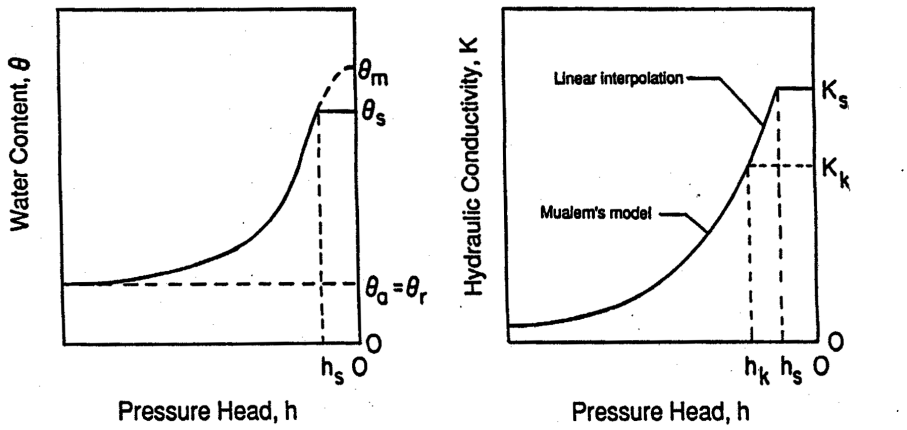

Figure 5.2: Soil water retention (on the left) and hydraulic conductivity (on the right) functions as given by Eqs. 5.11 and 5.12, respectively.

interactions along the boundaries of the flow region. In addition there is the possibility of imposing other three different types of system-dependent boundary conditions.

The first three refer to pressure head (Dirichlet type, Eq. 5.17), flux (Neumann type,Eq. 5.18) and gradient boundary conditions (Eq. 5.19) given by the following functions, respectively:

$$h(x,z,t) = \psi(x,z,t)\text{hspace6mm for}(x,z) \in \Gamma_D \tag{5.17}$$

$$-[K(K_{ij}^A \frac{\partial h}{\partial x_j} + K_{iz}^A)]n_i = \sigma_1(x,z,t)\text{hspace6mm for}(x,z) \in \Gamma_N \tag{5.18}$$

$$(K_{iz}^A \frac{\partial h}{\partial x_j} + K_{iz}^A)n_i = \sigma_2(x,z,t)\text{hspace6mm for}(x,z) \in \Gamma_G \tag{5.19}$$

where Γ_D, Γ_N and Γ_G indicate Dirichlet, Neumann and gradient type boundary segments; $\psi[L]$, $\sigma_1[LT^{-1}]$ and σ_2 [nondimensional] are prescribed functions of x, z, and t; n_i are the components of the outward unit vector normal to boundary Γ_N or Γ_G. The code implements the gradient boundary condition only in terms of a unit vertical hydraulic gradient simulating free drainage from a relatively deep soil profile.

The last three types of dependent boundary condition can not be defined a priori. One of these involves soil-air interfaces which are exposed to atmospheric conditions. The potential fluid flux across these interfaces is controlled exclusively by external condition. In the absence of surface ponding the numerical solution of Eq. 5.3 is obtained by satisfying the following two conditions ([148]):

$$\left| K(K_{ij}^A \frac{\partial h}{\partial x_j} + K_{iz}^A)n_i \right| \leq E \tag{5.20}$$

$$h_A \leq h_S \tag{5.21}$$

where E is the maximaum potential rate of infiltration or evaporation under the analyzed atmospheric conditions, h is the pressure head at the soil surface, h_A and h_S are minimum and maximum pressure heads allowed under the prevailing soil conditions, respectively. In general, h_A is determined from the equilibrium conditions between soil water and atmospheric water vapor ([156]) while h_S is set equal to zero.
the second type of system-dependent boundary condition is a seepage face through which water leaves the saturated part of the flow domain. The pressure head along a seepage face is automatically set uniformly equal to zero. Additionally the code assumes that water leaving the saturated zone across a seepage face is immediately removed by overland flow or some other removal process.
The third class of system-dependent boundary conditions concerns the drains. The code assumes that as long as a drain is located in the saturated zone, the pressure head along the drain is equal to zero. The drain acts as a pressure head sink.

5.4.4 Numerical solution

The solution of the governing flow equation 5.3 is obtained by using the Galerkin finite element method with linear basis function. This method has been covered in detail by many authors as i.e. Neuman 1975 ([149]) or Pinder and Gray, 1977 ([157]). In the following only the most pertinent steps in the solution process are given.
The method is composed by the following steps:

- Space discretization
- Time discretization
- Numerical iterative process

Firstly the flow region is divided into a network of triangular elements. The corner of these elements are taken to be the nodal points. The pressure head function $h(x, z, t)$ is approximated by a function $h'(x, z, t)$ as follows

$$h'(x, z, t) = \sum_{n=1}^{N} \Phi_n(x, z) h_n(t) \tag{5.22}$$

where $\phi_n$are the linear basis functions satisfying the condition $\Phi_n(x_m, z_m) = \delta_{nm}$, h_n are unknown coefficients representing the solution of 5.3 at nodal points and N is the total number of nodes. The Galerkin method postulates that the differential operator associated with the Richard's equation (5.3) is orthogonal

to each of the N basis function, i.e.

$$\int_{\Omega} \left\{ \frac{\partial \vartheta}{\partial t} - \frac{\partial}{\partial x_i} \left[K \left(K_{ij}^{A} \frac{\partial h}{\partial x_j} + K_{iz}^{A} \right) \right] + S \right\} \Phi_n d\Omega = 0 \tag{5.23}$$

Applying Green's first identity to 5.23 and replacing h by h' leads to:

$$\sum_{e} \int_{\Omega_e} \left(\frac{\partial \vartheta}{\partial t} \Phi_n + K K_{ij}^{A} \frac{\partial h'}{\partial x_j} \frac{\partial \phi_n}{\partial x_i} \right) d\Omega \tag{5.24}$$

where Ω_e represents the domain occupied by the element e.
After imposing additional simplifying assumptions and performing integration over the elements, the procedure leads to a system of time-dependent ordinary differential equations with non linear coefficients ([158]).
Integration in time of the system of time-dependent ordinary differential equations is achieved by discretizing the time domain into a sequance of finite intervals and replacing the time derivatives by finite differences for both unsaturated and saturated conditions. Because of the nonlinear nature of the system to be solved, an iterative process must be used in order to obtain solution of the global matrix equation at each new time step. For each iteration a system of linearized algebraic equations is first derived from the general matrix, which, after incorporation of the boundary conditions, is solved using either Gaussian elimination or the conjugate gradient method. After inversion, the coefficients are re-evaluated using the first solution and the new equation s are again solved. The iterative process continues until a satisfactory degree of convergences is obtained.
The next subsection deals with the description of *HYDRUS* application in studying BDS efficiency. This kind of analysis represents the first step for a complete numerical simulation of the drainage behavior placed below a sandy beach, in order to obtain a numerical model able to be used in BDS design.

5.4.5 First simulation of the BDS

HYDRUS-2D simulation focuses on the numerical analysis of the water table lowering in a medium sandy beach equipped by a drain. In this first step of numerical analysis only the static conditions have been considered in order to validate the model by using the experimental data collected during GWK experiments. As mentioned before, the numerical study of the drain efficiency, coupled with field and laboratory experiments, is useful in defining BDS design guidelines.
The geometry reproduced the physical model adopted for GWK tests. The finite-element mesh is constructed by dividing the flow region into triangular elements. The mesh is almost uniform except in the zone close to the drain where a local refinement has been used in order to obtain more accurate results

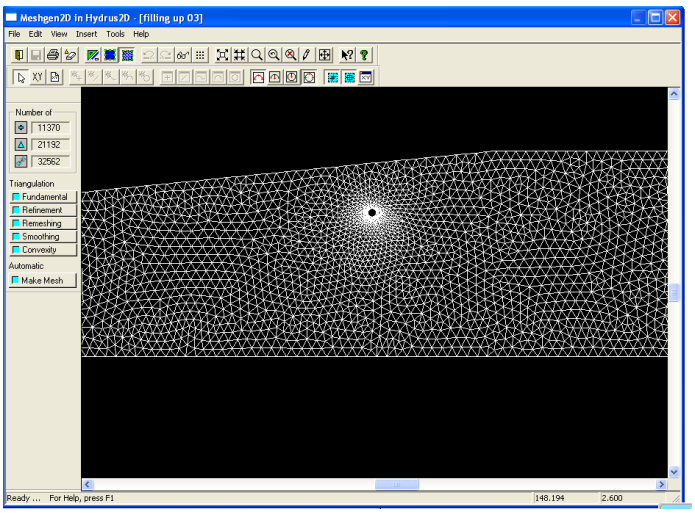

Figure 5.3: Embedded mesh in the zone close to the drain

(Fig. 5.3) for a total number of nodes equal to 11370 and 21192 triangles. The beach is assumed homogeneous and isotropic. Running the model requires the hydraulic parameters θ_s,θ_r, K_s, n, α and l, as well as the initial water content distribution. For sand characteristics the code allows to use some standard parameters which depend on the soil type (grain size, soil classification, etc.). For the present simulation the sand used is a fine sand. Only the hydraulic conductivity K_s has been changed and equal to that measured in laboratory ($3.2 * 10^{-3}$ cm/s). The drainage system is defined by one drain corresponding to the drain D3 placed in laboratory experiments (see Chapter 4). This drain, as discussed in the previous chapters, during experiments showed the better efficiency in terms of water table lowering and drained flows. The drain is modeled by a circular hole in the mesh, whose boundary is defined by a specific condition discussed in detail later.

The initial water content distribution has not been defined a priori. In order to recreate the real laboratory initial conditions, the channel filling-up has been simulated. The boundary conditions of this first simulation are represented in Fig. 5.4. A constant hydraulic head (4.00 m) has been imposed on the bottom of the beach, causing the gradual beach saturation from the bottom to the top, as the channel filling-up in laboratory. The output of this simulation give the hydraulic head distribution in the region, then used as initial condition for the drainage (Fig. 5.5).

The boundary conditions of the drainage simulations are showed in Fig. 5.6. All beach contours are *no flux* boundaries, while the drain is a *free drainage* surface. On the left side (Fig. 5.6 the static water levels in the channel (4.00 m and 4.20 m) have been simulated by imposing a constant hydraulic head during

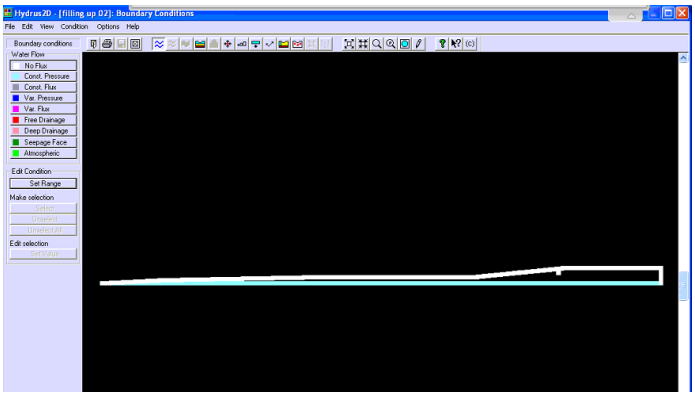

Figure 5.4: Boundary conditions for the filling up simulation

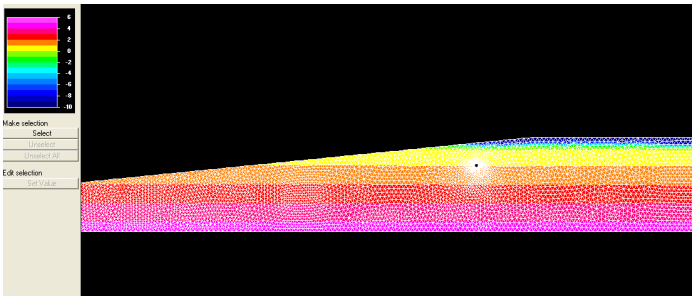

Figure 5.5: Initial conditions

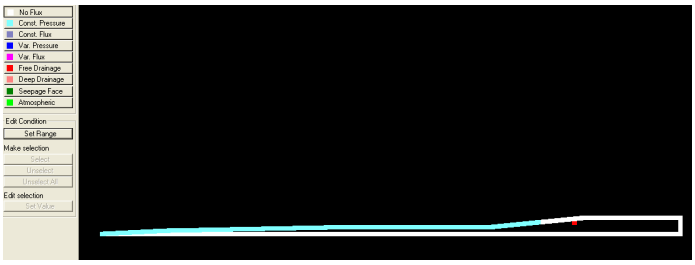

Figure 5.6: Boundary conditions

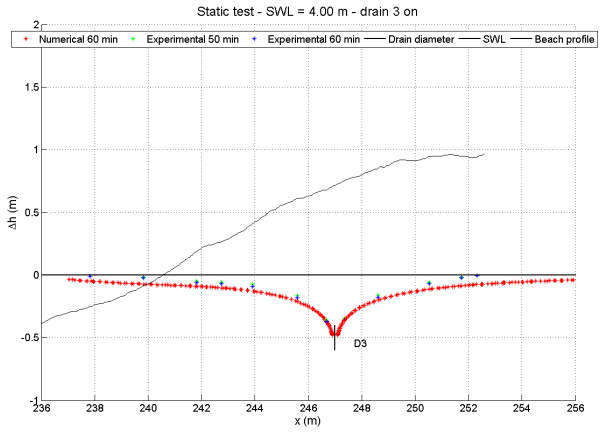

Figure 5.7: Comparison between experimental and analytical solution with the drain D3 on - t=60 min

the drainage processes.
The time of simulation has been set at 60' (as for laboratory runs) and the time discretization Δt has be set equal to 0.001. A time interval Δt smaller than 0.001 cause the bad convergence of the numerical solution.

First result and future applications

Figure 5.7 shows an example of the comparison between experimental and analytical results for a test with a working drain in constant hydraulic head conditions. The simulated water level in the channel is equal to 4.00 m. Moreover the beach profile measured at the end of test is reported. Red stars represented the spatial variation of water table modeled by numerical code at the end of simulation (t= 1h), while blue and green stars represented the local piezometric head measured in laboratory at t=50 min and t=60 min, respectively with the dran D3 open.
The numerical model well simulates the water table lowering due to the drain opening. In general the experimental measurements give a smaller water table lowering with respect to the numerical simulation even if the difference is negligible with respect the total hydraulic head loss, especially in the zone close to the drain. The maximum water table lowering occurs in correspondence of the drain. Moreover it tends to the undisturbed levels of the initial saturation line inside the beach and of the static water level seawards. However the difference between the numerical and experimental results is more evident in the inner part of the beach (right-side with respect to the drain position).
The most remarkable results obtained by simulating the drainage process is

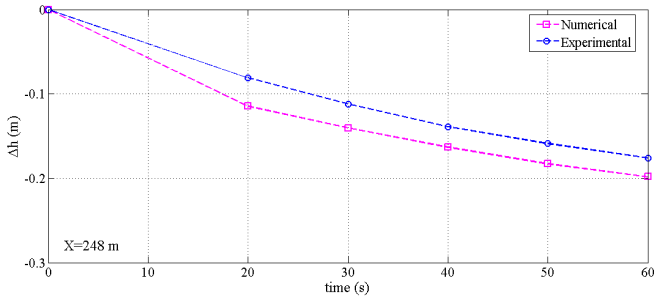

Figure 5.8: Comparison between the numerical and the experimental time variation of local pressure head near the drain

the groundwater behavior in correspondence of drain. The analysis of laboratory data (see Chapter 4) show that the internal drain flow is an open-channel flow, while in the sand a residual hydraulic head on drain can be observed. On the contrary the numerical simulation would confirm that no residual hydraulic head on drain occurs. Indeed the saturation line reaches the drain contours. The lack of a pressure transducers placed over the drain at the same section of that placed inside does not allow to understand the really hydraulic conditions. Figure 5.8 reports both experimental and numerical time variation of the local piezometric head every 10 minutes. The experimental data are obtained from the piezometers placed in the sand. In particular the figure shows the measurement performed by piezometer p9 placed at about 248 m from the wave generator and near the drain D3 (see Chapter 4). The numerical results are referred to the mesh node at the same piezometer plano-altimetric position in order to compare the data.

The comparison between two kind of data allow to state that the numerical model well simulate the time variation of the local piezometric head in the sand to the drain. In both numerical and experimental models the water table lowering velocity in the first 20 minutes is higher than for the residual time until the process reaches the stationary conditions. After t=20 min the two models show almost the same velocity in the water table lowering.

The reported simulations represents a first step for a complete numerical modeling of the phenomena interested in a drainage process. Future applications mainly regard the possibility of improving the adopted numerical model by simulating the drainage efficiency under different wave attacks. Previous simulations conducted by using the *Beachwin* model, which simulate simultaneously the external and wave motion, have furnished not very good results. In undrained conditions (Fig. 5.9) the numerical model (continuous line) simulate the increasing of the saturation line inside the beach due to the wave attack quite well with respect to the experimental results (dotted line). The Fig. 5.10 shows

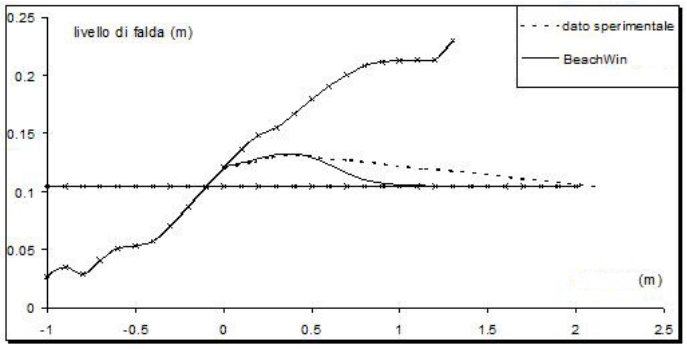

Figure 5.9: Comparison between the numerical (*BEACHWIN*) and the experimental spatial water table variation in undrained conditions

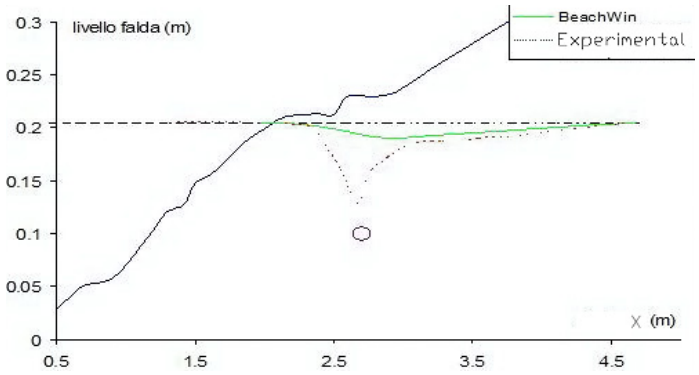

Figure 5.10: Comparison between the numerical (*BEACHWIN*) and the experimental spatial water table variation with drain on

an example of drain effect on water table simulated by *Beachwin* under a low energy wave attack. The green line in the Fig. 5.10 represents the numerical water table lowering induced by drain. It is evident that the model does not correctly reproduce the drain efficacy in lowering the local hydraulic head measured in laboratory.

For this reason the numerical simulations performed by *HYDRUS-2D* has firstly regarded the correct simulation of the groundwater flow inside the beach. Once this process is numerically well understood the simulation can be completed with the other to macro processes regarding the external wave motion modeling and the sediment transport in the swash zone.

Bibliography

[1] Battjes J. A. Surf-zone dynamics. *Annual Review of Fluid Mechanics*, 20(1):257–291, 1988.

[2] Peregrine D. H. Breaking waves on beaches. *Annual Review of Fluid Mechanics*, 15(1):149–178, 1983.

[3] Hansen U. A. Wave set up and design water level. *Journal Waterways Port Coast. Ocean. Div.*, 104:227–240, 1978.

[4] M. S. Longuet-Higgins and R. W. Stewart. Radiation stress and mass transport in gravity waves, with application to âsurf beatsâ. *Journal of Fluid Mechanics*, 13(04):481–504, 1962.

[5] Longuet-Higgins M. S. and Stewart R. W. A note on wave set-up. *Marine Research*, 21:4 – 10, 1963.

[6] Longuet-Higgins M. S. and Stewart R. W. Radiation stresses in water waves; a physical discussion, with applications. *Deep Sea Research and Oceanographic Abstracts*, 11(4):529 – 562, 1964.

[7] Young K. C. *Handbook of Coastal and Ocean Engineering.* World Scientific, 2009.

[8] Bowen A. J., Inman D. L, and Simmons V. P. Wave âSet-Downâ and Set-Up. *J. Geophys. Res.*, 73(8):2569–2577, 1968.

[9] Battjes J. A. Set-up due to irregular waves. In *Proceedings of the 13th International Conference on Coastal Engineering, Vancouver*, pages 1993–2004. ASCE, 1972.

[10] Stive M.J.F, Wind H.G., and Waterloopkundig Laboratorium. A study of radiation stress and set-up in the nearshore region. *Coastal Engineering*, 6:1–26, 1982.

[11] Guza R. T. and Thornton E. B. Wave Set-Up on a natural beach. *J. Geophys. Res.*, 86(C5):4133–4137, 1981.

[12] King B. A., Blackley M. W. L., Carr A. P., and Hardcastle P. J. Observations of wave-induced set-up on a natural beach. *J. Geophys. Res.*, 95(C12):22289–22297, 1990.

[13] Yanagishima S. and Katoh K. Field observation on wave set-up near the shoreline. *Proceedings of the International Conference on Coastal Engineering*, 1(22), 1990.

[14] Greenwood B. and Osborne P. D. Vertical and horizontal structure in cross-shore flows: An example of undertow and wave set-up on a barred beach. *Coastal Engineering*, 14(6):543–580, 1990.

[15] D.J. Hanslow and Nielses P. Shoreline set-up on natural beaches. *Journal of Coastal Research*, SI15, 1993.

[16] Hunt I.A. Design of seawalls and breakwaters. *J. Waterways and Harbors Div.*, 85(WW3), 1959.

[17] N.W.H. Allops, Hawkes P.J., F.A. Jackson, and L. Franco. *Wave run-up on steep slopes - model tests under random waves.* Report SR2, 1985.

[18] John P. A and M. S. Heimbaugh. Irregular wave runup on riprap revetments. *Journal of Waterways Port Coast. Ocean. Eng.*, 114(4):524–530, 1988.

[19] van der Meer J. W. and Stam C. M. Wave runup on smooth and rock slopes of coastal structures. *Journal of Waterways Port Coast. Ocean. Eng.*, 118(5):534–550, 1992.

[20] Wiegel. R.L. *Oceanographical Engineering.* Prentice Hall, New York, 1964.

[21] Svendsen I.A. Mass flux and undertow in a surf zone. *Coastal Engineering*, 8:347–365, 1984.

[22] Putrevu U. and Svendsen I. A. Vertical structure of the undertow outside the surf zone. *Journal of Geophysical research*, 98(C12):22707– 22716, 1993.

[23] Dyhr-Nielson M. and Sorensen T. Some sand transport phenomena oh coasts with bars. *Proceedings of the International Conference on Coastal Engineering*, 1(12):855–866, 1970.

[24] Dally W.R. A numerical model for beach profile evolution. Master's thesis, University of Delaware, 1980.

[25] Borekci O.S. *Distribution of wave-induced momentum fluxes over depth and application within the surf zone.* PhD thesis, University of Delaware, 1982.

[26] Dally W. R. and Dean R.G. Suspended sediment transport and beach profile evaluation. *Journal of Waterw. Port Coastal Ocean Eng. Am. Soc. Civ. Eng.*, 110(1):15–33, 1984.

[27] Stive M.J.F and Wind H.G. Cross-shore mean flow in the surf zone. *Coastal Engineering*, 10(4):325–340, 1986.

[28] Svendsen I.A. and Hansen J. B. Cross-shore currents in surf zone modelling. *Coastal Engineering*, 12:23–42, 1988.

[29] Bagnold R.A. Beach formation by waves: some model experiments in a wave tank. *Journal of the ICE*, 15(1):27–52, 1940.

[30] Nadaoka K. and Kondoh T. Laboratory measurements of velocity field structure in the surf zone by LDV. *Coastal Engineering Jpn.*, 25:125–145, 1982.

[31] Svendsen I.A. and Hansen J. B. Interaction of wavesand currents over a longshore bar. *Proceedings of the International Conference on Coastal Engineering*, 20:1580–1594, 1986.

[32] Okayasu A., Shibayama T., and Mimura N. Velocity field under plunging waves. *Proceedings of the International Conference on Coastal Engineering*, 1(20):660–674, 1986.

[33] Okayasu A., Shibayama T., and Mimura N. Vertical variation of undertow in the surf zone. *Proceedings of the International Conference on Coastal Engineering*, 1(21):478–491, 1988.

[34] Elgar S., Guza R. T., and Freilich M. H. Eulerian measurements of horizontal accelerations in shoaling gravity waves. *Journal of Geophysical Research*, 93:9261–9269, 1988.

[35] Diane P Horn and Travis Mason. Swash zone sediment transport modes. *Marine Geology*, 120(3-4):309–325, September 1994.

[36] Hughes M. G., G.Masselink, and Brander R. W. Flow velocity and sediment transport in the swash zone of a steep beach. *Marine Geology*, 138(1-2):91 – 103, 1997.

[37] Larson, S. Kubota, and L. Erikson. Swash-zone sediment transport and foreshore evolution: field experiments and mathematical modeling. *Marine Geology*, 212(1-4):61–79, 2004.

[38] Madsen O. S. Mechanics of cohesionless sediment transport in coastal waters. In *Proceedings of Coastal Sediments '91*, pages 15–27, 1991.

[39] Van De Graaff and J. Van Overeem. Evaluation of sediment transport formulae in coastal engineering practice. *Coastal Engineering*, 3(1-3):1–32, 1979.

[40] Akira Watanabe. Total rate and distribution of longshore sand transport. *Proceedings of the International Conference on Coastal Engineering*, 1(23), August 1992.

[41] Masselink G. and Hughes M. Field investigation of sediment transport in the swash zone. *Continental Shelf Research*, 18(10):1179–1199, 1998.

[42] Bagnold R. A. The flow of cohesionless grains in fluids. *Philosophical Transactions of the Royal Society of London. Series A, Mathematical and Physical Sciences*, 249(964):235–297, 1956.

[43] Nielsen P. *Coastal bottom boudary layers and sediment transport*, volume 4. World Scientific Publishing, 1992.

[44] Engelund F. *Transport of bed load at high shear stress.* Institute of Hydrodynamics and Hydraulic Engineering, ISVA, Technical University of Denmark, 1981.

[45] Meyer-Peter E. and Muller R. Formulas for bed-load transport. In *Proceedings of the 2nd Meeting, International Association for Hydraulic Structures Research*, pages 36–64, Stockholm, Sweden, 1948.

[46] Benno Brenninkmeyer S.J. In situ measurements of rapidly fluctuating, high sediment concentrations. *Marine Geology*, 20(2):117–128, 1976.

[47] Nadaoka K., Hino M., and Koyano Y. Structure of the turbolent flow field under breaking waves in the surf zone. *J. of Fluid Mechanics*, 204:359–387, 1989.

[48] Hinze J. O. *Turbulence.* McGraw-Hill, May 1975.

[49] Engelund F. A criterion for the occurrence of suspended load. *La Houille Blanche*, (6):607, 1965.

[50] van Rijn L.C. Sediment transport, part ii: suspended load transport. *Journal of hydraulic engineering*, 110(11):1613–1641, 1984.

[51] Nielsen P. Three simple models of wave sediment transport. *Coastal Engineering*, 12(1):43–62, 1988.

[52] Munch-Peterson J. Littoral drift formula. *Beach Erosion Board Bulletin U.S. Army Engineer Waterways Experiments Station*, 4(4):1–31, 1938.

[53] Eaton R. Littoral processes on sandy coasts. *Proceedings of the International Conference on Coastal Engineering*, 1(1):140–154, 1950.

[54] Watts G.M. A study of sand movement at south lake worth inlet, folrida. *Beach Erosion Board, Technical memorandum,U. S. Army Corps of Engineers*, 42, 1953.

[55] Caldwell J.M. Wave action and sand movement near anaheim bay, california. *Beach Erosion Board, Technical memorandum,U. S. Army Corps of Engineers*, 8, 1956.

[56] Savage R.P. Laboratory determination of littoral transport rates. *J. Waterways and Harbors Div.*, 88(WW2):69–92, 1962.

[57] Ribberink J. S. and Al-Salem A. Bed forms, sediment concentrations and sedimen transport in simultaed wave conditions. *Proceedings of the International Conference on Coastal Engineering*, 1(22), August 1990.

[58] Bagnold R.A. *Beach and nearshore processes - Part I, Mechanics of marine sedimentation*. The sea - ideas and observations on progress in the study of the sea, vol.3. Interscience Wiley, 19963.

[59] Bagnold R. A. An approach to the sediment transport problem from general physics. *USGS Professional Paper*, 422-I(I):42, 1966.

[60] Hardisty J. and Holman R.A. A calibration of the bagnold beach equation. *Marine Geologyg*, 61(1), 1984.

[61] Holland K. T., Sallenger A. H., Raubenheimer B., and Elgar S. Swash zone morphodynamics and sediment transport processes. *Proceedings of the International Conference on Coastal Engineering*, 1(26), August 1998.

[62] Bruun P. Coastal erosion and development of beach profiles. Technical report, U.S. Army Corps of Engineers, Washngton, DC, July 1954.

[63] Dean R.G. *Equilibrium beach profiles: U. S. Atlantic and Gulf coasts*, volume 12. Department of Civil Engineering, University of Delaware, Newark, DE, 1977.

[64] R.G. Dean, D.L. Kriebel, and T.L Walton. *Cross-shore secdiment transport processes*. Department of Civil Engineering, University of Delaware, Newark, DE, 2002.

[65] Moore B.D. *Beach profile evolution in response to changes in water level and wave height*. Department of Civil Engineering, University of Delaware, Newark, DE, 1982.

[66] Vellinga P., Bijker, Civil Engineering, Geosciences, and TU Delft. Beach and dune erosion during storm surges, dec 1986.

[67] Swart D.H., Bijker E.W., Civil Engineering, Geosciences, and TU Delft. Offshore sediment transport and equilibrium beach profiles, December 1974.

[68] Richard Silvester and John R. C. Hsu. *Coastal stabilization: innovative concepts*. PTR Prentice Hall, 1993.

[69] Johnson J. W. Scale effects in hydraulic models involving wave motion. *Transactions of the American Geophysical Union*, 30(4):517–525, 1949.

[70] Yuichi Iwagaki and Hideaki Noda. LABORATORY STUDY OF SCALE EFFECTS IN TWO-DIMENSIONAL BEACH PROCESSES. *Proceedings of the International Conference on Coastal Engineering*, 1(8):194–210, June 1962.

[71] Irvathur Vasudeva Nayak. EQUILIBRIUM PROFILES OF MODEL BEACHES. *Proceedings of the International Conference on Coastal Engineering*, 1(12), July 1970.

[72] Dean R.G. Heuristic models of sand transport in the surf zone. In *First Australian Conference on Coastal Engineering: Engineering Dynamics of the Coastal Zone*, pages 215–221, Sydney: Institution of Engineers, Australia, 1973.

[73] Tsuguo Sunamura and Kiyoshi Horikawa. TWO-DIMENSIONAL BEACH TRANSFORMATION DUE TO WAVES. *Proceedings of the International Conference on Coastal Engineering*, 1(14), July 1974.

[74] Nubuo Mimura, Yukinori Otsuka, and Akira Watanabe. Laboratory study on two-dimensional beach transformation due to irregular waves. *Proceedings of the International Conference on Coastal Engineering*, 1(20), August 19861.

[75] Horikawa K., Sunamura T., Kondo H., and Okada S. On two-dimensional shoreline change due to the waves. In *Proceedings of Japanese Conf. Coastal Eng. (in Japanese)*, volume 22, pages 329–334, 1975.

[76] Andrew D. Short. WAVE POWER AND BEACH-STAGES: a GLOBAL MODEL. *Proceedings of the International Conference on Coastal Engineering*, 1(16), August 1978.

[77] Hattori M. and Kawamata R. Onshore-offshore transport and beach profile change. In *Summeries of 17th Conf. Coastal Eng.*, volume 17, pages 254–255, 1980.

[78] Kriebel D.L. Verification study of a dune erosion model. *Shore and Beach*, 54(3):13–21, 1986.

[79] Nicholas C Kraus, Magnus Larson, Coastal Engineering Research Center (U.S.), U.S. Army Engineer Waterways Experiment Station, and United States. *Beach profile change measured in the tank for large waves : 1956-1957 and 1962 / by Nicholas C. Kraus and Magnus Larson.* available from National Technical Information Service,, Springfield, Va. :, 1988.

[80] Magnus Larson and Nicholas C Kraus. SBEACH: numerical model for simulating Storm-Induced beach change. report 1. empirical foundation and model development. Technical report, US Army Corps of Engineers, July 1989.

[81] Seymour R. J. and Castel D. Validation of cross-shore transport formulations. *Proceedings of the International Conference on Coastal Engineering*, 1(21):1676–1688, August 1988.

[82] Dalrymple R.A. Prediction of storm/normal beach profiles. *Journal Waterways Port Coast. Ocean. Div.*, 118(2):193–200, 1992.

[83] Nicholas C Kraus, Magnus Larson, and David L Kriebel. Evaluation of beach erosion and accretion predictors. In *Proceedings of Coastal Sediments*, pages 572–587, 1991.

[84] Mangor K. *Shoreline Management Guidelines.* DHI Water and Environment (DHI), 2001.

[85] L.D. Wright. Beach cut in relation to surf zone morhodynamics. *Proceedings of the International Conference on Coastal Engineering*, 1(17), 1980.

[86] A D Short and P A Hesp. Wave, beach and dune interactions in southeastern australia. *Marine Geology*, 48(3-4):259–284, 1982.

[87] Thornton, J. Macmahan, and A. Sallengerjr. Rip currents, mega-cusps, and eroding dunes. *Marine Geology*, 240(1-4):151–167, 2007.

[88] Vesterby H. Coastal drain system: a new approach to coastal restoration. In *Proceedings of GeoCoast*, pages 651–654, Yokohama, Japan, September 1991.

[89] Vesterby H. Beach face dewatering - the european experience. In *Proceedings of 7th National COnference on Beach Preservation Technology*, pages 53–68, Tampa, Florida, February 1994.

[90] Elfrink B. and Baldock T. Hydrodynamics and sediment transport in the swash zone: a review and perspectives. *Coastal Engineering*, 45(3-4):149 – 167, 2002.

[91] Larson M., Kubota S., and Erikson L. Swash-zone sediment transport and foreshore evolution: field experiments and mathematical modeling. *Marine Geology*, 212(1-4):61–79, 2004.

[92] D. Horn. Beach groundwater dynamics. *Geomorphology*, 48(1-3):121–146, 2002.

[93] Grant U.S. Effects of groundwater table on beach erosion. *Bullettin of the Geological Society of America*, 57, 1946.

[94] Grant U.S. Influence of the water table on beach aggradation and degradation. *Marine Research*, 7(3):655–660, 1948.

[95] Robinson C., Gibbes B., and Li L. Driving mechanisms for groundwater flow and salt transport in a subterranean estuary. *Geophysical Research Letters*, 33(3):L03402, February 2006.

[96] John R. and Duncan Jr. The effects of water table and tide cycle on swash-backwash sediment distribution and beach profile development. *Marine Geology*, 2(3):186–197, November 1964.

[97] Turner I. L. and Masselink G. Swash infiltration-exfiltration and sediment transport. *Journal of Geophysical Research*, 103(C13):30813–30824, 1998.

[98] Chappell J., Eliot I.G, M.P. Bradshaw, and Lonsdale E. Experimental control of beach face dynamics by watertable pumping. *Engineering Geology*, 14(1):29–41, June 1979.

[99] R. Rossetti. L. Damiani, G. Ranieri. Costal protection with bms: the first experience in italy. *Coastal Engineering*, 6:365–376, 2003.

[100] Bowman D., Ferri S., and Pranzini E. Efficacy of beach dewatering - alassio, italy. *Coastal Engineering*, 54:791–800, 2007.

[101] Ciavola P., Fontana E., and Vicinanza D. Performance of a beach drainage system at lido adriano (ravenna â italy). In *Proceedings of 33rd IAHR Congress: Water Engineering for a sustainable environment*, pages 7312–7319, Vancouver, British Columbia, August 2009.

[102] Vicinanza D., Ciavola P., and S. Biagi. Field experiment to control coastline subsidence: a unique case study at lido adriano (italy). *Special Issue of Coastal Research*, 56:1105–1109, 2003.

[103] Vicinanza D., A. Giuda, Ferrante P., and Ciavola P. Performance of a beach drainage system at chiaiolella beach (procida island, italy). *Journal of Coastal Research*, in press, 2009.

[104] Machemehl J.L, French T. J., and Huang N. E. New method for beach erosion control. In *Proceedings of Civil Engineering in the Oceans*, volume 1, pages 142–160. ASCE, 1975.

[105] Kawata Y. and Tsuchiya Y. Applicability of sub-sand system to beach erosion control. *Proceedings of the International Conference on Coastal Engineering*, 1(20), 1986.

[106] Oh T. M. and Dean R.G. *Beach face dynamics as affected by ground water table elevations*. University of Florida. Department of Coastal and Oceanographic Engineering, 1992.

[107] G. Masselink, I.L. Turner, and J.J. Williams. Large-scale laboratory investigation into the effect of the beach groundwater table on gravel beach morphology. *Journal of Coastal Research*, SI(56):93–97, 2009.

[108] Damiani L., Petrillo A.F., and Saponieri A. Beach dewatering systems: Modelling coastal groundwater flow. In *Proceedings of 33rd IAHR Congress: Water Engineering for a sustainable environment*, pages 7304–7311, Vancouver, British Columbia, August 2009.

[109] Hughes S.A. *Physical Models and Laboratory Techniques in Coastal Engineering - Advanced Series on Ocean Engineering - Vol. 7*. World Scientific, 1993.

[110] Ranieri G. The surf zone distortion of beach profiles in small.scale coastal models. *Journal of Hydraulic Researchy*, 45(2):261–269, 2007.

[111] Hallermeier R.J. Unified modelling guidance based on a sedimentation parameter for beach changess. *Coastal Engineering*, 49:37–70, 1985.

[112] Chiaia G., Damiani L., and Ranieri G. Experimental analysis of the water table of a beach equipped with a drainage system. In *Proceedings of 31st IAHR Congress - Water Engineering for the Future: Choices and Challenges*, volume 31, pages 5919–5929, COEX, Seoul, Korea, September 2005.

[113] L. Damiani, A. F. Petrillo, and G. Ranieri. Il laboratorio di ricerca e sperimentazione per la difesa delle coste - politecnico di bari. *Studi Costieri*, 5:97–106, 2002.

[114] Kraus N. and Larson M. *Beach profile change measured in the tank for large waves 1956-1957 and 1962*. U.S. Army Engineer Waterways Experiment Station; available from National Technical Information Service, 1988.

[115] Ranieri G. A standard method for measuring the average fall velocity of sands. In *Proceedings of the Hydraulic measurement experimental method conference*, Estes Park Colorado, USA, 2002. EWRI-ASCE.

[116] Cartwright N., Nielsen P., and Jessen O. Z. Swash zone and near-shore watertable dynamics. volume 1-3, pages 1006–1015. World Scientific Publishing Co. Pte. Ltd., 2003.

[117] Vesterby H. Modelling groundwater flow in beach profile for optimising stabilization measures. In *Proceedings of International Coastal Simposium 2000*, Rotorua, New Zeland, 2000.

[118] Li L., Barry D. A, Pattiaratchi C. B., and Masselink G. BeachWin: modelling groundwater effects on swash sediment transport and beach profile changes. *Environmental Modelling Software*, 17(3):313–320, 2002.

[119] Karambas T.V. Numerical study of the beach profile evolution due to a âcoastal drain system. In *Proceedings of 33rd IAHR Congress: Water Engineering for a sustainable environment*, pages 1–8, Vancouver, British Columbia, August 2009.

[120] Hansen J. B. and Svendsen I.A. A theoretical and experimental study of undertow. *Proceedings of the International Conference on Coastal Engineering*, 1(19):2246–2262, 1985.

[121] Ciavola P., Vicinanza D., Aristodemo F., and Contestabile P. Large-scale morphodynamic experiments on a beach drainage system. *Journal of hydraulic research*, 49(4):523–528, 2011.

[122] Thornton E. B., Humiston R. T., and Birkemeier W. Bar/trough generation on a natural beach. *Journal of Geophysical Research*, 101(C5):12097–12110.

[123] Masselink G. and Russell P. Flow velocities, sediment transport and morphological change in the swash zone of two contrasting beaches. *Marine Geology*, 227(3-4):227–240, March 2006.

[124] Baldock T. E., Baird A. J., Horn D. P., and T.E. Mason. Measuremtns and modelling of swash induced pressure gradients in the surface layers of a sand beach. *Journal of Geophysical Research*, 106(C2):2653–2666, 2001.

[125] Conley D. C. and Inman D. L. Ventilated oscillatory boundary layers. *Journal of Fluid Mechanics*, 273:261–284, 1994.

[126] Turner I. L. and Masselink G. Swash infiltration-exfiltration and sediment transport. *Journal of Geophysical Research*, 103(C13):30813–30824, 1998.

[127] van Gent, d'Angremond, Civil Engineering, Geosciences, and TU Delft. Wave interaction with permeable coastal structures, December 1995.

[128] M. S. Longuet-Higgins and E. D. Cokelet. The deformation of steep surface waves on water. i. a numerical method of computation. *Proceedings of the Royal Society of London. A. Mathematical and Physical Sciences*, 350(1660):1 –26, July 1976.

[129] Vinje T. and Brevig P. Numerical simulation of breaking waves. *Adv. Water Res.*, 4:77–82, 1981.

[130] Peregrine D.H. *Equations for water waves and the approximations behind them.* Academic Press, New York, 1972.

[131] Packwood A.R. The influence of beach porosity on wave uprush and backwash. *Coastal Engineering*, 7(1):29–40, February 1983.

[132] Damiani L. and G. Ranieri. Contirbuto allo studio delle oscillazioni della linea di riva. *Atti e relazioni - Accademia Pugliese delle Scienze*, 45(2):93–119, 1988.

[133] Kobayashi N. and Wurjanto A. Numerical model for waves on rough permeable slopes. *Journal of Coastal Research*, pages 149–166, April 1990. ArticleType: research-article / Issue Title: SPECIAL ISSUE NO. 7. Rational Design of Mound Structures / Full publication date: SPRING 1990 / Copyright Â© 1990 Coastal Education & Research Foundation, Inc.

[134] Nielsen. Tidal dynamics of the water table in beaches. *Water Resources Research*, 26(9):2127â2134, 1990.

[135] Kang H. Y. and P. Nielsen. Watertable dynamics in coastal areas. *Proceedings of the International Conference on Coastal Engineering*, 1(25), August 2011.

[136] L. Li, D. A. Barry, and C. B. Pattiaratchi. Modeling coastal groundwater response to beach dewatering. *JOURNAL OF WATERWAY PORT COASTAL AND OCEAN ENGINEERING-ASCE*, 122(6):273–280, 1996.

[137] L. Li, Barry D.A., and Pattiaratchi C.B. Numerical modelling of tide-induced beach water table fluctuations. *Coastal Engineering*, 30:105–123, March 1997.

[138] Vesterby H., Mangor K., and Refsgaard A. The beach drainage concept. development of an engineering design tool. *Proceedings of COPEDEC V*, 2:961–971, April 1999.

[139] Li, D A Barry, C B Pattiaratchi, and G. Masselink. BeachWin: modelling groundwater effects on swash sediment transport and beach profile changes. *Environmental Modelling Software*, 17(3):313–320, 2002.

[140] Ioannidis D. and Karambas Th. V. 'soft' shore protection methods: Beach drainage system. *Proceedings of International Conference on Environmental Science and Technology*, 10:528–535, September 2007.

[141] Tony Butt, P. Russell, and I. Turner. The influence of swash infiltrationâexfiltration on beach face sediment transport: onshore or offshore? *Coastal Engineering*, 42(1):35–52, 2001.

[142] Magnus Larson, Susumu Kubota, and Li Erikson. A model of sediment transport and profile evolution in the swash zone. *ASCE Conference Proceedings*, 260(40566):93, jun 2001.

[143] Simunek J., Vogel T., and van Genuchten Th. The $SWMS_2 code for simulating water flow and solute transport in two - dimensional variably saturated media. version 1.1. research report 126. Technical report, U.S. Salinity Lab$

[144] Simunek J. and van Genuchten Th. The $CHAIN_2 D code for the two - dimensional movement of water, heat and multiple solutes in variably saturated media, version 1.1. resear$

[145] Vogel T. SWMII - numerical model of two.dimensional flow in a variably saturated porous medium. research report 87. Technical report, Dept. of Hydraulics and Catchment Hydrology, Agricultural University, Wageningen, The Netherlands, 1987.

[146] Neuman S.P. Finite element computer programs for flow in saturated-unsaturated porous media. second annual report, project a10.swc-77. Technical report, Hydraulic Engineering Lab., Haifa, Israel, 1972.

[147] Neuman S.P. Saturated-unsaturated seepage by finite elements. second annual report, project a10.swc-77. *J Hydraulic Div., ASCE*, pages 2233–2250, 1973.

[148] Neuman S.P., Feddes R.A., and E. Bresler. Finite element simulation of flow in saturated-unsaturated soil considering water uptake by plants. third annual report, project a10.swc-77. Technical report, Hydraulic Engineering Lab., Haifa, Israel, 1974.

[149] Neuman S.P. *Galerkin approach to saturated-unsaturated flow in porous media, Chapter 10 in Finite elements in fluid*, volume 1. Wiley, 1975.

[150] R. A. Feddes, P. J. Kowalik, and Henryk Zaradny. *Simulation of field water use and crop yield*. Wiley, January 1978.

[151] van Genuchten Th. A numerical model for water and solute movement in and below the root zone. research report 121. Technical report, U.S. Salinity Laboratory, USDA, ARS, Riverside, CA, 1987.

[152] Brooks R.H. and A.T. Corey. Properties of porous media affecting fluid flow. *Journal of the Irrigation and Drainage Division*, 92(2):61–90, 1966.

[153] M TH Van Genuchten. A closed-form equation for predicting the hydraulic conductivity of unsaturated soils. *Soil Science Society of America Journal*, 44(5):892–898, 1980.

[154] Mualem. A new model for predicting the hydraulic conductivity of unsaturated porous media. *Water Resources Research*, 12(3):513–522, 1976.

[155] Tomas Vogel and Milena Cislerova. On the reliability of unsaturated hydraulic conductivity calculated from the moisture retention curve. *Transport in Porous Media*, 3:1–15, February 1988.

[156] R. A. Feddes, E. Bresler, and S. P. Neuman. Field test of a modified numerical model for water uptake by root systems. *Water Resources Research*, 10(6):PP. 1199–1206, 1974.

[157] G. F. Pinder. *Finite Element Simulation in Surface and Subsurface Hydrology*. Academic Pr, 1ST edition, June 1977.

[158] Simunek J., Senja M., and van Genuchten M. Th. *HYDRUS-2D Simulating wtaer flow, heat and solute transport in two-dimensional variably saturated media*. Colorado School of Mines, Apr 1999.

List of Figures

List of Tables